Fatigue Evaluation of Steel Bridges

DETAILS

115 pages | 8.5 x 11 | PAPERBACK
ISBN 978-0-309-25826-5 | DOI 10.17226/22774

AUTHORS

Bowman, Mark D.; Fu, Gongkang; Zhou, Y. Edward; Connor, Robert J.; and Godbole, Amol A.

NATIONAL COOPERATIVE HIGHWAY RESEARCH PROGRAM

NCHRP REPORT 721

Fatigue Evaluation of Steel Bridges

Mark D. Bowman
PURDUE UNIVERSITY
West Lafayette, IN

Gongkang Fu
ILLINOIS INSTITUTE OF TECHNOLOGY
Chicago, IL

Y. Edward Zhou
URS CORPORATION
Hunt Valley, MD

Robert J. Connor
PURDUE UNIVERSITY
West Lafayette, IN

Amol A. Godbole
PURDUE UNIVERSITY
West Lafayette, IN

Subscriber Categories
Highways • Bridges and Other Structures

Research sponsored by the American Association of State Highway and Transportation Officials
in cooperation with the Federal Highway Administration

TRANSPORTATION RESEARCH BOARD

WASHINGTON, D.C.
2012
www.TRB.org

NATIONAL COOPERATIVE HIGHWAY RESEARCH PROGRAM

Systematic, well-designed research provides the most effective approach to the solution of many problems facing highway administrators and engineers. Often, highway problems are of local interest and can best be studied by highway departments individually or in cooperation with their state universities and others. However, the accelerating growth of highway transportation develops increasingly complex problems of wide interest to highway authorities. These problems are best studied through a coordinated program of cooperative research.

In recognition of these needs, the highway administrators of the American Association of State Highway and Transportation Officials initiated in 1962 an objective national highway research program employing modern scientific techniques. This program is supported on a continuing basis by funds from participating member states of the Association and it receives the full cooperation and support of the Federal Highway Administration, United States Department of Transportation.

The Transportation Research Board of the National Academies was requested by the Association to administer the research program because of the Board's recognized objectivity and understanding of modern research practices. The Board is uniquely suited for this purpose as it maintains an extensive committee structure from which authorities on any highway transportation subject may be drawn; it possesses avenues of communications and cooperation with federal, state and local governmental agencies, universities, and industry; its relationship to the National Research Council is an insurance of objectivity; it maintains a full-time research correlation staff of specialists in highway transportation matters to bring the findings of research directly to those who are in a position to use them.

The program is developed on the basis of research needs identified by chief administrators of the highway and transportation departments and by committees of AASHTO. Each year, specific areas of research needs to be included in the program are proposed to the National Research Council and the Board by the American Association of State Highway and Transportation Officials. Research projects to fulfill these needs are defined by the Board, and qualified research agencies are selected from those that have submitted proposals. Administration and surveillance of research contracts are the responsibilities of the National Research Council and the Transportation Research Board.

The needs for highway research are many, and the National Cooperative Highway Research Program can make significant contributions to the solution of highway transportation problems of mutual concern to many responsible groups. The program, however, is intended to complement rather than to substitute for or duplicate other highway research programs.

NCHRP REPORT 721

Project 12-81
ISSN 0077-5614
ISBN 978-0-309-25826-5
Library of Congress Control Number 2012940789

COPYRIGHT INFORMATION

NOTICE

The project that is the subject of this report was a part of the National Cooperative Highway Research Program, conducted by the Transportation Research Board with the approval of the Governing Board of the National Research Council.

The members of the technical panel selected to monitor this project and to review this report were chosen for their special competencies and with regard for appropriate balance. The report was reviewed by the technical panel and accepted for publication according to procedures established and overseen by the Transportation Research Board and approved by the Governing Board of the National Research Council.

The opinions and conclusions expressed or implied in this report are those of the researchers who performed the research and are not necessarily those of the Transportation Research Board, the National Research Council, or the program sponsors.

The Transportation Research Board of the National Academies, the National Research Council, and the sponsors of the National Cooperative Highway Research Program do not endorse products or manufacturers. Trade or manufacturers' names appear herein solely because they are considered essential to the object of the report.

Published reports of the

NATIONAL COOPERATIVE HIGHWAY RESEARCH PROGRAM

are available from:

Transportation Research Board
Business Office
500 Fifth Street, NW
Washington, DC 20001

and can be ordered through the Internet at:

http://www.national-academies.org/trb/bookstore

Printed in the United States of America

THE NATIONAL ACADEMIES

Advisers to the Nation on Science, Engineering, and Medicine

The **National Academy of Sciences** is a private, nonprofit, self-perpetuating society of distinguished scholars engaged in scientific and engineering research, dedicated to the furtherance of science and technology and to their use for the general welfare. On the authority of the charter granted to it by the Congress in 1863, the Academy has a mandate that requires it to advise the federal government on scientific and technical matters. Dr. Ralph J. Cicerone is president of the National Academy of Sciences.

The **National Academy of Engineering** was established in 1964, under the charter of the National Academy of Sciences, as a parallel organization of outstanding engineers. It is autonomous in its administration and in the selection of its members, sharing with the National Academy of Sciences the responsibility for advising the federal government. The National Academy of Engineering also sponsors engineering programs aimed at meeting national needs, encourages education and research, and recognizes the superior achievements of engineers. Dr. Charles M. Vest is president of the National Academy of Engineering.

The **Institute of Medicine** was established in 1970 by the National Academy of Sciences to secure the services of eminent members of appropriate professions in the examination of policy matters pertaining to the health of the public. The Institute acts under the responsibility given to the National Academy of Sciences by its congressional charter to be an adviser to the federal government and, on its own initiative, to identify issues of medical care, research, and education. Dr. Harvey V. Fineberg is president of the Institute of Medicine.

The **National Research Council** was organized by the National Academy of Sciences in 1916 to associate the broad community of science and technology with the Academy's purposes of furthering knowledge and advising the federal government. Functioning in accordance with general policies determined by the Academy, the Council has become the principal operating agency of both the National Academy of Sciences and the National Academy of Engineering in providing services to the government, the public, and the scientific and engineering communities. The Council is administered jointly by both Academies and the Institute of Medicine. Dr. Ralph J. Cicerone and Dr. Charles M. Vest are chair and vice chair, respectively, of the National Research Council.

The **Transportation Research Board** is one of six major divisions of the National Research Council. The mission of the Transportation Research Board is to provide leadership in transportation innovation and progress through research and information exchange, conducted within a setting that is objective, interdisciplinary, and multimodal. The Board's varied activities annually engage about 7,000 engineers, scientists, and other transportation researchers and practitioners from the public and private sectors and academia, all of whom contribute their expertise in the public interest. The program is supported by state transportation departments, federal agencies including the component administrations of the U.S. Department of Transportation, and other organizations and individuals interested in the development of transportation. **www.TRB.org**

www.national-academies.org

COOPERATIVE RESEARCH PROGRAMS

CRP STAFF FOR NCHRP REPORT 721

Christopher W. Jenks, *Director, Cooperative Research Programs*
Crawford F. Jencks, *Deputy Director, Cooperative Research Programs*
Waseem DeKelbab, *Senior Program Officer*
Danna Powell, *Senior Program Assistant*
Eileen P. Delaney, *Director of Publications*
Maria Sabin Crawford, *Assistant Editor*

NCHRP PROJECT 12-81 PANEL
Field of Design—Area of Bridges

Barton J. Newton, *California DOT, Sacramento, CA* (Chair)
Sreenivas Alampalli, *New York State DOT, Albany, NY*
Laura M. Amundson, *Parsons Brinckerhoff, Minneapolis, MN*
Lian Duan, *California DOT, Sacramento, CA*
Hussam Z. "Sam" Fallaha, *Florida DOT, Tallahassee, FL*
Thomas K. Koch, *North Carolina DOT, Raleigh, NC*
Keith L. Ramsey, *Texas DOT, Austin, TX*
Joey Hartmann, *FHWA Liaison*
Stephen F. Maher, *TRB Liaison*

AUTHOR ACKNOWLEDGMENTS

The research reported in this Final Report was performed under NCHRP Project 12-81, "Evaluation of Fatigue on the Serviceability of Highway Bridges" by the School of Civil Engineering at Purdue University in West Lafayette, IN. Purdue University is the prime contractor for this study, with Dr. Fu as a private consultant to Purdue, and URS Corporation serving as a sub-contractor to Purdue. Dr. Mark D. Bowman, Professor of Civil Engineering at Purdue, is the Project Director and Principal Investigator. The other authors of this report are: Dr. Gongkang Fu, Professor of Civil Engineering at Illinois Institute of Technology; Dr. Y. Edward Zhou, National Practice Leader—Bridge Instrumentation and Evaluation at URS Corporation; Dr. Robert J. Connor, Associate Professor of Civil Engineering at Purdue; and Amol A. Godbole, Research Assistant and Ph.D. Candidate at Purdue University.

FOREWORD

By Waseem DeKelbab
Staff Officer
Transportation Research Board

The report provides proposed revisions to Section 7—Fatigue Evaluation of Steel Bridges of the *AASHTO Manual for Bridge Evaluation* with detailed examples of the application of the proposed revisions. The proposed revisions and examples were developed based on analytical and experimental research conducted to improve existing methods to evaluate and assess the serviceability of bridge structures for the fatigue limit state. The material in this report will be of immediate interest to highway design engineers.

The *AASHTO Guide Specifications for Fatigue Evaluation of Existing Steel Bridges (Guide)* and the *2003 AASHTO Guide Manual for Condition Evaluation and Load and Resistance Factor Rating (LRFR) of Highway Bridges (Manual)* provide guidance on fatigue evaluation of steel bridges. The Guide is more than 17 years old, and the material in the Manual is derived from the Guide. Section 7—Fatigue Evaluation of Steel Bridges of the *AASHTO Manual for Bridge Evaluation (MBE),* First Edition/2008, incorporates the material in the Manual. In recent years, more information on steel bridges has been developed that provides a foundation upon which to update the procedures for fatigue evaluation of steel bridges. Areas in need of improvement include: (a) methods of estimating total and remaining fatigue life as the current methods can result in unrealistic and inaccurate predictions, (b) guidance on the evaluation of retrofit and repair details used to address fatigue cracks, and (c) guidance for the evaluation of distortion-induced fatigue cracks.

The research was performed under NCHRP Project 12-81, "Evaluation of Fatigue on the Serviceability of Highway Bridges", by a team led by Dr. Mark D. Bowman, the School of Civil Engineering at Purdue University in West Lafayette, IN. The objectives of NCHRP Project 12-81 were to (1) propose updates to Section 7—Fatigue Evaluation of Steel Bridges of the *AASHTO Manual for Bridge Evaluation* and (2) provide detailed examples of the application of the proposed revisions.

A number of deliverables are provided as appendices. Only Appendix E—Proposed Section 7 of MBE and Appendix F—Fatigue Examples are published herein. Other appendices are not published but are available on the TRB website at http://www.trb.org/Main/Blurbs/167233.aspx. These appendices are titled as follows:

- APPENDIX A— Survey Interview Forms
- APPENDIX B— AASHTO Fatigue Truck Validation Analysis Results
- APPENDIX C— Tack Weld Tests
- APPENDIX D— Distortion Induced Fatigue Tests

CONTENTS

1 Summary

5 **Chapter 1** Background

7 **Chapter 2** Research Approach

7 History of AASHO/AASHTO Provisions for Fatigue Design and Evaluation of Bridges

8 Review of Fatigue Specifications in Other Countries

9 Eurocode Specification

9 Australian Specification

9 Survey

9 Summary of DOT Survey Results

10 Summary of Identified Fatigue Expert Survey Results

10 Identify Critical Issues and Needed Research

10 The S-N Curve

10 Unnecessary Approximation Leading to Unreliable Estimates

11 Negative Remaining Fatigue Life

12 Multiple Presence Factor

12 Lack of Detailed Guidance for Field Measurement as an Option

12 Lack of Guidance on Tack Welds and Riveted Members

14 Lack of Guidance for the Evaluation of Distortion-Induced Fatigue Cracks

16 Fatigue Serviceability Index

16 Additional Factors

16 Experimental Setup and Test Procedures

16 Tack Weld Tests

18 Distortion-Induced Fatigue Tests

24 **Chapter 3** Findings and Applications

24 S-N Curve

24 Validation of AASHTO Fatigue Truck

25 Multiple Presence Factor

26 Concept of Multiple Presence Factor

27 Analysis Overview and WIM Data Used

27 Sensitivity Analysis

27 Negative Remaining Life

30 R_R Factor

32 Fatigue Serviceability Index

36 More Accurate Estimation for Truck Traffic

36 Example 1

37 Example 2

39 Tack Weld Tests

40 Bolt Tightening Procedure

42 Finite Element Analysis of Tack Weld Specimen
44 Test Results
45 Comparison of Test Results
46 Distortion-Induced Fatigue Tests
46 Finite Element Analysis for Distortion-Induced Fatigue Tests
57 Test Results

61 **Chapter 4** Conclusions
62 Proposed Revisions to MBE Section 7
62 Options for Design Consideration

64 References

65 **Appendices A–D**

E-1 **Appendix E** Proposed Section 7 of MBE

F-1 **Appendix F** Fatigue Examples

Note: Many of the photographs, figures, and tables in this report have been converted from color to grayscale for printing. The electronic version of the report (posted on the Web at www.trb.org) retains the color versions.

SUMMARY

Fatigue Evaluation of Steel Bridges

The following report summarizes the results of the research effort undertaken as part of NCHRP Project 12-81. This research project has a focus on Section 7 "Fatigue Evaluation of Steel Bridges" in AASHTO's The Manual for Bridge Evaluation (MBE) first issued in 2008. The MBE combines the Manual for Condition Evaluation of Bridges, Second Edition (2000) and its 2001 and 2003 Interim Revisions with the Guide Manual for Condition Evaluation and Load and Resistance Factor Rating (LRFR) of Highway Bridges, First Edition in 2003 and its 2005 Interim Revisions. The objective of this research is to develop a revised and updated Section 7 for the MBE, to meet the needs of the user.

A view exists among some fatigue evaluation engineers that the MBE is overly conservative, because some bridges with satisfactory service history are accordingly determined to have negative remaining fatigue lives. A number of factors may have contributed to this conservatism: overestimated load distribution factors, unintended composite action ignored, the S-N curve's lower bound being used, etc. However, not all cases of fatigue evaluation are believed to be overly conservative. For example, truss or two-girder bridges carrying more than one lane of traffic may have un-conservative fatigue life estimates because of the single lane loading prescribed in the MBE. When multiple lanes are carried by the two trusses or girders, the fatigue life may be significantly overestimated because possible simultaneous loads on other lanes are ignored. On the other hand, conventional analysis methods generally overestimate the live load stress ranges in truss bridges because unintended composite actions are often ignored.

In general, a larger amount of uncertainty is involved in fatigue evaluations compared with bridge strength evaluations or load ratings. Furthermore, the demand for a realistic fatigue evaluation is much higher than that for a fatigue design, because an over-conservative evaluation result could cost considerably more than an over-conservative design. An un-conservative result is, of course, not desired either. Besides the uncertainty factors mentioned above, there are also other sources of uncertainty in the fatigue evaluation process. They include the scatter nature of the S-N curves, variable truck loads including significant site-to-site variations, approximations in structural analysis or load effect estimation, etc. The inherent uncertainties, however, can be reduced using more refined analyses or field measurements to better define the stress range at the details in question.

The research program of this project aims toward the revision of Section 7 of the MBE to advance the state of the art and the practice. Items specifically identified as in need of improvement include:

1. Improved methods utilizing a reliability-based approach to assess the fatigue behavior and aid bridge owners in making appropriate operational decisions.
2. Guidance on the evaluation of retrofit and repair details used to assess fatigue cracks.
3. Guidance for the evaluation of distortion-induced fatigue cracks.

To address these needs a number of analytical and experimental studies were performed. The analytical studies were used to examine various aspects that influence the fatigue behavior. These topics ranged from truck loading effects on bridge structures to fatigue resistance related factors that affect the predicted fatigue life. Both analytical and experimental studies were used to further develop an understanding of distortion-induced deformations and the structural behavior of various retrofit details used to repair a bridge structure with distortion-induced fatigue cracking. Moreover, early in the study it was decided that it would be beneficial to perform a series of experimental tests to study the influence of tack welds on riveted joints. A summary of some of the key findings from the study is provided below.

Finite fatigue life predictions based upon use of an approximate curve to estimate the lifetime average ADTT (average daily truck traffic) based upon the present single lane ADTT were found to lead to inconsistencies and errors in the prediction of the remaining fatigue life. The use of a closed form solution for the effect of traffic growth developed in NCHRP 12-51 is recommended for inclusion in the updated version of Section 7.

The resistance factor for the finite fatigue life was found to be well correlated with the 95th percentile for the minimum life. The values for R_R were correspondingly recalculated for the evaluation fatigue life and the mean fatigue life levels and are suggested for inclusion in the revised Section 7 provisions.

Multiple presence of trucks was found to have some influence on the loading used for fatigue evaluation. The primary factors involved were the ADTT level, the number of lanes available, and the bridge span length. WIM (weigh-in-motion) data with a high-resolution time stamp of 0.01 seconds from four different states and for different bridge configurations were used to study the effect of multiple trucks on various bridge structures. It was found that an equation involving the three predominant variables could be used to reasonably model multiple truck presence.

Remaining fatigue life was found to have an undesirable connotation and it was believed that a new methodology to evaluate fatigue serviceability would be useful. Hence, a non-dimensional parameter, named the fatigue serviceability index, was developed to evaluate the condition and the assessment outcome with respect to fatigue. The method uses bridge age, predicted fatigue life, structural configuration, and bridge importance to determine the fatigue evaluation.

When the bridge age exceeds the predicted fatigue life of a given bridge detail then the remaining life predicted in the current MBE Section 7 provisions gives a negative fatigue life. In the current Section 7 requirements, the user has the option to either reassess the life using new information, to assume a greater risk in the fatigue life estimation, or to retrofit the detail that has developed the problem. Using "new" information involves some additional effort and cost since better information such as WIM data or strain measurements are needed. Consequently, an additional option was developed to recalculate the cumulative frequency distribution based upon satisfactory performance with no observed fatigue cracking so that a positive remaining life would be produced at all times. The new option utilizes a modified frequency distribution with the same reliability factor as the original estimate.

An experimental study was conducted to evaluate the fatigue strength of members with tack welds. A number of existing bridge structures, especially older riveted structures, have tack welds that were used for fit-up during construction and which were simply left in place. The tack welds are currently classified as Category E details in the LRFD Bridge Design Specification. This fatigue category provides a correspondingly low fatigue life prediction, which may require a costly retrofit or removal by grinding the tack welds off the primary structure when the bridge evaluation is performed. Consequently, cyclic tests were conducted to determine if the fatigue strength is indeed higher than Category E, since few data on tack welded members are available. A higher fatigue strength classification may remove the need for unnecessary

retrofits or repairs. The following observations were made based on the tack weld analysis and testing results:

- Finite element analysis indicates that the weld toe of the first line of tack welds experiences the maximum stress. Hence, it was expected that the weld toe of the first tack weld would be the critical location for fatigue due to the stress concentration at that location. This was confirmed through the fatigue testing, as all of the fatigue cracks that formed were observed to initiate at the weld toe of the first tack weld.
- Variations in the number of tack welds, length of tack welds, position of the tack weld relative to the fastener hole, and orientation of the tack welds relative to the load were all studied. The number, length, and orientation of the tack welds were not observed to significantly affect the fatigue strength of the tack welds.
- Based upon the results of seventeen cyclic tests, it was found that the cyclic strength of the tack welds all exceeded the mean value of the Category D curve and was closest to the mean fatigue strength for the Category C curve. Moreover, all of the fatigue test results exceeded the Category C fatigue design curve. Hence, it was concluded that the fatigue strength can be adequately modeled using a Category C design life as given per the LRFD Bridge Design Specification.

Distortion-induced fatigue cracking of steel bridge web gap details was studied. A survey of state transportation officials was conducted to evaluate current fatigue inspection and evaluation procedures. The results of the survey revealed that distortion-induced fatigue cracking is the most frequently encountered type of fatigue distress observed by various state transportation agencies. Both softening and stiffening, in addition to hole drilling, were reported as methods being used to retrofit distortion-induced cracking. Both analytical modeling and experimental testing were used to evaluate the behavior of retrofits used to stiffen the connection and mitigate distortion-induced fatigue cracking. The following observations were made:

- Finite element analysis was used to study the stiffness and response of WT sections used for retrofit elements to mitigate distortion-induced cracking. The WT section is typically installed to bridge the gap between the vertical connection plate and the girder flange, with the WT flange attached to the girder flange and the WT web stem attached to the vertical connection plate or stiffener. It was found that increasing the thickness of the flange of the WT section is significantly more effective in controlling out-of-plane distortions than increasing the web thickness.
- Finite element analysis was conducted to analytically study forces developed in cross frame angle members of representative bridges since they frequently provide the out-of-plane forces that cause distortion of the girder web. It was found that out-of-plane deformations decreased significantly after a retrofit was installed, but the force in the brace was found to increase notably, often twofold or more for a given differential girder displacement. Predicting the out-of-plane force in the retrofit is difficult because it was found to be influenced by the differential deflection of adjacent girders, the size and length of the cross-brace members, the length of the girder web gap, the thickness of the girder web, and the geometry of the retrofit detail. These factors must be accounted for through refined analysis or field measurement if the retrofit forces are to be accurately assessed. Otherwise, a sufficiently stiff retrofit must be installed to minimize the distortion and transfer the out-of-plane force to the girder flange.
- Experimental testing was used to evaluate the cyclic performance of three retrofit details bolted to the girder flange and the vertical connection plate: WT sections, double angles, and single angles. Thirteen test specimens were used with variations in the retrofit thicknesses and web gap dimensions. It was observed that fatigue cracking initiated very quickly in the

subcomponent girder web at the web gap for all girder sections tested when subjected to out-of-plane distortions. Although the cracks initiated quickly, growth slowed considerably as it propagated away from the web gap region due to softening of the connection. (After the retrofit, the fatigue cracks were not removed by hole drilling to permit evaluation while still in this most critical condition.) No subsequent fatigue cracks were observed to occur for any of the WT or double-angle retrofit details which were installed. The fatigue cracks left intact were observed to not grow further or to only grow by a small amount. A number of single-angle retrofits were observed to develop active fatigue cracks, but none of them failed after at least 5,000,000 additional loading cycles after retrofit. The cracking is believed to be due to a lack of symmetry and greater flexibility of the single-angle retrofit.

- If a stiffening retrofit is used, it is recommended that either a WT section or a pair of angles should be used if possible. Thicknesses greater than ½-in should be utilized to provide sufficient connection stiffness with at least four bolts used to connect the retrofit to the web and flanges. If single angles are used for the retrofit, then a relatively thick angle should be used. Also, retrofit holes should always be drilled to remove the crack tip of the distortion-induced fatigue cracks that have been detected.

CHAPTER 1

Background

Optimal performance of a bridge under normal service loads is essential for full and effective use by the motoring public. Problems that occur as a result of excessive deflections, deteriorating deck conditions, or fatigue cracking of steel girders or beams under normal operating service loads can cause delays and inconvenience for the public as these problems are being corrected. In extreme cases, inadequate serviceability performance may require that portions of a bridge be closed as it is being repaired, or the bridge may need to be replaced altogether. Moreover, repair operations also pose a safety hazard for both the motoring public and the construction personnel. Clearly, the need exists to develop modern and effective methods to assess the serviceability of a bridge structure so that the optimal performance can be achieved.

This research project has a focus on Section 7 "Fatigue Evaluation of Steel Bridges" in AASHTO's The Manual for Bridge Evaluation (MBE) Second Edition issued in 2011. The MBE combines the Manual for Condition Evaluation of Bridges, Second Edition (2000) and its 2001 and 2003 Interim Revisions with the Guide Manual for Condition Evaluation and Load and Resistance Factor Rating (LRFR) of Highway Bridges, First Edition and its 2005 Interim Revisions. The objective of this research is to develop a revised and updated Section 7 for the MBE, to meet the needs of the user.

A view exists among some fatigue evaluation engineers that the MBE is overly conservative because some bridges with satisfactory service history are accordingly determined to have negative remaining fatigue lives. A number of factors may have contributed to this conservatism: overestimated load distribution factors, unintended composite action ignored, the S-N curve's lower bound being used, etc. On the other hand, not all cases of fatigue evaluation are believed to be overly conservative. For example, truss or two-girder bridges carrying more than one lane of traffic may have unconservative fatigue life estimate because of the single lane loading prescribed in the MBE. When multiple lanes are carried by the two trusses or girders, the fatigue life may be significantly overestimated because possible simultaneous loads on other lanes are ignored. On the other hand, conventional analysis methods generally overestimate the live load stress ranges in truss bridges because unintended composite actions are often ignored.

In general, a larger amount of uncertainty is involved in fatigue evaluations compared with bridge strength evaluations or load ratings. Furthermore, the demand for a realistic fatigue evaluation is much higher than that for a fatigue design because an over-conservative evaluation result could cost considerably more than an over-conservative design. An un-conservative result is, of course, not desired either. Besides the uncertainty factors mentioned herein, there are also other sources of uncertainty in the fatigue evaluation process. They include the scatter nature of the S-N curves, variable truck loads (including significant site-to-site variation), approximations in structural analysis or load effect estimation, etc. The inherent uncertainties, however, can be reduced using more refined analyses or field measurements to better define the stress range at the details in question.

The research program of this project aims toward the revision of Section 7 of the MBE to advance the state of the art and the practice (AASHTO 2011). This research includes analytical and experimental studies which will lead to the effective development of an improved Section 7 of the MBE.

The primary objective of the research is to revise and update Section 7, "Fatigue Evaluation of Steel Bridges" of the Manual for Bridge Evaluation. Items specifically identified as in need of improvement include the following:

1. Improved methods utilizing a reliability-based approach to assess the fatigue behavior and aid bridge owners in making appropriate operational decisions.

2. Guidance on the evaluation of retrofit and repair details used to assess fatigue cracks.
3. Guidance for the evaluation of distortion-induced fatigue cracks.
4. Guidance for evaluation of tack weld induced fatigue cracks.
5. Adjustment of truck loading factors to account for multiple lane loading.

Experimental tests performed to evaluate tack weld induced fatigue cracks examine the effect of different stress ranges and weld parameters on the fatigue life of the tack welds. The objective of the tests is to classify the tack weld detail into the appropriate fatigue category based on the observed fatigue life of the tack welds. Experimental tests to evaluate distortion-induced fatigue cracks examine the effectiveness and fatigue behavior of different types of retrofit options. The retrofits used to address the distortion-induced fatigue include only stiffening retrofits: particularly WT, double-angle retrofits, and single-angle retrofits. New methodologies and provisions to enhance the fatigue evaluation procedure of bridge details are researched in order to improve Section 7 of the MBE. Existing fatigue provisions are also examined for improvement.

CHAPTER 2

Research Approach

A review of the history of provisions for fatigue design and evaluation of bridges was performed in order to identify specific provisions that can be improved, as well as to identify items that need to be researched further so that new provisions handling such items can be included. An effort was also spent in reviewing fatigue evaluation provisions of other countries in order to compare and contrast with existing provisions. Also, a survey was sent out to state DOTs, agencies, Canadian Provinces, and selected consultants in order to gain insight into the various issues related to bridge loadings and the effect they have on the assessment of the fatigue strength of bridge structures.

History of AASHO/AASHTO Provisions for Fatigue Design and Evaluation of Bridges

The first fatigue design provisions of the AASHTO Standard Specifications for Highway Bridges appeared in 1965. In the 10th edition (1969) in Section 1.7.3 Fatigue Stresses, an allowable fatigue stress range was determined as a function of loading, highway classification, detail type, strength of steel, and 'R' ratio (i.e., the algebraic ratio of the minimum stress to the maximum stress, which was not necessarily a live load stress range, as the minimum stress could have been produced by dead load). Eleven detail categories were defined, completely different than in use today, and are known as categories A through K. In the 11th Edition (1973), the fatigue provisions remained essentially unchanged with little modifications.

The 12th Edition (1977) contained a completely revised approach for fatigue design of highway bridges. These changes were essentially a direct result of the NCHRP research conducted by Dr. John Fisher and colleagues. Section 1.7.2, titled "Repetitive Loading and Toughness Considerations," was added and addressed both fatigue and fracture. This section of the Standard Specifications contained guidance related to the fatigue design of common steel details found in highway bridges. The Specifications contained illustrations of common bolted and welded details that are known to be fatigue sensitive, along with their associated fatigue resistance. These illustrations remain essentially unchanged to this day. The details were grouped into categories of similar fatigue resistance that were labeled 'A' through 'F,' with 'A' being the highest.

The most significant change was the introduction of the stress range concept for fatigue design. The results of NCHRP studies confirmed that for welded details, fatigue life was primarily a function of stress range, detail category, and the number of applied cycles. The other parameters previously included in the earlier specifications, such as material strength and 'R' ratio, had no significant effect on the fatigue life of welded details commonly used in bridge construction. The allowable stress range at a specific number of loading cycles was provided for each of the new categories in Table 1.7.2A1. These effectively define the allowable fatigue resistance based upon the stress range concept. The fatigue endurance limit was also defined. Section 1.7.2 of the 12th Edition of the Standard Specifications also provided guidance on the number of cycles for which a given bridge member should be designed (indirectly this is the design life). Similar to the previous versions, the required design life is a function of member type, highway classification, and ADTT. This also includes infinite-life design. Infinite-life design is required in cases where a very high number of cycles are expected and/or no fatigue cracking can be tolerated.

The fatigue provisions changed very little between the 14th and 16th editions of the Standard Specifications. The AASHTO LRFD Bridge Design Specifications, introduced in 1994, incorporated a reliability-based approach to all aspects of design related to highway bridges. The fatigue provisions were substantially revised, with the most significant changes being made to the load model used for fatigue design. The illustrative examples and detail resistance (i.e., CAFL [constant amplitude fatigue limit]) essentially remained unchanged.

The specification utilized the concept of an "effective fatigue truck" of prescribed loading and axle spacing.

The Guide Specifications for Fatigue Evaluation of Existing Steel Bridges (1990)—or Guide—was a significant development that introduced a comprehensive method to evaluate the fatigue life of steel bridges. The fatigue evaluation procedures in the Guide Specifications were developed in NCHRP Project 21-83 and presented in *NCHRP Report 299* by Moses et al. (1987). The procedures provided an alternative to the design specification requirements, which were not well suited to the evaluation of existing bridges.

Section 7 of the AASHTO Manual for Condition Evaluation and LRFR of Highway Bridges (2003) (or LRFR Manual) represents a notable update of the AASHTO Guide Specifications that were issued in 1990. Language was added denoting the difference between load-induced fatigue versus distortion-induced fatigue. For load-induced fatigue damage evaluation, the fatigue requirements in the LRFR Manual utilize the equations and categories in the AASHTO LRFD Bridge Design Specification rather than the comparable values in the AASHTO Standard Specifications that were used by the Guide Specifications. Nevertheless, the same calibration was used to establish the values for the fatigue S-N curves for both the Guide Specification and the LRFR Manual. The LRFR Manual further indicates that the effective stress range shall be estimated as either the measured stress range or a calculated stress range value determined by using a fatigue truck as specified in the LRFD Bridge Design Specification, or a fatigue truck determined by a truck survey or weigh-in-motion study. The LRFR Manual makes use of partial load factors that adjust the stress range as uncertainty in the estimate is reduced as a result of improved analysis or site-specific information. The lowest possible partial load factor is associated with the use of measured strains to obtain the stress range values. Once the effective stress range has been determined, then a check is made to determine whether or not the details are prone to load-induced fatigue damage.

In the LRFR Manual, a resistance factor, R_R, was used in the fatigue life expression to account for one of the three types of life estimates being determined: a minimum expected fatigue life that would be conservative and be equal to the design fatigue life, an evaluation fatigue life that would give a conservative estimate of fatigue life, and the mean fatigue life, which is the most likely fatigue life estimate. A table is given for R_R to account for the appropriate type of fatigue life value being estimated for each of the various AASHTO detail categories. According to the Commentary of the LRFR Manual, the probability of failure associated with the fatigue life approaches 2%, 16%, and 50% for the minimum, evaluation, and mean fatigue lives, respectively. This represents an offset of one and two standard deviations from the mean fatigue life for the evaluation and minimum fatigue lives, respectively.

The fatigue life estimate also accounts for the growth in truck traffic volume. In the LRFR Manual, the correlation is made to the average lifetime daily truck traffic for a single lane. A figure is provided to correlate the present $[(ADTT)_{SL}]_{PRESENT}$ with the lifetime average daily truck traffic $(ADTT)_{SL}$. A section is also provided in the LRFR Manual with a number of different strategies to increase the remaining fatigue life, should it be deemed undesirable. The commentary indicates that retrofit or load-restriction decisions should be based upon use of the Evaluation Life rather than the minimum life. Use of the mean life (with a 50% probability of failure) for remaining life estimates is also permitted if the estimate from the Evaluation Life is still unacceptable. Additional options that are prescribed include the recalculation of the fatigue life using more accurate data as input to the fatigue life estimate. These include improvements in the effective stress range, effective truck weight, the average daily truck traffic, or the number of cycles per truck passage. The fatigue life can also be improved by retrofitting the critical detail to improve the detail category rating and thereby increase the fatigue life.

A section is provided in the LRFR Manual that deals with distortion-induced fatigue evaluation. The section is quite brief, and it indicates that distortion-induced fatigue is typically a low-cycle fatigue phenomenon, with few stress range cycles needed to initiate cracking at distortion-induced prone details. The provisions state that "distortion-induced fatigue is a stiffness problem (more precisely the lack thereof) versus a load problem." No provisions are provided for how to address distortion-induced cracking when it occurs. Another addition to the LRFR Manual requirements is the prescription of a required fracture mechanics analysis if fatigue cracks have been visually detected. Alternatively, retrofitting measures are recommended once fatigue cracking is detected.

Section 7 titled "Fatigue Evaluation of Steel Bridges" of AASHTO's The MBE was first issued in 2008 with a second edition in 2011 that combined the Manual for Condition Evaluation of Bridges, Second Edition (2000) and its 2001 and 2003 Interim Revisions with the Guide Manual for Condition Evaluation and LRFR of Highway Bridges, First Edition and its 2005 Interim Revisions. With this, all the previous bridge evaluation titles were archived by AASHTO. Section 7 of the MBE has been directly adopted from the LRFR Manual with minor changes in referencing.

Review of Fatigue Specifications in Other Countries

An effort was spent on collecting and reviewing selected fatigue design and evaluation specifications of other countries representing the state of the practice in the world. A review of Eurocode and Australian specification codes is presented in the following sections.

Eurocode Specification

The Eurocode (2005) has been revised since its first version reviewed in *NCHRP Report 299* by Moses et al. (1987) when the Guide Specification was developed. It also uses the S-N curve concept for assuring an adequate life of bridges considering steel fatigue. Different from the AASHTO counterpart for normal stress ranges in members, the slope of the S-N curves is not a constant for the entire life range or stress range. Two slopes, 3 and 5, are used for different regions of the curves. In addition, 14 fatigue categories are used instead of 8 as in the AASHTO MBE (2011). Furthermore, for shear stress ranges, another set of S-N curves are provided with a constant slope of 5. The S-N curves for normal stress ranges have different infinite-life limits for constant and variable amplitude cases, whereas those for shear have only one limit for both cases. The Eurocode specification also allows the use of the hot-spot stress method. Lastly, the provisions in the Eurocode for non-welded details or stress-relieved welded details allow the mean stress influence on fatigue strength to be taken into account by determining a reduced effective stress range $\Delta\sigma_{E,2}$ (corresponding to 2 million cycles) in the fatigue assessment when part or all of the stress cycle is compressive. The effective stress range may be calculated in the Eurocode by adding the tensile portion of the stress range and 60% of the magnitude of the compressive portion of the stress range.

Australian Specification

The Australian bridge design standard (Council of Standards Australia, 2004a) and rating standard (Council of Standards Australia, 2004b) both contain provisions regarding the fatigue failure mode in steel bridge components. The S-N curves in the Australian specifications are similar to those in the Eurocode as discussed above. Nevertheless, one more fatigue strength category is adopted in the Australian standards, which is at the high-strength end of the spectrum whose failure (cracking) perhaps more likely will not be observed very often. Two different slopes of the S-N curves are included, as in the Eurocode, as well as two levels of limit stress for infinite life, one for constant, and the other for variable amplitude stress variation. The Australian standards also include S-N curves for shear stress ranges appearing to be identical to those for the Eurocode. The Australian standards also explicitly include bolts and shear studs into the fatigue strength categorization, being different from the Eurocode. Note also that Australia is the only country found in this effort of literature review to have a separate bridge rating standard covering fatigue, although the rating procedure refers to the design S-N curves without many additional provisions directly dealing with the variety of situations possibly encountered in rating. Some examples of such situations may include, but are not limited to, how to use truck load records when an inadequate life is found, or what needs to be done when a fatigue crack is observed in the bridge.

Survey

Surveys were received from 30 of the more than 80 sent out, with 26 received from DOTs and other agencies and 4 from fatigue experts. A blank copy of the DOT survey, a summary of the DOT survey responses, and a blank copy of the fatigue expert survey is included in Appendix A.

Summary of DOT Survey Results

The results of this survey can be summarized as follows:

1. It is extremely rare for states to perform regularly scheduled fatigue evaluations. While states acknowledge that many common types of bridges require fatigue evaluations, they are only performed when cracks are discovered during inspections. Several states do not perform any fatigue analyses whatsoever. The reasons given are low traffic volumes and the absence of fatigue issues in the past.
2. When considering requirements utilized for fatigue evaluation, the Guide Specification is more popular among states, and those states that utilize Section 7 of the Manual indicate that they also use the Guide. The majority of states feel that these two documents meet their current needs, but some states who are content feel that the evaluations are often too conservative. The MBE had just recently been published when this survey was carried out.
3. The majority of agencies make use of field measurements in their evaluations. More states reported using external consultants, but many also make use of in-house programs. Roughly one-third of states reported collecting and using WIM data.
4. Almost all states have observed distortion-induced fatigue cracking and the majority indicated that it is more common than load-induced fatigue. Two types of retrofit/repair details are commonly used to address distortion-induced fatigue cracking. Most states "soften" the detail by removing rivets or bolts and drilling holes to relieve stresses and arrest cracks. A smaller group of states will stiffen the detail by welding or bolting the vertical stiffener to the flanges of the girder.
5. Nearly all states retrofit details that have cracked from load-induced fatigue. The method used by all states is almost identical. Holes are drilled to arrest the crack, and the section is stiffened by adding bolted splice plates.

Summary of Identified Fatigue Expert Survey Results

A short questionnaire was sent out to identified fatigue experts in order to gain useful information and opinions.

The first question inquired about recent test data that may be useful for revising Section 7 of the Manual. All four experts provided some information on possibly useful experimental data.

The second question solicited the expert's opinion about which parts of the Manual (or other fatigue design and evaluation specifications) should be revised. The intention of the question was to identify areas of the Manual that need to be revised and/or updated considering the latest advancements of knowledge. One expert did not identify any areas in the current specifications. Another expert identified the need to address the issue of very few stress cycles above the CAFL known to produce fatigue failure, and this risk is not covered by CAFL. The third expert pointed to the same issue of very few but very high stress cycles, also related to an inconsistency on this subject between the design and evaluation provisions in the two sets of AASHTO specifications. The fourth expert pointed out that the Manual does not include non-destructive evaluation information as a tool to characterize fatigue damage.

The third question in the questionnaire specifically solicited ideas to deal with possible negative remaining life. One expert expressed the importance of refined analysis using a 3-D model of the bridge. Another expert agreed with this, but also pointed to the impact factor of 15% as overestimating dynamic stress effects but expressed a belief that these two factors alone (the overestimated static load effect and impact factor) still are not fully responsible for the problem. A third expert believes that the stress estimation must be wrong when a negative remaining life results, and the fourth expert offered no opinion.

The last question of the questionnaire was an open solicitation for any suggestions or comments that the expert may wish to express regarding revisions to the fatigue evaluation requirements of existing bridges. Two of the experts indicated nothing, a third one expressed support of the needed revision of the Manual, and the fourth one suggested including methods for estimating the effective stress range.

Identify Critical Issues and Needed Research

A review was conducted to decide specific directions for revising and updating Section 7 of the MBE. The review involved identification and prioritization of issues and procedures needing revision based on existing knowledge. Where additional research is needed to revise the MBE, a number of items were individually identified for revision based on the literature review and survey results. These items and factors are noted herein and briefly discussed.

The S-N Curve

The S-N curve is the foundation underlying the fatigue evaluation of steel bridges in the MBE. The curves were developed primarily based on fatigue test data under constant amplitude cyclic loading. These curves were the result of a significant effort as part of NCHRP Project 12-15(5) by Keating and Fisher (1986) published as *NCHRP Report 286* to gather available fatigue data and establish a consistent design methodology. They drew heavily from experimental fatigue test data reported in *NCHRP Report 102* (Fisher et al. 1970) and *NCHRP Report 147* (Fisher et al. 1974) on steel bridge details. A new set of fatigue curves was established with a consistent slope of −3.0 to better model the behavior of welded bridge details.

Since the development of the MBE, technical advancement has been made for understanding long-life fatigue behavior under low-magnitude and variable amplitude cyclic loading. The current use of the S-N curves with a linear extension below the CAFL to account for long-life behavior was examined, and the behavior contrasted with that obtained by using S-N curves as in the Eurocode and the Australian code which utilize multiple slopes. The impact of changing the S-N curves from the present behavior to one that more closely follows the practice in foreign countries also was examined in terms of the accuracy of the predicted cyclic life. It also should be noted that S-N curve development based on constant amplitude stress range testing results is different from that using variable amplitude test data, because the latter involves a new dimension of uncertainty associated with the load effect. It is worth mentioning that in bridge applications, this uncertainty is often more pronounced than that associated with the strength that is treated as the only uncertainty in S-N curve regression using constant amplitude test data.

Unnecessary Approximation Leading to Unreliable Estimates

In Article 7.2.5, "Estimating Finite Fatigue Life," of the Manual (AASHTO 2003), or equivalently in Article 3.2 of the Guide (AASHTO 1990) and Article 7.2.5 of the MBE (AASHTO 2011), the following equation is provided to compute the estimated finite fatigue life Y of a fatigue-prone detail.

$$Y = \frac{R_R A}{365 n \left(ADTT\right)_{SL} \left(\left(\Delta f\right)_{eff}\right)^3} \tag{1}$$

As seen, $ADTT_{SL}$ in the denominator is required to find Y, as the average number of trucks per day in a single lane averaged over the fatigue life Y. Since the fatigue life Y is being sought, $ADTT_{SL}$ cannot be found directly. Conceptually, $ADTT_{SL}$ needs to be found by iteration, using this equation. Nevertheless, the commentary to Article 7.2.5 in the Manual

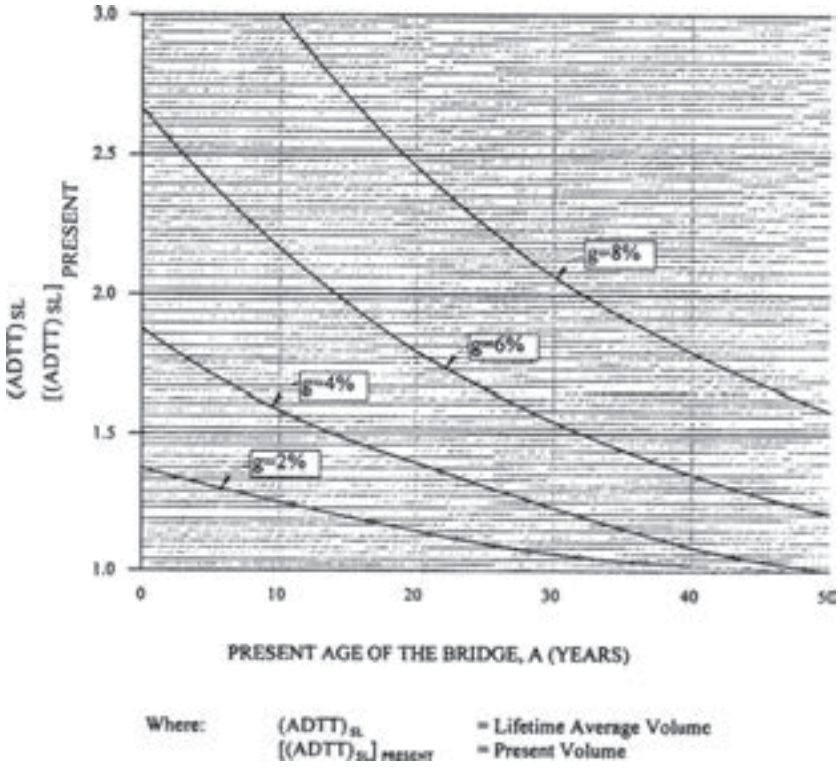

***Figure 1. Figure C7-1 in the manual for estimating* $ADTT_{SL}$.**

(and Article 3.5 in the Guide) recommends an approximation using the chart in Fig. C7-1 in the Manual (Figure 3.5A in the Guide) to estimate $ADTT_{SL}$, and then in turn *Y*. This chart, as seen in Figure 1, does not include the unknown *Y* but only present age *A* (*a* in the commentary) that is only part of *Y*. Therefore, this chart contains an approximation, which can be reduced to enhance the reliability of estimation.

Negative Remaining Fatigue Life

A negative fatigue life occurs when the bridge age exceeds the predicted cyclic life. This situation is conceptually depicted in Figure 2. The current Section 7 of the AASHTO MBE (2011) provides a couple of options for handling situations where the evaluation computation results in a negative remaining life (estimated) and field inspection has observed no fatigue cracking for the particular steel connection detail in the bridge. These options involve accepting a greater degree of risk, using more accurate data to compute fatigue life, or retrofitting the detail altogether.

As illustrated in Figure 2, the real fatigue life of the detail is a random variable, expressed by the probability distribution curve shown with little triangle symbols. The total life estimated according to the MBE is a deterministic value, also indicated on the abscissa. It is defined in the calibration process of the specifications (*NCHRP Report 299* by Moses et al. [1987]) as a value, up to which the failure probability (the shaded area) is equal to the failure probability corresponding to the target reliability index. In other words, the probability of the real life being smaller than this value is controlled to be under the targeted (acceptable) risk level associated with the target reliability index. Due to conservatism required in the process and a significant amount of uncertainty involved, sometimes this estimated total life is so small that subtracting the present age of the detail (bridge) from it results in a

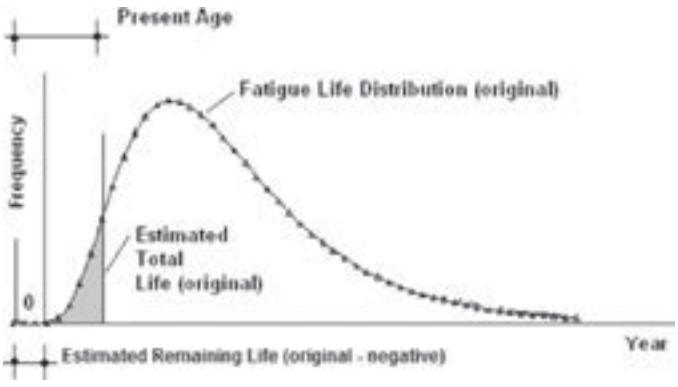

Figure 2. Negative remaining life resulting from uncertainty in fatigue life estimation (shaded area is equal to targeted failure probability).

negative remaining life (also as an estimate). As indicated in Figure 2, the estimated remaining life ends at the left side of the origin, being negative. As symbolically indicated in Figure 2, the fatigue life distribution is widely "spread," modeling a wide range of random variation or uncertainty. Therefore, without further information, it is difficult to insure the estimated remaining life to be positive.

When it is known that no fatigue cracking has been identified for the detail, this information should be taken into account in the evaluation process. In other words, it would be desirable if the information for suitable performance (no cracking) could be used to revise the life estimate with the same level of risk maintained.

Multiple Presence Factor

Truck loading is the primary cause of steel bridge fatigue damage. Heavy trucks may appear on a highway bridge span in one or more lanes simultaneously. Depending on the structure's configuration, trucks in multiple lanes can induce much higher load effects to bridge components than those in one lane. Therefore, the governing load effects due to these loading configurations need to be addressed in bridge evaluation. However, the AASHTO MBE (2011) prescribes an approximate approach to counting truck loads for their effect in inducing fatigue failure. It specifies that only the truck load on the shoulder lane needs to be counted for fatigue evaluation. This decision was made without rigorous investigation (*NCHRP Report 299* by Moses et al. (1987)) and also perhaps because there were almost no WIM data available at the time.

Regarding multiple presence of trucks on a bridge span, it is obvious that ignoring trucks in other lanes can lead to underestimation of the real load. This effect can be significant especially when a two-girder, two-truss, or two-arch system with multiple lanes is concerned. In addition, when the shoulder lane carries relatively less traffic, i.e., when other lanes carry relatively more truck traffic, such under-estimation of stress can also be more pronounced. Note that the current AASHTO MBE (2011) prescribes a uniform 80% to be the percentage of the total traffic carried by the shoulder lane, which has been verified to be often an overestimate of the shoulder lane's truck traffic. This subject has been investigated in this research project using a large amount of WIM data.

Lack of Detailed Guidance for Field Measurement as an Option

Field measurement of load effect (in strain, displacement, etc.) for the stress range histogram is a practical approach to reducing uncertainties associated with load effects in a fatigue evaluation. The MBE (AASHTO 2011) has listed this method as an alternative method to determine the effective stress range. However, there is a lack of sufficient details for the user to adequately employ this method for producing consistent results. This situation results in significantly different, or sometimes inconsistent, results depending on the individual who performs the work. The method used to collect strain data is critically important. Clearly, the collection of incorrect or inadequate strain data could lead to significant errors if the fatigue life is predicted to be significantly greater than the true behavior. Consequently, it is anticipated that additional guidance is needed to describe the minimum procedures to be used when collecting strain data to assess the fatigue strength. For example, the use of detailed analysis and/or proper modeling should be considered as a tool to assist in determining proper gage locations.

Lack of Guidance on Tack Welds and Riveted Members

The MBE (AASHTO 2011) does not include any provisions or guidance on treating tack weld induced cracks. The MBE mentions riveted members but refers to the LRFD specifications for details. The information provided in the latter is not adequate for evaluation, either.

Tack welds are mostly in existence on many bridges having built up sections, such as trusses. They often have been used to temporarily hold members in place before they are riveted, bolted, or welded. Tack welds have many start/stop locations during placement and therefore run the risk of weld flaws at the weld termination. Often these welds do not have a particularly high quality since they were not detailed or designed to carry any measurable load per se but are only placed to facilitate the fabrication.

Cracking of the tack welds through the throat of the tack weld will probably not pose a great danger to the structure. In cases where the tack weld is only partially cracked through the throat, it may be prudent to grind off the tack weld before the crack has a chance to propagate into the base metal of the primary structural element. Although certainly not common, there are documented cases where a fatigue crack has developed at the toe of a tack weld.

Figure 3 shows some examples of typical tack welds used in bridges. Also shown in the figure is an example of a tack weld that has developed a fatigue crack through its throat.

Tack welds are currently classified as Category E details with a corresponding very low fatigue strength. However, data are insufficient to support this classification. As a matter of fact, one of the reasons for this classification originally was to discourage the use of tack welds. This category likely underestimates their fatigue strength. If the fatigue strength is actually higher than Category E, and the tack weld presents little risk to seriously damage the primary structural members, then considerable cost savings may be realized if the need to repair tack welds is delayed or avoided altogether. This can be significant

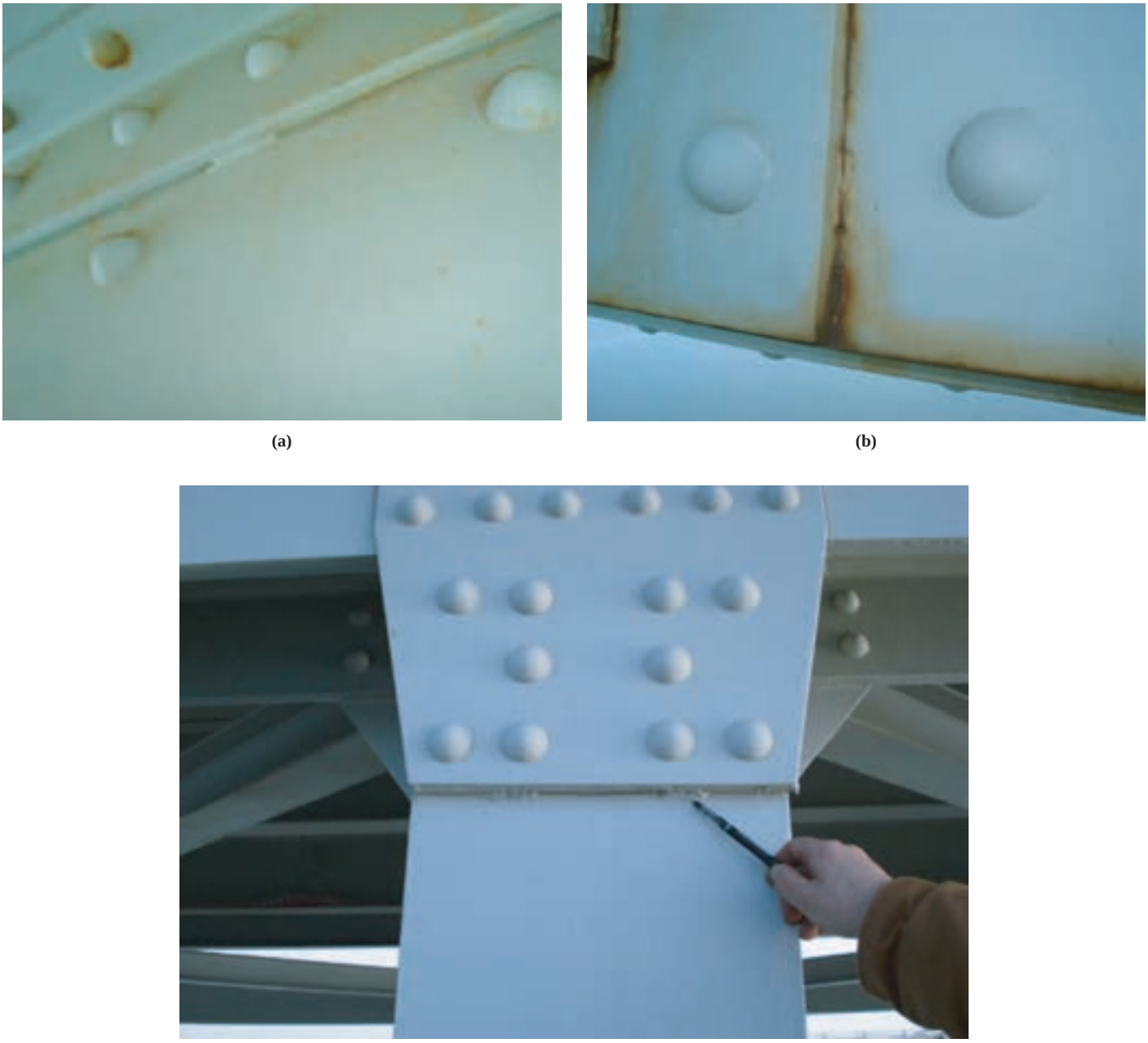

(a) (b)

(c)

Figure 3. Examples of tack welds used in bridge structures: (a) tack weld left in place after riveting, (b) tack weld throat crack, and (c) transverse tack weld.

for some older riveted structures that may have literally hundreds of tack welds that may need to be ground off otherwise.

The survey sent out to state Departments of Transportation contained two questions specifically addressing tack welds. The first question asked if fatigue cracks associated with tack welds had been observed in any bridges. A total of 13 states out of the 23 that answered the question, or slightly more than one-half, indicated that they had observed fatigue cracks at tack welds. Unfortunately it was not clear if the fatigue cracks reported were simply a severing of the tack weld through the throat, which is fairly benign, or if the fatigue crack was at a weld toe, which can be potentially serious. Nevertheless, numerous fatigue cracks were detected at tack weld details. The second question asked if the agency performed a fatigue evaluation for tack welds. In this case, only three states of the 23 who responded to the question answered in the affirmative. Hence, it appears that most states are not thoroughly evaluating the tack weld details at present.

The literature search located very few data collected to assess tack welds. Therefore, laboratory testing was conducted to better quantify their fatigue strength and their influence on built-up members.

Lack of Guidance for the Evaluation of Distortion-Induced Fatigue Cracks

The AASHTO MBE (2011) indicates that distortion-induced fatigue is more of a stiffness problem (or lack thereof) than a loading problem. The frequency of distortion-induced fatigue cracking is quite extensive. In fact, Connor and Fisher (2006) estimate that 90% of all fatigue cracking is the result of out-of-plane distortion at fatigue sensitive details. Common distortion-induced fatigue cracking sites include the web gap region at the end of vertical stiffeners or connection plates for floor beams, or in the web gap region of lateral gusset plates that intersect vertical connection plates. An example of distortion-induced fatigue cracking at the ends of vertical connection plates is shown in Figure 4.

An experimental examination of distortion-induced fatigue damage was reported by Fisher et al. (1979) in *NCHRP Report 206*. In this study, several types of fatigue damage at various fatigue susceptible details were investigated, including welded partial length cover plates, vertical stiffeners, and web penetrations by a flange. The fatigue testing demonstrated that for cyclic out-of-plane displacement of web gap regions, the fatigue strength increased as the web gap length increased. The relationship between web gap length and the initiation of fatigue cracking, however, was found not to be directly proportional. Small web gaps (less than five times the web thickness) were found to have very erratic behavior under cyclic out-of-plane displacement. Fatigue cracks at the end of the stiffeners for the normal beam testing were found to be satisfactorily retrofitted by using drilled holes.

A comprehensive study was conducted by Fisher et al. (1990) in *NCHRP Report 336* to examine various types of distortion-induced fatigue cracking. The goal of this NCHRP study was to develop recommended criteria for designing steel girders so that distortion-induced fatigue cracking problems are minimized. Both transverse connection plate and lateral gusset plate details were studied. Experimental tests of specimens that simulated details used in practice were conducted to evaluate the structural behavior. It was found that drilled retrofit holes were effective in arresting fatigue crack growth when they conformed to the following relationship:

$$\Delta K/\sqrt{\rho} < 4\sqrt{\sigma_y} \quad (\text{for } \sigma_y \text{ in ksi units}) \tag{2}$$

where ρ is the retrofit hole radius, σ_y is the yield strength of the steel, and ΔK is the stress intensity range for a given nominal stress range level, S_r. This relationship was developed by Fisher et al. (1980) in *NCHRP Report 227* in a study of the fatigue behavior of welded bridge attachments.

The retrofit used for positive attachment of the lateral connection detail consisted of a WT section that was bolted to both the flange of the beam and the transverse connection plate. No retrofit hole was used along with the WT section that was bolted to the flange and transverse plate to evaluate the effectiveness of the bolted attachment. It was found that little additional crack growth occurred and that the positive attachment was effective in repairing the transverse connection plate detail. Of course, the small additional crack growth that did occur could be completely eliminated if a retrofit hole were used together with the bolted positive attachment.

A number of observations were made from the cyclic testing program. First, the stress gradient for the web gap region varied significantly and produced larger stresses at

(a) (b)

Figure 4. Distortion-induced fatigue cracking at (a) lower end of vertical connection plate and (b) upper end of connection plate.

the transverse connection plate weld toe than at the lateral gusset plate weld toe. Second, for an in-plane stress range of 41.4 MPa (6 ksi), no cracking was detected for details A and B after 10,000,000 cycles of loading. Third, fatigue cracks did develop at the weld toe of the transverse stiffener opposite the gusset plate for detail C, where there was not a positive attachment of the lateral gusset plate to the transverse stiffener. Fourth, when the data were plotted on an S-N curve, with the stress plotted on the basis of the sum of the in-plane flexural stress plus the estimated out-of-plane bending stress, then all of the data exceeded the AASHTO category C level. Fifth, drilled holes at the crack tips were found to arrest the crack growth when the stress range levels did not exceed 138 MPa (20 ksi); higher stress levels require a positive attachment between the gusset plate and the transverse stiffener, even for large web gaps. A couple of additional comments in this study are worth noting. They mention that fitting gusset plates around a transverse stiffener without a direct attachment does not appear to be desirable. Moreover, even with a positive attachment, the web gap between the weld toes should be at least four times the web thickness. Large stress gradients can occur in the gap region, even for very small gaps. Lastly, it is stated that the intersection of the gusset longitudinal weld and the transverse stiffener weld must be avoided. Weld shrinkage strains will produce severe restraint and contribute to the possibility of weld discontinuities and inclusions at the weld intersection.

Additional test data on the repair of distortion-induced web cracking at a vertical connection plate for variable amplitude, long-life cyclic loading is also provided in *NCHRP Report 354* (Fisher et al. 1993). The report states that:

> The test results suggest that fatigue cracks are not likely to develop at transverse stiffener details in actual bridge structures unless out-of-plane distortion develops. The studies on out-of-plane distortion of transverse connection plates confirmed the findings given in *NCHRP 336.* Rigid connections of the plate to the top and bottom flanges by bolted or welded connections are needed to prevent fatigue cracks from out-of-plane deformation.

Proper retrofit procedures to address and mitigate distortion-induced cracking are critically important. General methods for evaluating and retrofitting bridges, as well as a case study involving out-of-plane distortion cracking at the web gap, are presented by Connor and Fisher (2006). Web gap details are generally classified as Category C for fatigue strength evaluation. While this may be adequate for in-plane bending stresses, the out-of-plane distortions that occur make this a fatigue-prone detail. Methods of instrumentation discussed include gage placement and type as well as monitoring times and methods. A case study is reviewed of a three-span continuous haunched plate girder bridge which had been retrofitted once the fatigue cracks had been discovered at the ends of the vertical stiffeners and at the gusset plate to stiffener details. Angles were attached to the top flange of the girder and to the transverse connection plates. They were also installed between the lateral gusset plates and the intersected transverse stiffeners. The results of this instrumentation and monitoring were used to determine that several existing details required retrofitting and that some previously installed retrofits were not effective. Specifically, the $3 \times 3 \times \frac{3}{8}$ angles attached with only two bolts at the gusset plate to the stiffener web gap were not capable of providing sufficient rigidity to fully mitigate fatigue cracking. The web gap at the top of the transverse connection plate detail was retrofitted with an $8 \times 8 \times \frac{5}{8}$ angle connected with four bolts that resulted in a significantly stiffer connection. Measurements obtained at the top web gap at three separate locations where heavier angles and more bolts had been installed indicated that the angle retrofit was sufficiently stiff to decrease distortional displacements and subsequent stresses to a level that was effective in mitigating further fatigue cracking. As a general guideline, Connor and Fisher conclude that for retrofitting transverse connection plates, heavy back-to-back angles (19 mm minimum thickness) or comparable WT sections be used with four high-strength bolts in each leg. The main point is that retrofits for out-of-plane distortion must provide sufficient stiffness to prevent relative deflection and distortion between adjacent components.

The survey that was sent to all of the state Departments of Transportation confirmed that the most commonly observed fatigue cracks in steel bridges are those due to distortion-induced localized stresses. In practice, there have been two general approaches for repairing distortion-induced fatigue cracks: stiffening or softening. Either approach may work satisfactorily if designed and installed properly. On the other hand, neither approach will work if not done properly in design and/or installation. The stiffening approach is to stiffen the distorted web and other elements of the detail. The key to the stiffening approach is to properly assess the required connection forces and provide a retrofit that has not only sufficient strength but, more importantly, very high stiffness to eliminate localized deformation. On the other hand, the key to the success of the softening approach is to properly analyze the load paths as well as the overall behavior of the structural system so that the softened structure will not cause adverse effects by allowing excessive local deformations. If done properly, the softened structure is flexible enough to deform under the required distortion so that the induced stresses do not cause significant fatigue damage.

The MBE does not include proscriptive provisions as to how distortion-induced fatigue cracking can be evaluated or treated. Section 7 of the MBE contains a separate subsection for distortion-induced fatigue. The section indicates that distortion-induced fatigue is a stiffness problem rather than a load problem.

However, no guidance is provided on how to evaluate or retrofit details that have developed distortion-induced fatigue cracks. Additional information is needed on how to evaluate details susceptible to distortion-induced fatigue cracking. Considerable information is already available in the literature on use of the hole drilling and softening method to retrofit cracked details. However, more proscriptive recommendations on methods to design effective retrofit details for stiffening the web gaps of vertical connection plates would be helpful to increase the service life of details that have experienced distortion-induced fatigue cracking. Consequently, a series of distortion-induced fatigue tests were conducted to provide additional information on the behavior of the connection.

Fatigue Serviceability Index

The fatigue serviceability index (FSI), Q, is one of the methods envisioned to assess the fatigue serviceability limit state. The FSI provides a relative measure of the performance of a structural detail, at a particular location in the structure, with respect to the overall fatigue resistance of the member. Although the remaining fatigue life is used to determine the FSI, the final value for the fatigue serviceability index is dimensionless. Relative values of this coefficient are intended to be used to characterize the overall serviceability relative to the fatigue limit state. Based on a combination of the quantitative value of the FSI and the overall qualitative assessment, engineers can make planning decisions regarding the viability of given bridges in their bridge inventory.

Additional Factors

Two additional factors that will be considered further for incorporation into Section 7 of the Manual are the use of fracture mechanics and hot-spot methods to assist the user in estimating the remaining cyclic life, which will then in turn be used to evaluate the FSI.

Experimental Setup and Test Procedures

Two of the factors identified previously require experimental testing. They are tack weld details and retrofits for distortion-induced fatigue cracks. The test setups and procedures that were implemented for the testing of these types of details are described in the following sections.

Tack Weld Tests

The tack weld tests involve a simple lap connection loaded in tension. A pair of plate members is attached to a test central plate using tack welds on the sides of the plate members. A typical tack weld specimen is shown in Figure 5. Various variables were examined in the tack weld program. These include the number of tack welds along the side of the bolted plates, the length of the tack welds, the stress range applied, the position of the tack welds relative to the adjacent bolt hole, longitudinal vs. transverse position of the tack weld, and the effect of the bolt clamping force. All steel plates are ASTM A36.

The purpose in examining different numbers of tack welds along the side of the bolted plates is to examine the degree to which the overall stiffness of the connection is influenced by the number of tack welds. It is well known that there is a shear lag effect that can occur in a long weld. The stresses in a long weld, or even a long bolted joint, tend to be greater at the ends than near the middle. If this influence is valid here, then cracking at the ends may be more likely for the three tack weld configuration than for the two tack weld geometry.

The tack weld length is also examined. Most of the tack welds for the test program are about one inch long. If the "tack welds" are too long and placed in series, then they would be better classified as intermittent welds, rather than as tack welds. To evaluate this difference, a few tests were conducted with weld lengths of about 1.5 inches to see if there is a discernable difference in the fatigue strength. The tack welds were deposited on the plates at room temperature with no significant pre-heat. Since the weld cooling rate is related to the hardness of the material in the heat-affected zone adjacent to the weld toe, the short tack welds will probably cool more rapidly than longer tack welds, and thus may be more susceptible to cracking in the heat-affected zone.

Most of the tack welded connections were tested with tack welds parallel to the lines of fasteners in the joint. However, a few specimens were tested with the tack welds along the end

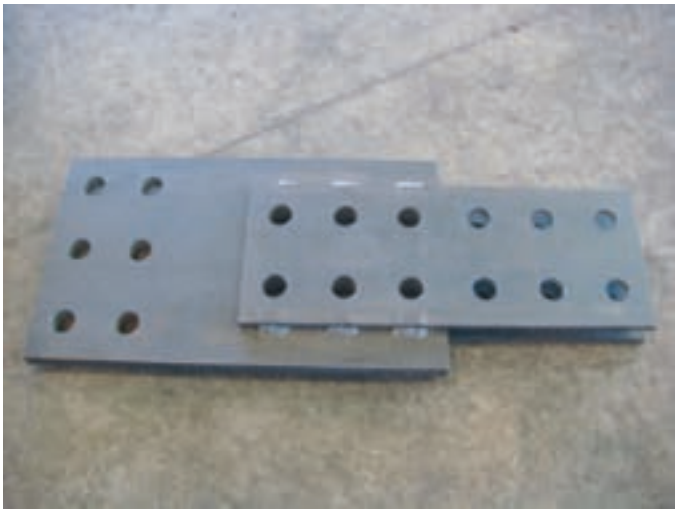

Figure 5. Typical tack weld test specimen.

Table 1. Test matrix for tack weld test program.

No. of Tack Welds	Tack Weld Position	Tack Weld Length	No. of Specimens Tested at S_r Value		
			20 ksi	12 ksi	12 ksi
2	L	<1-in.		2	
3	L	<1-in.	3	3	2 (FT)
2	L	<1-in.		3 (MP)	
2	T	<1-in.		2	
3	L	>1-in.		2	

of the connection in a line perpendicular to the fasteners. It is well known that welds are significantly more ductile when they are oriented parallel to the direction of the loading rather than perpendicular to the load. It is expected that the tack welds along the end of the connection will crack through the weld throat rather quickly and not play a significant role in the fatigue life of the connection. Nevertheless, this factor was examined.

Lastly, the role of nominal stress range on the "lightly" bolted joint is examined. The fatigue resistance of a connection with tack welds is often anticipated to be Category E. Hence, to evaluate overall cyclic performance, two different stress range levels are examined: one at about 20 ksi, which is likely in the finite-life region, and one at about 12 ksi, which is just above the endurance limit for a Category C detail. This provided a range of values from which the fatigue resistance could be evaluated and compared. Table 1 shows the test matrix for the tack weld test program. Here 'MP' denotes a modified position tack weld specimen where the leading line of tack welds is shifted such that the tack weld toes are in line with the center of the adjacent bolt holes. 'FT' indicates a specimen where the bolts are fully tightened along with the welds being in the modified position.

An R ratio of 0.1 was used to calculate loads to be applied for the different stress ranges. The R ratio is simply the ratio of the minimum stress to the maximum stress, and a positive value indicates that the stresses are of the same sign. In the test specimens being tested, both the minimum and maximum stresses are tensile. The tack welds are about a quarter of an inch in size. Normal length welds are about an inch in length, while longer welds are about 1.5 inches in length.

A 4-pole MTS servo-hydraulic test fixture is used to cyclically load the specimens. Two grip plates and two lap plates are used to grip the tack weld specimen. The grip plates fit into the grips of the MTS controller. The tack weld assembly, along with the dimensions of specimen plates and grip plates, is shown in Figure 6. All bolts on the assembly are fully tightened, except for the ones on the tack weld specimen. When replacing a specimen, only the bolts holding the specimen plates at the top and bottom in the assembly need to be loosened. The old specimen can then be slid out and replaced with a new specimen. A Campbell CR5000 Data Acquisition System was used to record the strains from the strain gages attached to some of the specimens, including the initial specimen. The strain gage readings were utilized to measure the stress distribution across the plates and the stress range near the weld toe. A photograph

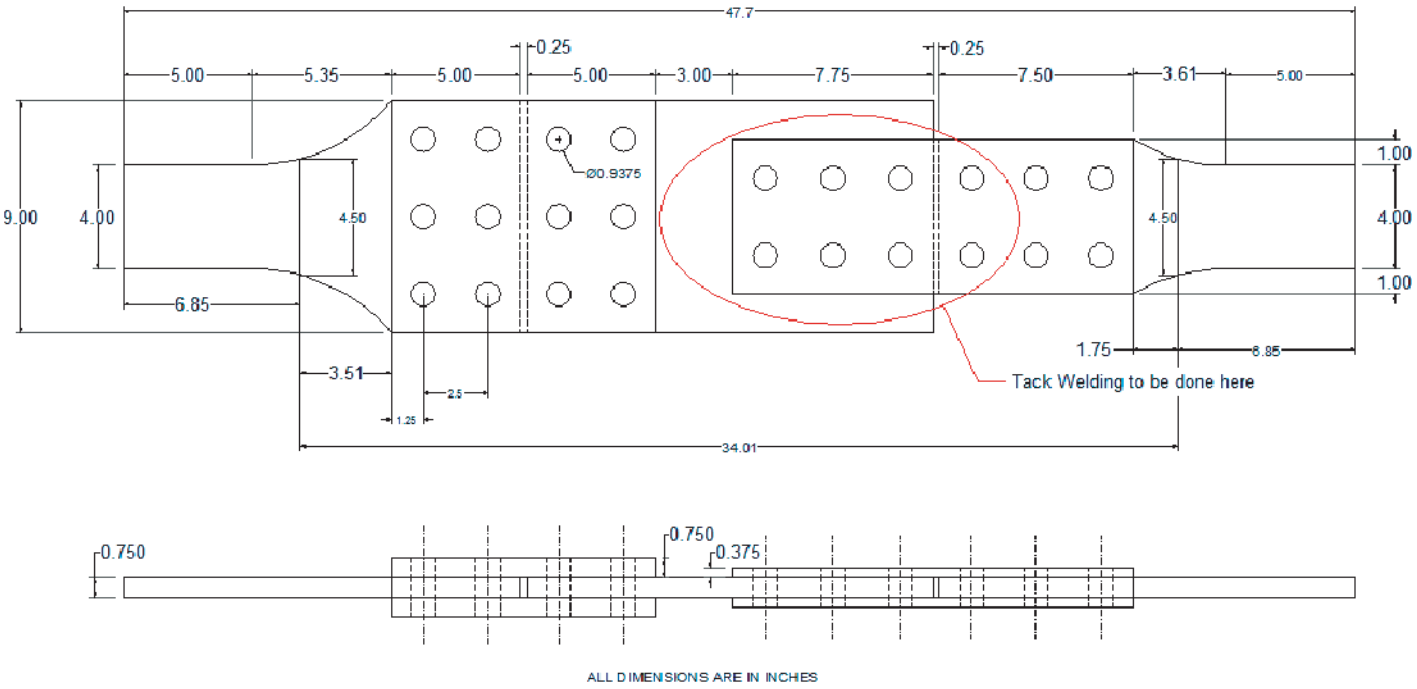

Figure 6. Tack weld test assembly (specimen shown is circled).

(a) (b)

Figure 7. Tack weld specimen in a 4 pole MTS servo-hydraulic actuator.

of the specimen fitted into the hydraulic grips along with the entire test setup is shown in Figure 7.

Distortion-Induced Fatigue Tests

One problematic condition that has not been well studied is the retrofit details for connections that exhibit distortion-induced cracking. A majority of fatigue cracks detected in steel bridges belong to this category. Several different methods have been used to repair these cracked details. In general, these include repairs that either stiffen the detail or make it more flexible.

Distortion-induced cracks often form at the end of vertical connection plates that are attached to the web of a girder, but not attached to the girder tension flange. Out-of-plane forces are developed in the cross frame members when one bridge girder deflects a different amount than an adjacent girder. The cross frame members are typically attached to the vertical connection plate, introduce pumping of the web region, and tend to develop out-of-plane stresses that combine with in-plane bending stresses. These elevated stresses can often lead to a premature cracking at the end of the weld to the vertical connection plate and/or the toe of the longitudinal weld attaching the web to the flange plate. A common retrofit used to prevent cracking at the end of the vertical connection plate is to use an attachment that is bolted to the vertical connection plate and to the flange of the girder. A variety of different attachment details are used to make this positive connection, including a WT section, a pair of angles, single angles, or a pair of plates that are welded together and then bolted to the girder flange and vertical connection plate. If the attachment is stiff enough, the out-of-plane stresses will be significantly reduced and the likelihood of distortion-induced cracking will be eliminated if it has not already occurred. However, the stiffness of the retrofit detail is critical. Connor and Fisher (2006) describe a situation where a retrofit detail with a small thickness was not fully effective in preventing further crack growth at a detail with distortion-induced fatigue cracking, while a thicker detail used elsewhere on the same bridge was effective in halting further crack growth. Clearly, the stiffness of the detail is quite important. But questions remain about determining the required stiffness to mitigate distortion-

induced fatigue cracking. Other than the experimental results reported by Fisher et al. (1990) in *NCHRP Report 336: Distortion-Induced Fatigue Cracking in Steel Bridges,* few data exist on the fatigue strength and performance of attachments used to repair distortion-induced cracking.

This subcomponent test involves testing a portion of a welded girder with a welded connection plate attached to the web. The cross section of the welded girder involves a section with a 34-in. × ⅜-in. web plate and 12-in. × 1-in. flange plates. These dimensions were intentionally selected to be very similar to the cross section dimensions used in *NCHRP Report 336.* The performance of the web region is evaluated by introducing a given displacement to the vertical connection plate. Since this type of a displacement occurs in an actual connection that experiences distortion-induced fatigue cracking, and because the large magnitude of the out-of-plane stresses developed when this transverse loading occurs, the subcomponent test is believed to be appropriate for studying the behavior of the web gap and the retrofit/repair details used in the web gap region.

It should be noted, however, that a limitation of the subcomponent test is that it does not effectively model primary bending stress that occurs parallel to the primary axis of the girder member. As cracks developed from distortion propagate away from the connection plate and begin to turn, then the influence of the primary bending stress would come into play. Nevertheless, it is believed that out-of-plane cracking behavior can still be effectively studied with the simple subcomponent test specimen.

The connection plate for an actual bridge structure would often be terminated short of the tension flange to prevent fatigue cracking at the plate to flange weld. This would result in a web gap between the end of the connection plate and the flange at one end only. However, for the subcomponent test, a web gap region exists at each end of the connection plate to obtain the greatest amount of possible information. Accordingly, two attachments are connected to the specimen, one at each end of the connection plate, which effectively allows for two tests to be conducted simultaneously (see Figure 8). The connection plate is loaded at two locations along the plate length. The dimensions for the test specimen subcomponent are shown in Figure 9.

The critical factors that are studied to examine their role on the repair of distortion-induced fatigue cracking include: the web gap size, the type of attachment detail, attachment thicknesses, magnitude of differential distortion, and attachment geometry.

The web gap for most of the WT specimens is 1.5 in., with two WT tests with a smaller web gap of 0.75 in. The 1.5-in. web gap corresponds to the web gap used in *NCHRP Report 336,* while a smaller value of 0.75 in. provides a more critical situation with greater out-of-plane stresses for the smaller gap.

Two of the WT specimens (labeled with an RH) were repaired with a drilled retrofit hole prior to installing the bolted retrofit detail to verify that the detail will fully arrest further distortion-induced cracking. Two additional WT specimens (labeled as B) were tested with a reduced number of bolts attaching the retrofit flange and web elements in order to study the influence of a reduced number of bolts on the effectiveness of the retrofit detail. Most of the retrofit details were tested with four bolts attached to each flange element and four bolts to the connection plate. For the "B" tests, however, only two bolts were used to attach the retrofit detail to the flange elements and to the connection plate. Variation of the number of bolts provides information on the importance of the connection stiffness on the fatigue performance.

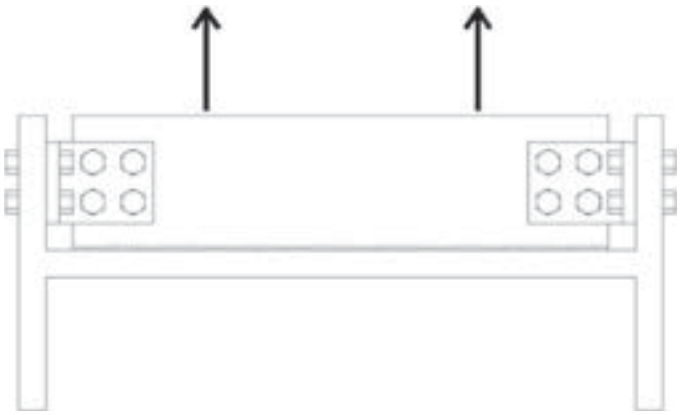

Figure 8. Subassembly unit with retrofit details installed.

The use of double-angle and single-angle retrofit specimens is also studied since there are situations where these details will be more convenient to use than a WT section due to geometric constraints, such as interference with a horizontal attachment plate or the elimination of the need to cut out part of the vertical connection plate to make the positive connection to the vertical plate. A smaller web gap is used here since it produces greater out-of-plane stresses and because this is an excellent example of where the angle(s) would simplify the retrofit since there will be no need to cut the vertical connection plate. Two different angle thicknesses were used to study the influence of detail stiffness.

A total of 13 subassembly tests were conducted, with two specimens per subassembly. Hence, a total of 26 specimens were tested that includes 14 WT retrofit specimens, 6 double-angle specimens, and 6 single-angle specimens. Two specimen web gaps of 0.75 in. and 1.5 in. were used, along with three different differential distortions. WT retrofit flange thicknesses tested were 0.5 in. and 0.75 in. Double angles of thicknesses of ⅝ in. and ¾ in. were tested. Single angles of thicknesses ¾ in. and 1 in. were tested. The test matrix for the distortion test program is given in Table 2.

Pre-cracking the specimens was found to range from 1.5 to 3.5 million cycles at a loading frequency of 4 Hz. Hence,

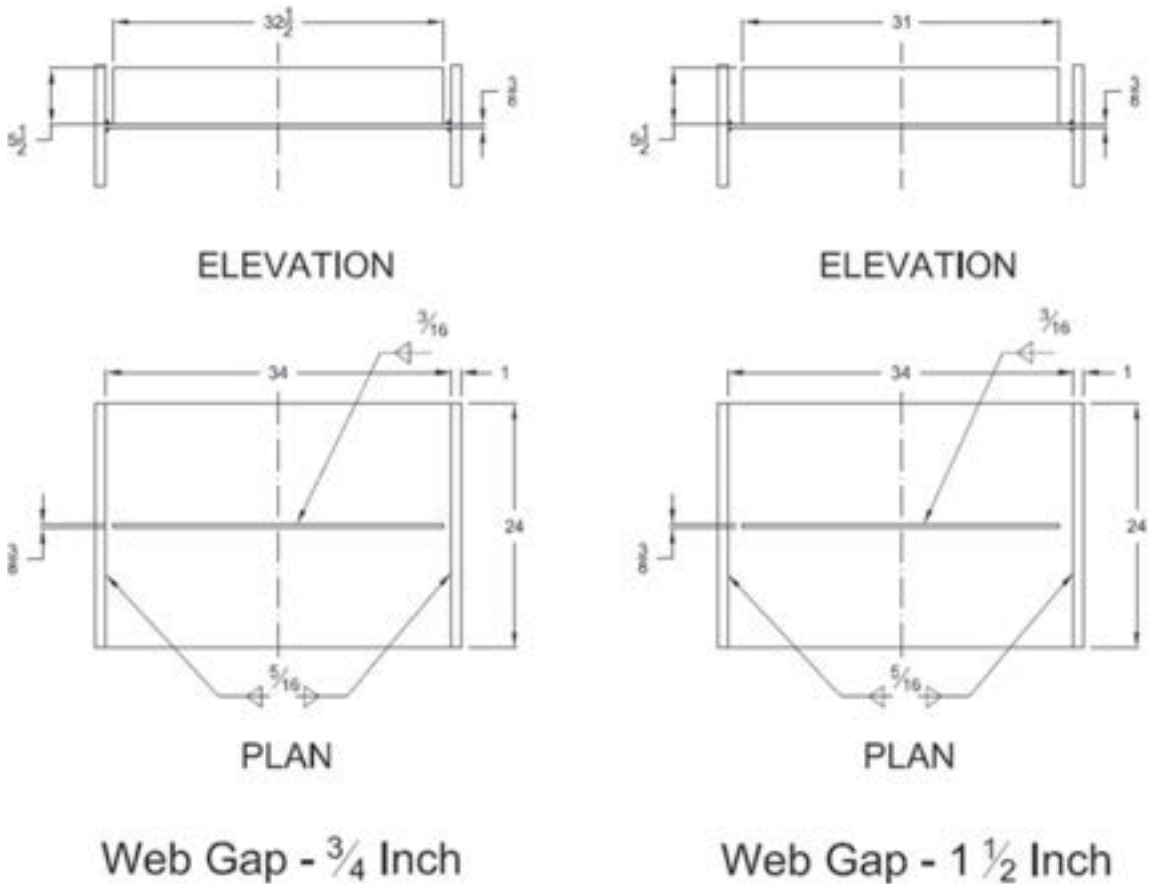

Figure 9. Top and side view of subcomponent test specimen.

Table 2. Test matrix for the distortion test program.

Connection Type	Detail Thickness (in.)	Differential Distortion, 0.01 in.		Differential Distortion, 0.02 in.	
		Web Gap, ¾ in.	Web Gap, 1-½ in.	Web Gap, ¾ in.	Web Gap, 1-½ in.
WT	1/2		X		X
			X		X
	3/4	X	X		X
		X	X		X
			X(RH)		
			X(RH)		
			X(B)		
			X(B)		
		Differential Distortion, 0.0075		Differential Distortion, 0.01	
DA	5/8	X		X	
		X		X	
	3/4	X			
		X			
SA	3/4	X		X	
		X		X	
	1	X			
		X			

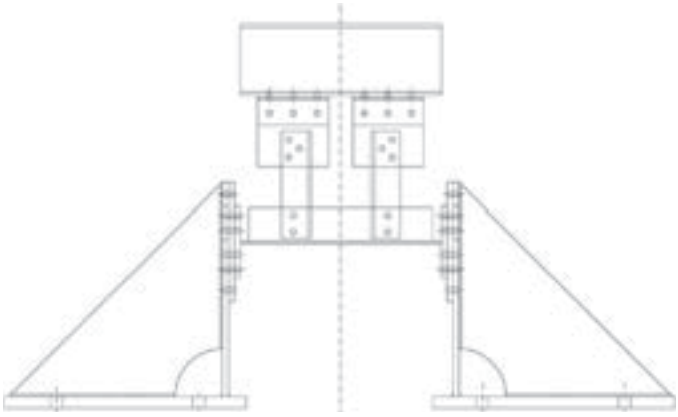

Figure 10. Test specimen mounted in test jig attached to strong floor.

in order to speed up the time required for testing, two test setups were used. A schematic of Test Setup 1 is shown in Figure 10. The top of the loading spreader beam is attached to a 220-kip capacity MTS servo-hydraulic actuator. The spreader beam is attached to a pair of angles that pulls on the specimen stiffener at two points while the specimen flanges are firmly bolted to the side supports. In between the flange and the side support is an extra plate which accommodates different bolt hole patterns for the retrofits to be tested without having to change the side supports. Test Setups 1 and 2 for the distortion tests are shown in Figure 11. Test Setup 2 is similar to Test Setup 1 except that concrete supports have been used to hold the specimen instead of steel supports. Also, a 55-kip capacity MTS servo-hydraulic actuator was used, rather than the 220-kip capacity actuator used for Test Setup 1.

The distortion of the stiffener was measured with an MTS clip-on gage. An aluminum attachment was fabricated so that the clip gage can be attached and held in position. The attachment, as shown in Figure 12, consists of two parts. The primary part sits on top of the specimen stiffener, reaching out horizontally over the specimen flange. It has a small steel knife edge at this end. The secondary part sits on top of the specimen flange and also has a small knife edge. This part will hold the clip gage in place during the test. The clip gage can latch on to the two knife edges, which effectively measures the deformation between the flange and the stiffener edge. The actuator can then pull on the stiffener according to the

(a)

(b)

Figure 11. Distortion test setups 1 and 2.

(a) (b) (c)

Figure 12. MTS clip-on gage fitted in aluminium attachment.

measured clip gage reading, and thereby control relative distortion of the web gap between the stiffener and the flange.

In order to evaluate the effectiveness of the clip gage in measuring the distortion of the stiffener, Linear Variable Differential Transformers (LVDTs) with a range of ±0.05 in. were used on the test specimen as shown in Figure 13. These LVDTs give a more accurate estimate of the actual distortion occurring in the stiffener-to-web weld toes at the two ends of the specimen.

The tests were initially planned to be run in distortion control with the help of the clip gage. This was achieved successfully, but the maximum frequency at which the test could be run was unsatisfactory. Hence the tests were instead run in a pseudo-distortion control, where force control was primarily employed, but the force was adjusted based on the monitoring of the resultant distortion, such that a nearly constant distortion was always maintained. The tests were mostly run at a frequency of 4 Hz.

The testing procedure involves running the test initially in pseudo-displacement control to initiate a distortion-induced fatigue crack that is about ½ to 1 in. long on each side of the vertical connection plate. At this point, holes are drilled through the specimen flange to install the retrofit at both ends of the vertical connection plate. It should be noted that the fatigue cracks in the web were not treated by drilling a stop hole to remove the fatigue crack tip. Although this would normally be done as recommended normal practice, it was not done in these tests so that the effectiveness of the retrofit detail repair could be assessed, even if the crack tips were not first blunted. (Note: stop holes were drilled for two retrofit specimens—labeled as RH—to assess expected normal practice.) The required initial load for cracking the specimen is roughly doubled, and the loading is resumed in force control. Since the retrofits are rigidly attached to the ends of the stiffener, force control also corresponds to a fixed amount of distortion at the ends of the specimen. The

(a) (b)

Figure 13. Linear variable differential transformers (LVDTs).

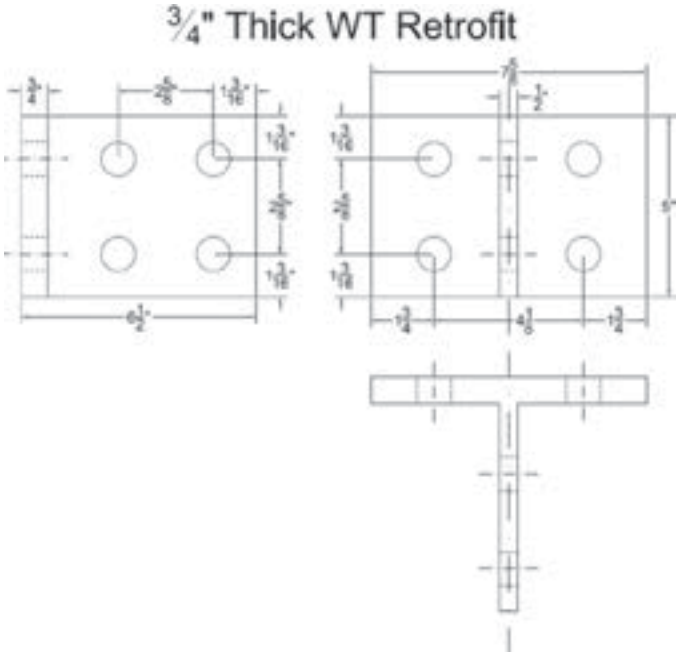

Figure 14. Typical WT retrofit bolt pattern.

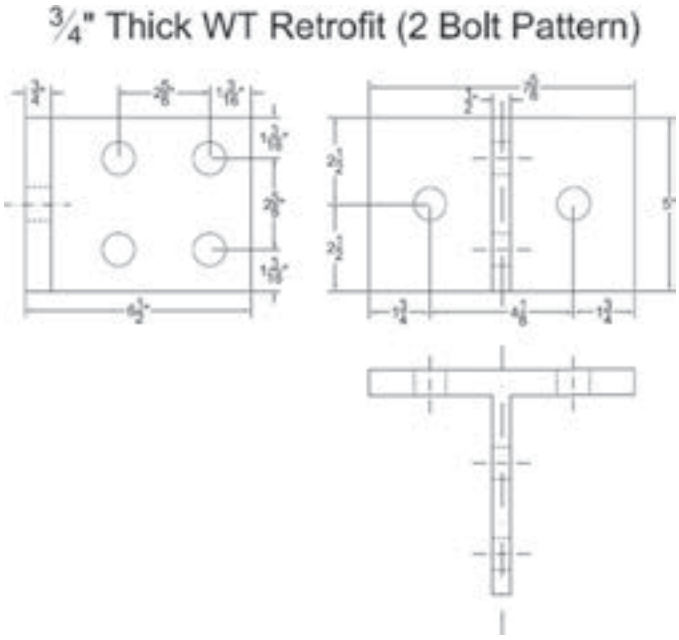

Figure 15. Two bolt WT retrofit pattern.

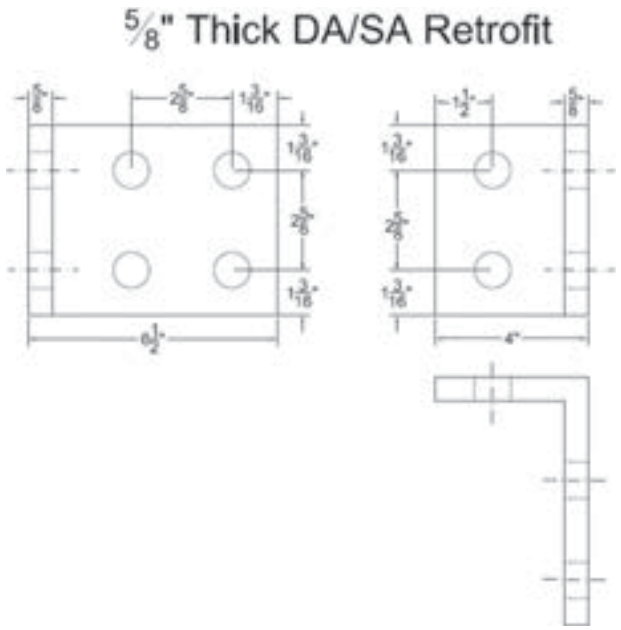

Figure 16. Typical double-angle/single-angle retrofit bolt pattern.

loading is continued until failure or completion of 5,000,000 loading cycles. At this point, the specimen is removed in order to examine any fatigue cracks to determine if the retrofit was effective in significantly slowing or halting further fatigue crack growth.

Strain gages were attached to the loading angles to measure the stress flowing through the angles. This is necessary to ensure that the load is being equally distributed to both ends of the specimen and also to observe the change in the distribution of load as fatigue cracks form at the ends of the specimen. The strains were recorded using a Campbell CR5000 Data Acquisition System. Strain gages were also attached to the initial specimen and some of the retrofits to measure the stress range at critical locations of interest.

Figure 14 shows a typical bolt pattern for a WT retrofit. The holes used in all retrofits have a diameter of 15/16 in. Figure 15 shows the bolt pattern for a 2 bolt WT retrofit. Figure 16 shows the typical bolt pattern for double-angle or single-angle retrofits.

CHAPTER 3

Findings and Applications

As described in the previous chapter, individual items in Section 7 that were identified for revision were examined. This chapter presents the results of the examination of the items. Also included are the details of finite element analysis carried out for the experimental tests as well as the results of experimental testing for tack weld and distortion-induced fatigue tests.

S-N Curve

Data regarding long cyclic life behavior are provided in *NCHRP Report 354* (Fisher et al., 1993) for three different types of welded details: partial-length cover plates, web attachments, and transverse web stiffeners. The results were found to support the conservative design assumption that a straight-line extension of the fatigue resistance curves can be used to predict fatigue lives with variable life loading. This was believed, however, to be overly conservative for higher strength details such as transverse stiffeners.

The test results from *NCHRP Report 336* (Fisher et al., 1990) for distortion-induced fatigue strength of transverse connection plates were used to compare the AASHTO and Eurocode S-N curves specified for this detail. For normal stress ranges, the Eurocode stipulates 14 detail categories for fatigue instead of the 8 stipulated by AASHTO. Each Eurocode detail category is designated by a number which represents, in N/mm^2, the reference value for the fatigue strength at 2 million cycles. When test data were used to determine the appropriate detail category for a particular constructional detail, the value of the stress range corresponding to 2 million cycles was calculated for a 75% confidence level of 95% probability of survival for log N, taking into account the standard deviation and the sample size and residual stress effects. The Eurocode S-N curves use a slope of 3 for up to 5 million cycles where the corresponding stress range is the CAFL for that curve. From 5 million cycles to 100 million cycles, a slope of 5 is used, and the stress range corresponding to 5 million cycles is the cutoff limit for the curves. Eurocode classifies vertical stiffeners welded to a beam or plate girder as detail category 80 while AASHTO classifies the details as Category C. Figure 17 shows the comparison of the test data with the Eurocode detail category 80 S-N Curve and AASHTO detail category C (CAFL: 10 ksi). The AASHTO S-N curve has been extended below the CAFL up to the variable amplitude fatigue limit (VAFL), which is half the CAFL.

As can be seen from the figure, the AASHTO S-N curve is also a reasonable curve for the distortion-induced fatigue cracking at ends of transverse connection plates, even in the long-life region. On comparison with the Eurocode S-N curve, the AASHTO S-N curve seems to equally fit the test data in the long-life region, where the Eurocode S-N curve changes its slope from 3 to 5. Changing the nature of the current AASHTO fatigue curves from linear to a more bi-linear slope would considerably increase the effort required in calculation of fatigue life. Neither does it seem that adopting a bi-linear slope can considerably increase the accuracy in prediction of fatigue life in the long-life region. The test data examined here also do not seem to justify the need to change the nature of S-N curves. Hence, it was decided to not change the linearly varying nature of the current S-N curves and keep them as they are.

Validation of AASHTO Fatigue Truck

An analysis was performed using WIM data collected from randomly selected states, sites, truck traffic volumes, and recording months. This investigation using the analysis results was aimed at better understanding whether the AASHTO fatigue truck reasonably models the real load and, if not, how to improve this model. The analysis results are gathered in Appendix B.

As seen in Appendix B, WIM data from the states of California, Florida, Idaho, New York, Michigan, Texas, and Vermont were used in this analysis. The road configuration

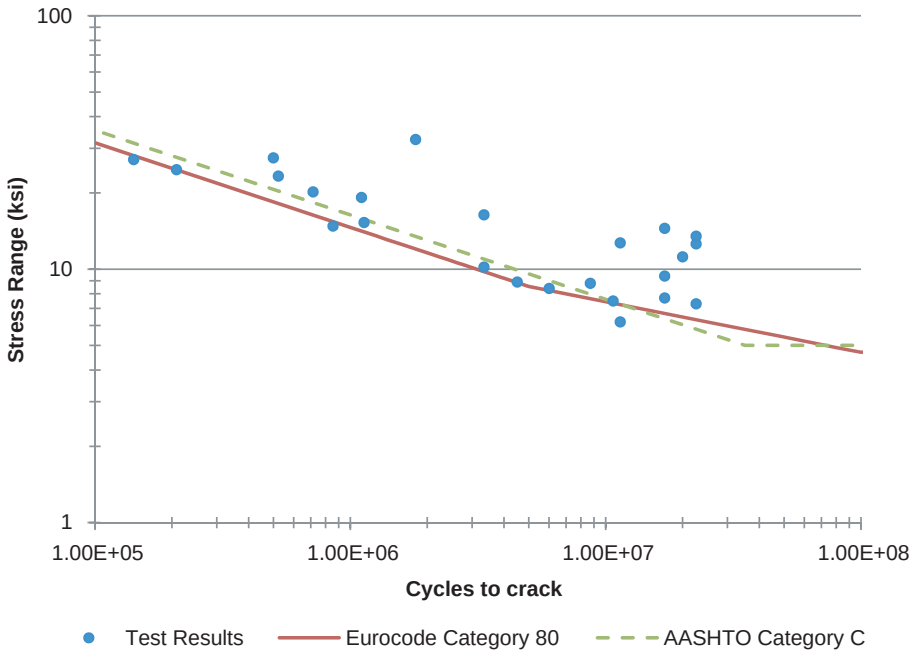

Figure 17. Comparison of test data with AASHTO and Eurocode S-N curves.

varied from 2 to 4 lanes of truck traffic in the same direction. Some states provided more cases with a varied number of lanes than others. The ADTT per lane of these sites varied from tens of trucks (61) to thousands (4,703). Please note that these ADTT values are averaged over the number of lanes recorded, used here merely as an indicator, while the real ADTT on each lane can vary more notably. Among different lanes at the same site, the truck traffic distribution can be quite uneven. One lane may have as much as 86% of the total truck traffic, compared to another lane with as little as 4%. Therefore the actual ADTT of each lane (not the averaged ADTT per lane) can vary much more significantly than from 61 to 4,703.

The figures gathered in Appendix B use one common quantity on the vertical axis. It is the quotient of the WIM truck load effects summed according to Miner's law and the corresponding AASHTO fatigue truck's load effect. If the ratio is larger than 1, it means that the AASHTO model underestimates the real fatigue load effect. Otherwise if the ratio is below 1, then the model over-estimates the real fatigue load effect.

As seen in the results shown in Appendix B, it was very difficult to conclude whether the AASHTO fatigue truck model over-estimates or underestimates the true loading effect or condition. In other words, the AASHTO model sometimes goes one way and at another time the other way. Higher ADTT values do not necessarily lead to a higher fatigue load effect, apparently relevant to what truck configurations (axle loads, axle distances, etc.) are more common at a particular site.

Given this observation, there have not been obvious reasons and motivation to recommend a new model to better describe the fatigue load effect than the current AASHTO fatigue truck, although the latter's lack of realistic modeling is obvious. At this point, it is recommended or further emphasized, as done in Section 7 of the AASHTO MBE, that WIM data gathered at or near a particular site with well maintained and calibrated equipment is clearly the most reliable data to be used for fatigue load effect estimation.

Multiple Presence Factor

The present study uses WIM data to derive the multiple presence factor (MPF). A large amount of WIM truck weight data is used to simulate and model the behavior of trucks and their load effects in bridge components. This data set provides a reliable basis for the MPF recommended in this report for steel bridge fatigue evaluation. In general, longer spans allow more trucks to be simultaneously present on the span, higher truck traffic volumes increase the probability of such simultaneous presence, and more lanes available reduce such likelihood. The proposed MPF is thus given as a function of these three major causal factors: span length, ADTT, and number of lanes.

To fully understand the behavior of truck load effects in bridge components, this study also has used a new truck-by-truck analysis approach to develop raw data of MPF. These data events are then used to perform regression analyses for developing the proposed MPFs as functions of the identified causal factors.

Concept of Multiple Presence Factor

For strength limit states, MPF is intended to facilitate estimation of the load effect in a structural component due to all truck loads on the span, with reference to the load effect in the same component due to only one lane of truck load. Therefore, MPF for evaluation is formulated similarly as follows:

$$\text{MPF} = \frac{\text{N-Lane Load Effect in Component}}{\text{One-Lane Load Effect in Component}} = \frac{\text{LE}_{\text{total}}}{\text{LE}_{\text{onelane}}} \quad (3)$$

where LE stands for load effect. The subscript "total" indicates the total load effect due to trucks in all the lanes on the bridge, and "onelane" indicates the total load effect due to only one lane of truck load.

The fatigue load effect is modeled herein using the Miner's law assuming linear accumulation of fatigue damage:

$$\frac{\text{LE}_{\text{total}}}{\text{LE}_{\text{onelane}}} = \frac{\sqrt[3]{\sum \text{f}_i \ \text{LE}_{\text{i\_total}}^3}}{\sqrt[3]{\sum \text{f}_j \ \text{LE}_{\text{j\_onelane}}^3}} \quad \text{i} = 1,2,3,\ldots;\ \text{j} = 1,2,3,\ldots \quad (4)$$

The LE_{total} in the numerator is the fatigue load effect of all trucks on the span in all lanes available. $\text{LE}_{\text{i\_total}}$ here is the total fatigue load effect of the ith load event (i.e., the ith platoon of trucks) in the WIM data, and f_i is the frequency or probability of load event i. Similarly, $\text{LE}_{\text{onelane}}$ in the denominator is the fatigue load effect of trucks in the driving lane. $\text{LE}_{\text{j\_onelane}}$ is the load effect of trucks in load event j (i.e., the jth platoon of trucks) in the driving lane, and f_j is its frequency. This definition of MPF in Equations 3 and 4 will allow convenient estimation of load effects from all lanes by multiplying MPF with one lane's load effect. The latter can be practically obtained and commonly performed using the WIM technique available with state transportation agencies throughout the United States.

In each load effect event (or truck platoon) i or j, there can be one or more trucks on the span contributing to the load effect in the bridge component. The superposition of two or more load effects of these trucks needs to cover two perpendicular directions. One is the traffic or longitudinal direction and the other the perpendicular or transverse direction. The former can be done using influence lines and the latter needs to consider lateral distribution of load effect to the interested bridge component. The superposition along the longitudinal direction is performed here based on the headway distance between the trucks on the span, with reference to the corresponding load effect's influence line. Both $\text{LE}_{\text{i\_total}}$ and $\text{LE}_{\text{j\_onelane}}$ need to include this superposition as deemed appropriate. On the other hand, only $\text{LE}_{\text{i\_total}}$ needs to consider lateral superposition to include trucks in different lanes. This effect is modeled accordingly as follows:

$$\text{LE}_{\text{i\_total}} = \text{DF}_1\text{LE}_{\text{i1}} + \text{DF}_2\text{LE}_{\text{i2}} + \text{DF}_3\text{LE}_{\text{i3}} + \text{DF}_4\text{LE}_{\text{i4}} \quad (5)$$

and also,

$$\text{LE}_{\text{j\_onelane}} = \text{DF}_1\text{LE}_{\text{j1}} \qquad (\text{LE}_{\text{j1}} = \text{LE}_{\text{i1}}) \quad (6)$$

where LE_{i1} to LE_{i4} are respectively load effects of trucks in Lanes 1 to N, up to all the available lanes. In this study, the maximum N is 4 because only up to 4 lanes of simultaneously recorded WIM data are available, although the concept can be extended further to more lanes. Note that LE_{i1} to LE_{i4} include longitudinally superimposed load effects in the respective same lanes. DF_1 to DF_4 in Equations 5 and 6 are lateral distribution factors to distribute loads in Lanes 1 through 4 to the focused bridge component.

For computation convenience, Equation 5 is rewritten as

$$\text{LE}_{\text{i}} = \text{DF}_1\left(\text{LE}_{\text{i1}} + \frac{\text{DF}_2}{\text{DF}_1}\text{LE}_{\text{i2}} + \frac{\text{DF}_3}{\text{DF}_1}\text{LE}_{\text{i3}} + \frac{\text{DF}_4}{\text{DF}_1}\text{LE}_{\text{i4}}\right) \quad (7)$$

In Equation 4, both the numerator and denominator have DF_1 as a factor. It will then be cancelled. Thus, only the ratios $\frac{\text{DF}_2}{\text{DF}_1}$, $\frac{\text{DF}_3}{\text{DF}_1}$, and $\frac{\text{DF}_4}{\text{DF}_1}$ in Equation 7 are needed for the analysis defined in Equations 3 and 4. These ratios indicate the relative weights of load in Lane k to Lane 1 (for k=2, 3, or 4) in load distribution. The following values of these ratios are used in this study, based on a review of available research results for a variety of highway bridge types and span lengths (AASHTO 2010, BridgeTech et al. 2007, Zokaie et al. 1991). Their possible variation is discussed in the following section on Sensitivity Analysis and given as:

$$\text{For 2-lane spans,} \quad \frac{\text{DF}_2}{\text{DF}_1} = 0.45 \quad (8)$$

$$\text{For 3-lane spans,} \quad \frac{\text{DF}_2}{\text{DF}_1} = 0.40; \quad \frac{\text{DF}_3}{\text{DF}_1} = 0.15 \quad (9)$$

$$\text{For 4-lane spans,} \quad \frac{\text{DF}_2}{\text{DF}_1} = 0.40; \quad \frac{\text{DF}_3}{\text{DF}_1} = 0.15; \quad \frac{\text{DF}_4}{\text{DF}_1} = 0.0 \quad (10)$$

Note that in the AASHTO MBE (2011) only one lane of loading is specified to be considered for the fatigue limit state evaluation. For longer spans and higher ADTTs, this approach apparently underestimates fatigue damage accumulation since more trucks are likely to be present on the span other than just Lane 1 or driving lane. Using MPF defined in Equation 3 will simplify analysis in bridge design and evaluation for these cases, by simply multiplying one lane load effect with N and MPF to obtain the total fatigue load effect. It will help estimate more reliably fatigue load effect, especially in fatigue evaluation of steel bridges for more reliable remaining life prediction. This will be particularly true

for two-girder-, two-truss-, and two-arch-systems, where each primary member needs to carry all the lanes (as opposed to multiple beams carrying several lanes so that some beams do not participate in carrying certain lanes at all). Note that current AASHTO specifications unconservatively ignore loads from lanes other than the shoulder lane.

Analysis Overview and WIM Data Used

The MPF proposed herein is developed using WIM data from California, Oregon, Michigan, and New York, related to span length, ADTT, and number of lanes. These states are the only ones found to have truck weight data with a time stamp of 0.01 second, the highest resolution available for WIM data. This high time stamp resolution allows identification of two trucks' headway distances as short as 1 ft at a speed of 70 miles per hour. This resolution therefore permits an accurate and reliable estimation of the additional load effect of another truck on the same span but in a different lane when two trucks are close to each other longitudinally.

The 2-lane, 3-lane, and 4-lane situations are analyzed separately using WIM data from these states. A total of 18.1 million trucks over 161 months from 17 sites is used for the case of 2-lane spans, 22.2 million trucks over 137 months from 13 stations for 3-lane spans, and 27.4 million trucks over 138 months from 13 sites for 4-lane spans. Simple spans have been included in this effort of developing MPF. The ADTT ranged from 777 to 8,421 for 2-lane, 740 to 10,734 for 3-lane, and 671 to 12,816 for 4-lane roadways. The WIM data were selected to cover a realistic range of ADTT, especially the high end where MPF is significant and more critical. The data were scrubbed first before the analysis, and typically less than 4% of the recorded data were eliminated when an apparent inconsistency was seen.

For the case of fatigue limit state, each month of WIM data is used to produce one point of MPF value as defined in Equation 3. A total of 8 span lengths (30, 50, 70, 100, 130, 160, 190, and 220-ft) has been analyzed to produce data points for the subsequent regression analysis. The resulting regression relation of MPF to the causal factors is proposed in Equation 11 for estimating the total fatigue load based on one lane of load effect. It is derived using MPF values for the WIM data from four states discussed previously, with an R^2 of 0.73.

$$\text{MPF} = 0.988 + 6.87 \times 10^{-5} \text{ span length} + 4.01 \times 10^{-6} \text{ ADTT} + 1.07 \times 10^{-2} / \text{N} > 1 \quad (11)$$

For both midspan moment and support shear, Figures 18 through 23 display comparisons of the regression relation in Equation 11 and the computed MPF values according to Equation 3 for three cases of number of lanes (N=2, 3, and 4) and three cases of simple span lengths (30, 100, and 220 ft) over a range of observed ADTT. Most MPF values are clustered near 1.0, and it would be difficult to see their behavior for the different number of lanes N. The figures were therefore plotted with the MPF value divided by the number of lanes of traffic N, so that the influence of traffic lanes could be displayed. As seen, the regression line or the recommended MPF fits very well with the observed values for the practically representative ranges of the parameters.

Sensitivity Analysis

As discussed in the previous section on the distribution factor ratios defined in Equations 8 through 10, these ratios may vary depending on a number of factors, such as type of deck (concrete deck, timber deck, whether composite or non-composite with the supporting members, etc.); type of deck supporting system (concrete beams, steel beams, pre-stressed concrete beams, etc.); aspect ratio of deck (width to length ratio), and so on. To understand the effect of possible variation in the distribution factor ratios, each of the ratio values in Equations 8 through 10 is individually varied by an amount of −0.05, 0, and +0.05. This range of variation is considered to be realistic for highway bridges in the United States. As a result, a total of 36 cases of analysis for the WIM data are repeated, and the resulting MPF values are compared with the regression result, as shown in Figures 18 through 23. They exhibit no significant deviations from the recommended regression lines. Thus, Equation 11 is accepted as robust for general application.

Negative Remaining Life

As discussed in Chapter 2, one of the serious practical issues with current Section 7 of the AASHTO MBE (2011) is that there are no provisions for the situation of negative remaining life resulting from calculation, even though field inspection has observed no fatigue cracking for the particular steel connection detail in the bridge. This situation is illustrated in Figure 24, duplicated here from Chapter 2.

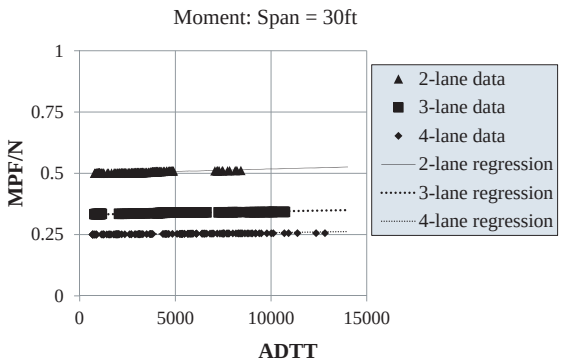

Figure 18. Comparison of proposed MPF and computed MPF using WIM data divided by number of lanes (midspan moment in 30ft span).

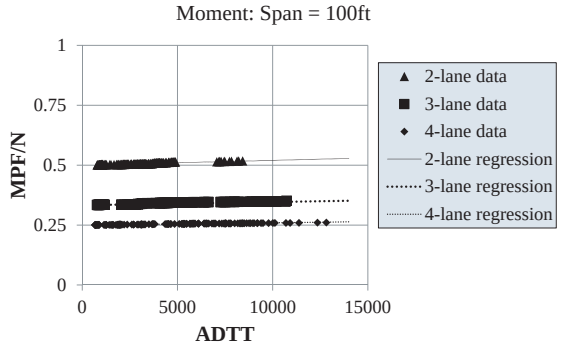

Figure 19. Comparison of proposed MPF and computed MPF using WIM data divided by number of lanes (midspan moment in 100ft span).

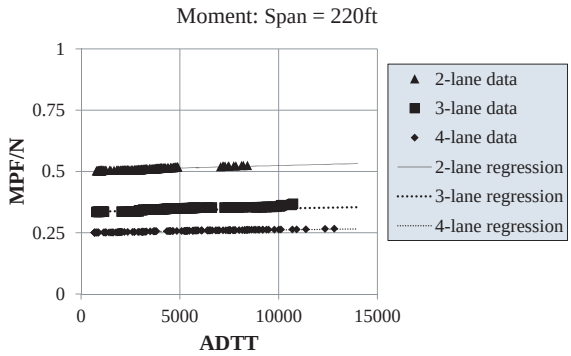

Figure 20. Comparison of proposed MPF and computed MPF using WIM data divided by number of lanes (midspan moment in 220ft span).

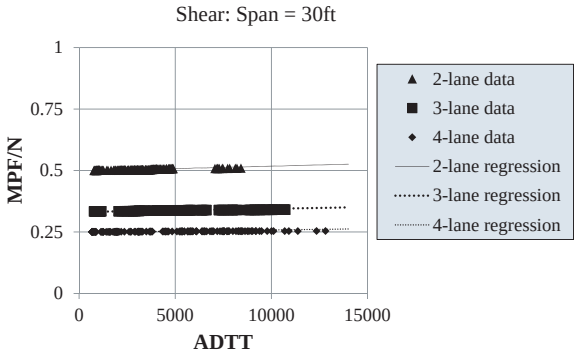

Figure 21. Comparison of proposed MPF and computed MPF using WIM data divided by number of lanes (shear in 30ft span).

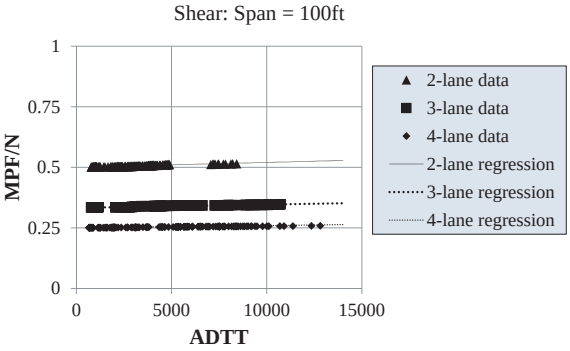

Figure 22. Comparison of proposed MPF and computed MPF using WIM data divided by number of lanes (shear in 100ft span).

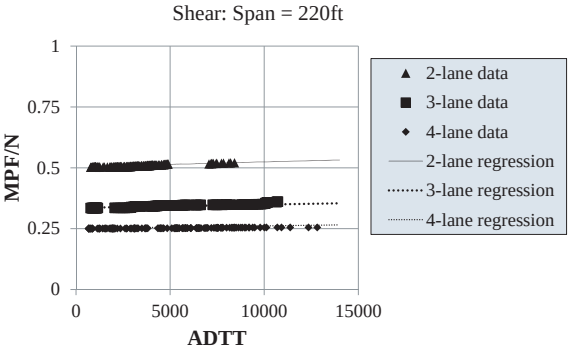

Figure 23. Comparison of proposed MPF and computed MPF using WIM data divided by number of lanes (shear in 220ft span).

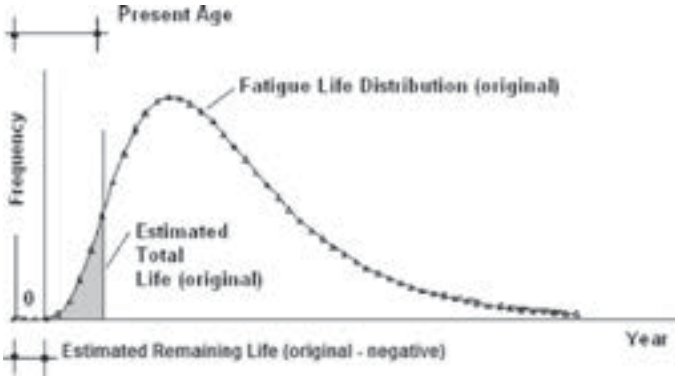

Figure 24. Negative remaining life resulting from uncertainty in fatigue life estimation (shaded area is equal to targeted failure probability).

As illustrated, the real fatigue life of the detail is a random variable, expressed using the curve of probability distribution with little triangle symbols. The total life estimated according to the AASHTO MBE (2011) is a deterministic value, as the right boundary of the shaded area as the target failure probability. In other words, the probability of the real life being smaller than this value is controlled to be under the targeted (acceptable) risk level expressed using the target reliability index. Due to conservative approach, the estimated remaining life ends at the left side of the origin, being negative. When it is known that no fatigue cracking has been identified at the detail, this information can be taken into account in the evaluation process to help reduce the uncertainty so that the evaluation result will better reflect the reality. This concept is illustrated in Figure 24.

Figure 25 continues from the situation in Figure 24, with the same original fatigue life distribution using the same symbol of little triangles on the curve. Given the fact that the detail has not failed (cracked), the possibility of the total life being shorter than the present age is excluded. As expressed in Figure 25, this elimination is modeled using truncation of the original probability distribution at the value of present age. The total area under the truncated curve will be less than 1.0 due to the truncation. Thus, the remaining curve beyond the present age is increased proportionally by dividing it by $1 - p_{truncated}$, where $p_{truncated}$ is the truncated area or truncated probability. The resulting curve is shown in Figure 25, named fatigue life distribution (updated).

In addition, the estimated total life of the detail can be updated using the same concept of controlling the failure probability or calibration, according to the updated fatigue life distribution. Namely, the total life computed as a deterministic value resulting from the evaluation process will be so determined such that the real life which is less than that value is controlled to be within the acceptable risk. Figure 26 indicates this updated total life as a point on the abscissa to the right of the truncation location or present age. The difference between the two values is then the updated remaining

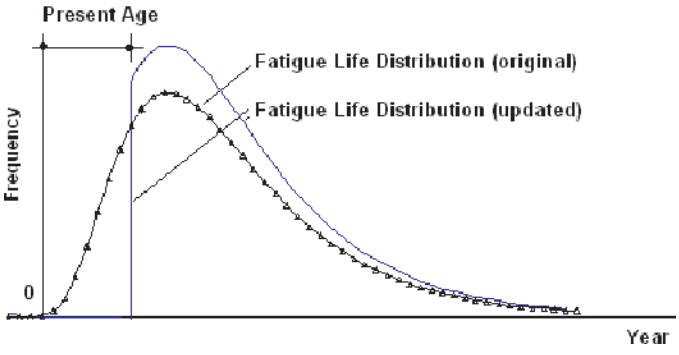

Figure 25. "No fatigue cracking observed" modeled by truncated fatigue life distribution.

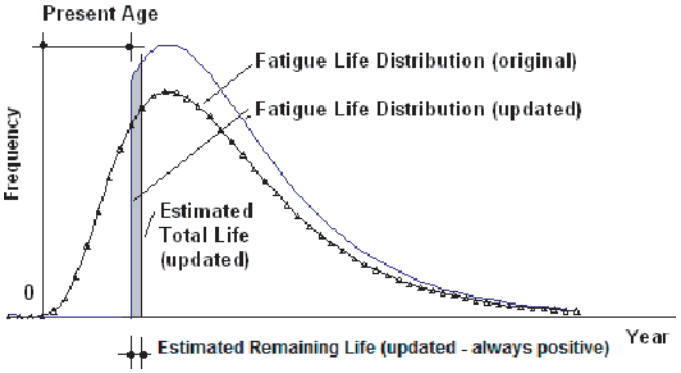

Figure 26. Updating remaining life estimation using updated fatigue life distribution (shaded area is equal to targeted failure probability).

life aimed as the evaluation result, also indicated in Figure 26. The shaded area in Figure 26 is to be made equal to the targeted failure probability corresponding to the target reliability index, also equal to the shaded area in Figure 24, since the same target reliability index is used in both calibration processes. This determination process is a high level of calibration taking into account the *in-site* information of no failure, or even detail cracking, observed for the detail.

Note also that this truncated distribution model has been used in a research effort to calibrate bridge proof load factors for load rating (Fu and Tang 1995), where the bridge capacity's distribution is truncated at the proof load level since the possibility for it to be below that level has been eliminated.

As seen in Figure 26, since the truncation is done at present age which is always positive, the updated estimated remaining life will be accordingly always positive. This will eliminate negative remaining life results when no cracking is observed in the field. Obviously, if no such field inspection result is available, a negative estimated remaining life may still result as illustrated in Figure 24. Such a result should indicate the need for further information, including but not limited to: field detail condition (whether cracked or not and possibly workmanship); WIM data for the site (for information on the load); stress range measured for the detail (more information on the load effect); and so on. The information specific for the particular detail will help reduce the random variation, or make the distribution curve in Figure 24 "narrower" so that the total life estimation will become less uncertain and more credible.

NCHRP Report 299 (Moses et al. 1987) provides the calibration basis for the current AASHTO MBE (2011). Consequently, the following information is used in determining the distribution in Figures 24 through 26:

Lognormal distribution with
Mean = 2.19 Y_{mean}
Coefficient of Variation = 0.84

Therefore, the truncated probability P at Y = a = current age is

P = probability of fatigue life being shorter than current age before updating based on no crack found

$$= \Phi\left[\frac{\mathrm{Ln}\left(\frac{a}{2.19Y_{mean}}\right)+0.27}{0.73}\right] \quad (12)$$

As discussed, the updated fatigue life Y′ is the one that leads to the same target reliability index β:

$$\Phi(-\beta) = \frac{\Phi\left[\frac{\mathrm{Ln}\left(\frac{Y'}{2.19Y_{mean}}\right)+0.27}{0.73}\right]-P}{1-P} \quad (13)$$

Y′ is then solved from the above equation as

$$Y' = 2.19Y_{mean}e^{0.73\Phi^{-1}[\Phi(-\beta)(1-P)+P]-0.27} \quad (14)$$

to be the updated fatigue life that will not lead to negative remaining fatigue life. In the revised Section 7 of the AASHTO specifications, four different levels of nominal fatigue life are used corresponding to four different levels of fatigue evaluation reliability, i.e., β values. The equations derived corresponding to these levels of fatigue evaluation reliability are as follows:

$$Y'_{mean} = 2.19Y_{mean}e^{0.73\Phi^{-1}[0.18(1-P)+P]-0.27} \quad (15)$$

$$Y'_{evaluation\ 2} = 2.19Y_{mean}e^{0.73\Phi^{-1}[0.12(1-P)+P]-0.27} \quad (16)$$

$$Y'_{evaluation\ 1} = 2.19Y_{mean}e^{0.73\Phi^{-1}[0.074(1-P)+P]-0.27} \quad (17)$$

$$Y'_{minimum} = 2.19Y_{mean}e^{0.73\Phi^{-1}[0.039(1-P)+P]-0.27} \quad (18)$$

R_R Factor

Section 7 of the MBE currently provides for three levels of finite fatigue life for estimation:

- Minimum expected fatigue life (which equals the conservative design fatigue life);
- Evaluation fatigue life (which equals a conservative fatigue life for evaluation); and
- Mean fatigue life (which equals the most likely fatigue life).

The desired fatigue life estimate is obtained by multiplying the resistance factor R_R times the detail category constant. A Table for the values of R_R corresponding to different levels of finite fatigue life is provided in the MBE as given in Table 3.

Table 3. Resistance factor for evaluation, minimum or mean fatigue life, R_R.

Detail Category	R_R		
	Evaluation Life	Minimum Life	Mean Life
A	1.7	1.0	2.8
B	1.4	1.0	2.0
B'	1.5	1.0	2.4
C	1.2	1.0	1.3
C'	1.2	1.0	1.3
D	1.3	1.0	1.6
E	1.3	1.0	1.6
E'	1.6	1.0	2.5

The accompanying commentary C7.2.5.1 explains that since much variability exists in the experimentally derived fatigue lives, a conservative fatigue resistance two standard deviations below the mean fatigue resistance or life is assumed for design. This corresponds to the minimum expected finite fatigue life given in the MBE. However, using the design-based finite fatigue resistance may be too conservative for fatigue evaluation purposes and, consequently, result in low fatigue lives. Hence, evaluation and minimum fatigue resistance curves have been provided, which are two and one standard deviations off the mean fatigue life S-N curves in log-log space, respectively. The probability of failure associated with each level of fatigue life approaches 2%, 16%, and 50% for the minimum, evaluation, and mean fatigue lives, respectively. The references for Section 7 include *NCHRP Report 299* (Moses et al. 1987) and other AASHTO specifications.

NCHRP Report 286: Evaluation of Fatigue Tests and Design Criteria on Welded Details by P. B. Keating and J. W. Fisher (1986) mentions that the initial AASHTO Fatigue Design Curves were derived from the linear regression analysis of the test data obtained in NCHRP Project 12-07 (*NCHRP Reports 102* and *147*) using the 95% confidence limits defining the lower bounds of the fatigue resistance for 95% survival. Keating and Fisher proposed to change the slope of all the design curves that existed then to a constant value of –3.0. Before this, all curves had slightly different slope values around –3.0. The proposed curves were developed using stress range intercept values at 2 million cycles. Hence, the earlier curves and the new curves have identical intercepts at 2 million cycles. In order to assess the adequacy of the new curves, the test data were compared with the new design curves. Since the new curves represent the 95% lower confidence limit, most of the test data should plot above the curve, as was shown in the report.

Since the current Section 7 of the MBE references *NCHRP Report 299*, it is assumed that the values for the resistance factor, R_R, were calculated using data presented in *NCHRP Report 299*. *NCHRP Report 299* specifies that it is typically assumed that scatter in fatigue data follows a lognormal sta-

Table 4. Fatigue data reported in *NCHRP Report 299*.

Detail Category	S_r at 2 x 10^6 cycles	S_{rD} at 2 x 10^6 cycles	Intercept on the nominal S-N curves	COV
A	33.0	23.2	2.500E+10	21.7%
B	22.8	18.1	1.191E+10	14.1%
B'	18.0	14.5	6.109E+09	13.2%
C	16.7	13.0	4.446E+09	15.3%
D	13.0	10.3	2.183E+09	14.2%
E	9.5	8.1	1.072E+09	9.7%
E'	7.2	5.8	3.908E+08	13.2%
Average				14.5%

tistical distribution for a given N. For design purposes, allowable nominal stress ranges are usually defined two standard deviations below the mean stress ranges. This design curve is defined as

$$NS_{95}^b = A$$

in which S_{95} is the stress range two standard deviations below the mean, and A is the intercept for this allowable design curve.

NCHRP Report 299 provides a Table of data for various fatigue detail categories as given in Table 4.

A normal distribution can have two-sided limits or one-sided limits. Since fatigue resistance curves are one-sided (i.e., survival on one side and failure on the opposite side), one-sided limits should be used. This was done as specified in *NCHRP Report 286* where 95% lower confidence limit was used with 95% survival to calculate the design curves. A 95% lower confidence limit ensures a probability of failure of 5%. On the other hand, a two standard deviation shift from the mean provides a probability of failure of 2.275% as shown in Figure 27. Thus, a two standard deviation shift from the mean does not provide the same level of safety as a 95% lower confidence limit. However, *NCHRP Report 299* mentions that the current fatigue design curves are based on a two standard deviation shift from the mean values at 2 million cycles. A calculation of the stress ranges at 2 million cycles was performed using a two standard deviation shift and a 95% lower one-sided confidence limit. The mean and standard deviation for the normal distribution corresponding to the lognormal distribution were calculated. The results are shown in Table 5.

The following are sample calculations of stress ranges and R_R for mean life for Category A:

$$\sigma = \sqrt{\ln(1+\text{cov}^2)} = \sqrt{\ln(1+0.217^2)} = 0.2145$$

$$\mu = \ln(S_{r_{Mean}}) = \ln(33) = 3.4965$$

95th Percentile for Standard distribution with Mean μ and Standard Deviation $\sigma = 3.144$
95th Percentile $S_r = e^{3.144} = 23.2$

2 Standard Deviation Shift for Standard distribution with Mean μ and Standard Deviation σ
$= \mu - 2\sigma$
$= 3.4965 - 2x0.2145$
$= 3.0675$
2 Standard Deviation Shift $S_r = e^{3.0675} = 21.5$

Constant A for Design Stress Range $= (S_{r_{DESIGN}})^3 x(2x10^6) = 23.2^3 x(2x10^6) = 2.5x10^{10}$
Constant A for Mean Stress Range $= (S_{r_{MEAN}})^3 x(2x10^6) = 33^3 x(2x10^6) = 7.19x10^{10}$

$$R_R \text{ for Category A Detail for Mean Life} = \frac{7.19\times10^{10}}{2.5\times10^{10}} = 2.9$$

As can be seen from Table 5, a 95th percentile line matches the design stress ranges currently used in the AASHTO LRFD Specifications (2010), whereas a two standard deviation shift gives lower stress range values. Hence, the data provided in *NCHRP Report 299* seem to indicate that the design fatigue curves are indeed based on a 95% lower confidence limit and

Figure 27. Standard normal distribution (two standard deviation shift vs. 95% lower confidence limit).

Table 5. Calculations for 95th percentile stress range vs. two standard deviation shift stress range.

Detail Category	S_r (Mean) at 2 million cycles	S_r (Design) at 2 million cycles	COV	σ (Std. Deviation)	μ (Mean)	95th Percentile	95th Percentile S_r	Two Standard Deviation Shift	Two Standard Deviation Shift S_r
A	33	23.2	21.70%	0.2145	3.4965	3.144	23.2	3.067	21.5
B	22.8	18.1	14.10%	0.1403	3.1268	2.896	18.1	2.846	17.2
B'	18	14.5	13.20%	0.1314	2.8904	2.674	14.5	2.628	13.8
C	16.7	13	15.30%	0.1521	2.8154	2.565	13.0	2.511	12.3
D	13	10.3	14.20%	0.1413	2.5649	2.333	10.3	2.282	9.8
E	9.5	8.1	9.70%	0.0968	2.2513	2.092	8.1	2.058	7.8
E'	7.2	5.8	13.20%	0.1314	1.9741	1.758	5.8	1.711	5.5

not on a two standard deviation shift which would give lower stress range values.

Based on this, using the 95th percentile line as minimum life, the resistance factor R_R was recalculated for mean life. Table 6 compares the R_R values given in Section 7 with the recalculated R_R values. As can be seen from the table, the recalculated R_R values are generally higher than the current Section 7 values, except for fatigue categories B′ and E′. Hence, the recalculated R_R values will provide a higher finite fatigue life for mean life (50% probability of failure).

Similar R_R values were recalculated for different levels of probability of failure from 5% to 50%. The values are given in Table 7.

These values are plotted in the graph shown in Figure 28. As can be seen from the figure, the relationship between probability of failure and R_R seems to be approximately linear. Table 8 provides the linearly interpolated values of R_R between minimum and mean fatigue lives. Comparing tables 7 and 8, the maximum difference between the values of R_R is about 0.1. Hence, a linear approximation between the mean and minimum finite fatigue life levels can be used to arrive at approximate values of R_R for different levels of probabilities of failure. Thus, this can be used to easily extend the finite fatigue life of the detail if the user is willing to accept a higher level of probability of failure.

Table 6. Comparison between Section 7 and recalculated R_R values for mean life.

Detail Category	Mean Life (50% Pf)	
	Section 7 Values	Recalculated Values
A	2.8	2.9
B	2.0	2.0
B'	2.4	1.9
C	1.3	2.1
C'	1.3	2.1
D	1.6	2.0
E	1.6	1.6
E'	2.5	1.9

Instead of providing multiple values of R_R for probabilities of failure, another solution would be to provide two different levels of safety besides the minimum and mean fatigue life. These would be Evaluation Life 1 and Evaluation Life 2 for probabilities of failure of 15.9% and 32.9% respectively. Evaluation Life 1 will correspond to the level of safety associated with one standard deviation shift from the mean. This is what is currently provided as "Evaluation Life" safety level in Section 7. Evaluation Life 2 will be halfway between Evaluation Life 1 and Mean Life. This level of safety will correspond to a probability of failure of 32.9%. The calculated values of R_R for these levels of safety are as shown in Table 9.

Fatigue Serviceability Index

The FSI, Q, is a method for providing a relative evaluation of the fatigue serviceability of a structural detail. The index itself is dimensionless, but it is expected that engineers can make planning decisions regarding bridge viability based on the quantitative value of the FSI and the overall qualitative assessment.

The expression for the FSI is given as follows:

$$Q = \left(\frac{Y-a}{N}\right) GRI \tag{19}$$

where:

N = Greater of Y or 100 years
G = Load Path Factor, as given in Table 10
R = Redundancy Factor, as given in Table 11
I = Importance Factor, as given in Table 12
Y = Calculated total fatigue life of the detail

The load path, redundancy, and importance factors are risk factors that modify the FSI. They reduce the index from its

Table 7. Variation of R_R with probability of failure.

Probability of Failure	Fatigue Category						
	A	B	B'	C	D	E	E'
5%	1.0	1.0	1.0	1.0	1.0	1.0	1.0
10%	1.3	1.2	1.2	1.2	1.2	1.1	1.2
15%	1.5	1.3	1.3	1.3	1.3	1.2	1.3
20%	1.7	1.4	1.4	1.4	1.4	1.3	1.4
25%	1.9	1.5	1.5	1.6	1.5	1.3	1.5
30%	2.1	1.6	1.6	1.7	1.6	1.4	1.6
35%	2.2	1.7	1.6	1.8	1.7	1.4	1.6
40%	2.4	1.8	1.7	1.9	1.8	1.5	1.7
45%	2.7	1.9	1.8	2.0	1.9	1.6	1.8
50%	2.9	2.0	1.9	2.1	2.0	1.6	1.9

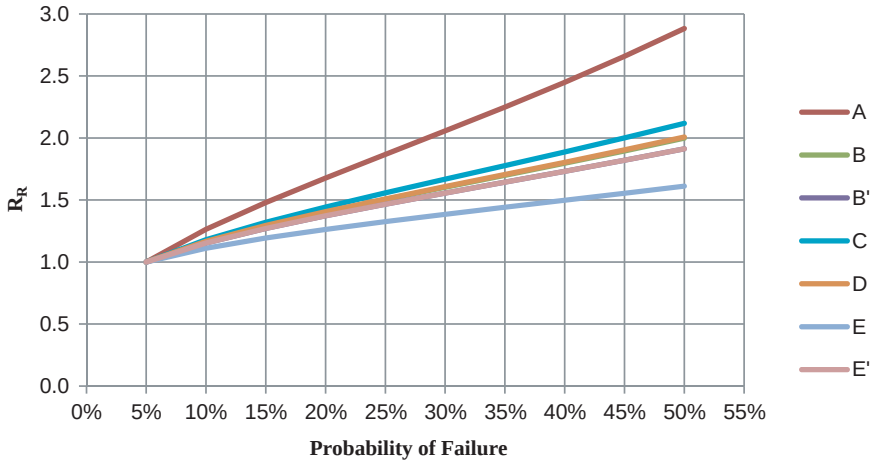

Figure 28. Variation of R_R with probability of failure.

Table 8. Linear interpolation of R_R between minimum and mean fatigue lives.

Probability of Failure	Fatigue Category						
	A	B	B'	C	D	E	E'
5%	1.0	1.0	1.0	1.0	1.0	1.0	1.0
10%	1.2	1.1	1.1	1.1	1.1	1.1	1.1
15%	1.4	1.2	1.2	1.2	1.2	1.1	1.2
20%	1.6	1.3	1.3	1.4	1.3	1.2	1.3
25%	1.8	1.4	1.4	1.5	1.4	1.3	1.4
30%	2.0	1.6	1.5	1.6	1.6	1.3	1.5
35%	2.3	1.7	1.6	1.7	1.7	1.4	1.6
40%	2.5	1.8	1.7	1.9	1.8	1.5	1.7
45%	2.7	1.9	1.8	2.0	1.9	1.5	1.8
50%	2.9	2.0	1.9	2.1	2.0	1.6	1.9

Table 9. Values of R_R for different levels of safety.

Detail Category	Minimum Life (5% Pf) (Design)	Evaluation Life 1 (15.9% Pf)	Evaluation Life 2 (32.9% Pf)	Mean Life (50% Pf)
A	1.0	1.5	2.2	2.9
B	1.0	1.3	1.7	2.0
B'	1.0	1.3	1.6	1.9
C	1.0	1.3	1.7	2.1
C'	1.0	1.3	1.7	2.1
D	1.0	1.3	1.7	2.0
E	1.0	1.2	1.4	1.6
E'	1.0	1.3	1.6	1.9

base value (i.e., based on fatigue resistance alone) to a reduced value that reflects greater consequences from the lack of ability to redistribute the load (load path factor); lack of redundancy (redundancy factor); or use of the structure (importance factor). The net effect of a reduction in the index will be to move the composite index value to a lower value that may result in a lower fatigue rating. These risk factors are similar to the ductility, redundancy, and operational classification factors in the *AASHTO LRFD Bridge Design Specifications.* Improved quantification with time will possibly modify these factors.

The number of members that carry load when a fatigue truck is placed on the bridge is used to select the load path factor; e.g., two members for a two-girder bridge and for a typical truss structure; four or more members for a multi-beam or multi-girder bridge; etc.

The fatigue rating and assessment outcomes are given in Table 13. These values and outcomes were selected based on several different fatigue assessment trials. While not exact, they can be used to provide some guidance in decision making.

In order to illustrate the behavior of the FSI, consider a hypothetical bridge. There can be various details on the bridge experiencing different stress ranges and thus having varying total fatigue lives. For the time being, neglect the load path factor, redundancy factor, and the importance factor, since these are penalizing factors that account for higher risk. Consider the variation of (Y-a)/N with the remaining life as shown in Figure 27. It can be seen that the curve remains bounded between zero and one for positive remaining lives. The curve follows a linear trend for fatigue lives less than 100 years. For fatigue lives less than 100 years, there is a direct linear correlation between remaining life and the FSI. For example, an FSI of 0.2 corresponds to remaining life of about 20 years, and an FSI of 0.1 indicates a remaining life of about 10 years. Also, a linear relationship helps define the boundaries for the FSI to which a fatigue rating can be assigned.

From the assessment outcomes noted, it is likely that only the last two assessment outcomes of 'Increase Inspection Frequency' and 'Assess Frequently' are significant from the Bridge Owner's point of view. The decision to monitor the bridge periodically or frequently is presently made by the owners based on the remaining life, which is in absolute years. Since the FSI is expected to provide an approximate guideline to the bridge owners for making this decision, the FSI should also vary linearly with the remaining life, at least when the FSI starts dropping into these last two assessment outcome ranges. Also, as can be seen from Figure 29, for bridge ages up to 80 years, the FSI still maintains a linear relationship below a value of 0.2. Hence the linear correlation between FSI and remaining life is maintained below 0.2 for bridge ages up to 80 years. This is advantageous as the fatigue engineer now has an approximate judgment of the remaining life in years left for the detail from the value of FSI.

The three additional factors—load path factor, redundancy factor, and the importance factor—lead to a reduction in the value of the FSI. A four-girder continuous span rural bridge is an example of a best possible condition of the bridge with respect to these risk factors, where all the factors have a value of 1.0. A two-girder simple span interstate bridge is an example of the worst condition. Various bridge conditions have been examined in Figure 30 for a bridge age of 35 years. The worst possible reduction in the value of FSI due to these risk factors is 35.2% ($1\text{-}0.8 \times 0.9 \times 0.9$). Hence, an FSI of 0.2 for the best condition gets reduced to 0.13 for the worst condition. Or said another way, a bridge detail with

Table 10. Load path factor G.

Number of Load Path Members	G
1 or 2 members	0.8
3 members	0.9
4 or more members	1

Table 11. Redundancy factor R.

Type of Span	R
Simple	0.9
Continuous	1

Table 12. Importance factor I.

Structure or Location	Importance Factor, I
Interstate Highway Main Arterial State Route Other Critical Route	0.90
Secondary Arterial Urban Areas	0.95
Rural Roads Low ADTT routes	1.00

Table 13. Fatigue rating and assessment outcomes.

Fatigue Serviceability Index, Q	Fatigue Rating	Assessment Outcome
1.00 to 0.50	Excellent	Continue Regular Inspection
0.50 to 0.35	Good	Continue Regular Inspection
0.35 to 0.20	Moderate	Continue Regular Inspection
0.20 to 0.10	Fair	Increase Inspection Frequency
0.10 to 0.00	Poor	Assess Frequently
< 0.00	Critical	Consider Retrofit, Replacement or Reassessment

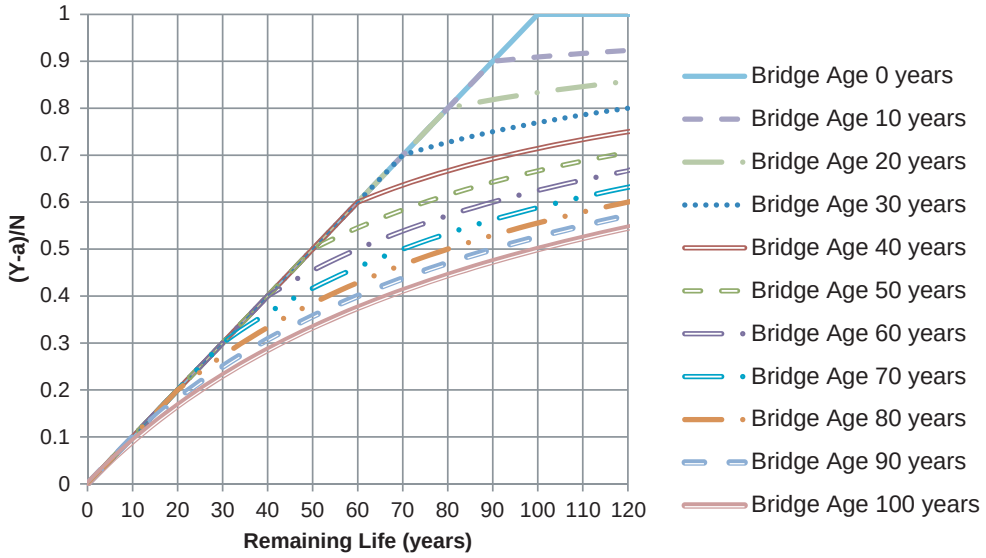

Figure 29. Variation of (Y-a)/N with remaining life for various bridge ages.

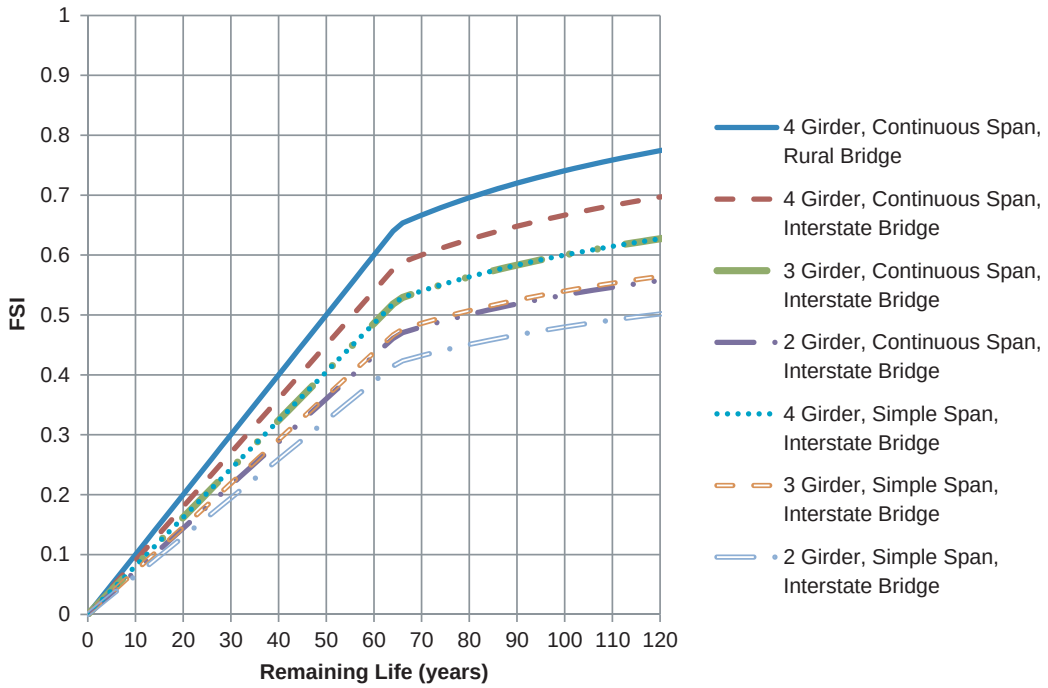

Figure 30. Variation of FSI for different bridge parameters (bridge age 35 years).

an approximate remaining life of 20 years gets reduced to a life of approximately 13 years for the worst possible bridge condition.

The FSI can also become negative if negative remaining lives are obtained. For negative FSI values, strategies that can be adopted to ameliorate the unsatisfactory condition include refinements to the analysis procedure for estimating the stress range, field stress measurements, and use of the truncated fatigue life distribution methodology.

More Accurate Estimation for Truck Traffic

The AASHTO MBE (2011) recommends an approximation to estimate the remaining fatigue life of a detail in Figure C7-1. This approximation may cause significant under- and over-estimation of the remaining life.

This approximation has been eliminated in the proposed revisions to Section 7 of the specifications using a closed form solution for *Y*. This solution was completed in conjunction with NCHRP Project 12-51 (Fu et al., 2003) and has been implemented in a computer program *Carris* as a product of that research effort. Using the analytical sum of the truck traffic, the finite fatigue life is revised as follows:

$$Y = \frac{\log\left[\dfrac{R_R A}{365n\left[(ADTT)_{SL}\right]_{PRESENT}\left[(\Delta f)_{eff}\right]^3} g(1+g)^{a-1} + 1\right]}{\log(1+g)} \tag{20}$$

which eliminates the need for Figure C7-1. In Equation 20, *a* is the present age of the detail, *g* is the estimated annual traffic volume growth rate, and $[(ADTT)_{SL}]_{PRESENT}$ is the present average number of trucks per day in a single lane, as defined in the AASHTO MBE (2011). As a result, iteration for an accurate $ADTT_{SL}$ has become unnecessary. Consequently, it is suggested that the updated Equation 20 be used for estimating the finite fatigue life in the revised Section 7 of AASHTO MBE (2011) to reflect this knowledge advancement.

Two examples of an E′ detail (from bridges in New York and Maryland) have been examined regarding this issue. For these two examples and the range of present age and traffic growth rate covered in Figure C7-1, it has been found that the maximum over-estimation is 37% and the maximum under-estimation is 183%. Under-estimation over 100% means a supposedly positive remaining life is approximated as a negative one. For example, in the Maryland example, a supposedly 18-year remaining life is approximated as –15 years, resulting in a 183% under-estimation. More details on this subject are described herein.

For an illustration of Equation 20 and demonstration of the approximation involved in using Figure C7-1 in current Section 7 of the specifications, the following two examples are considered.

Example 1

This example considers a cover plate weld detail in New York State belonging to Category E′ (Cohen et al., 2003). The situation is summarized as having the following characteristic parameters for Figure C7-1 in current Section 7 and Equation 20: R_R = 1.0 for minimum life, $A = 3.9'10^8$ ksi^3, $[(ADTT)_{SL}]_{PRESENT}$ = 1896 trucks / day, Δf_{eff} = 1.817 ksi, and n = 1 for a simple span longer than 40 ft. Conceptually, this case may occur with different growth rates and present ages. Accordingly, Table 14 shows a comparison between the closed form solution of Equation 20 and the Manual recom-

Table 14. Example 1—Comparison of Manual recommended approximation and exact solution Equation 20 for g = 0.02.

a (yr)	Minimum Remaining Life Using Manual Recommended Approach (yr)	Minimum Remaining Life Using Exact Approach (yr)	Manual Recommended Minimum Remaining Life/ Exact Approach Minimum Remaining Life
5	67	51	1.32
10	66	49	1.33
15	65	48	1.35
20	62	47	1.34
25	62	45	1.37
30	59	44	1.33
35	55	43	1.29
40	52	42	1.24
45	48	41	1.17
50	44	40	1.10

Table 15. Example 1—comparison of Manual recommended approximation and exact solution Equation 20 for $g = 0.04$.

a (yr)	Minimum Remaining Life Using Manual Recommended Approach (yr)	Minimum Remaining Life Using Exact Approach (yr)	Manual Recommended Minimum Remaining Life/ Exact Approach Minimum Remaining Life
5	50	38	1.31
10	49	37	1.31
15	48	36	1.33
20	48	36	1.34
25	48	35	1.37
30	47	35	1.35
35	47	34	1.37
40	47	34	1.37
45	47	34	1.34
50	43	34	1.30

mended approximation approach, for a range of a values and $g = 0.02$. The last column in the Table displays the ratio of two remaining minimum lives, using the closed form solution as the reference. It is seen that the Manual-recommended approach produces approximation results all with an error larger than 10% except one case when $a = 50$ years.

Tables 15 through 17 continue the comparison of the two approaches for $g = 0.04$, 0.06, and 0.08, to cover the range of the chart in AASHTO MBE (2011) (Figure C7-1). In Tables 16 and 17, the approximate approach generates cases of under-estimation, with the ratio in the last column less than 1. The worst case is 0.37 indicating a 63% under-estimation of the remaining life. Apparently, if the stress range Δf_{eff} is large enough, this could cause a negative remaining life, while the closed form solution still produces a positive one. In addition, Table 17 does not include the case $a = 5$ years because the chart in AASHTO MBE (2011) (Figure C7-1) does not include that case, while Equation 20 could still produce an exact solution.

Example 2

This example considers a cover plate weld detail with a fatigue strength of Category E′ as well. The following parameters for Figure C7-1 in current Section 7 and Equation 20 are identified: $R_R = 1.0$ for minimum life; $A = 3.9 \times 10^8$ ksi^3; $[(ADTT)_{SL}]_{PRESENT} = 1081$ trucks/day; $\Delta f_{eff} = 2.62$ ksi; and $n = 1$ for a simple span longer than 40 ft. Again, this case may occur for different growth rates and present ages.

Tables 18 to 21 show comparisons between the closed form solution Equation 20 and the Manual recommended approximation approach, for different average traffic growth rates g and a range of present life a. The last column in the Tables displays the ratio of two remaining minimum lives,

Table 16. Example 1—comparison of Manual recommended approximation and exact solution Equation 20 for $g = 0.06$.

a (yr)	Minimum Remaining Life Using Manual Recommended Approach (yr)	Minimum Remaining Life Using Exact Approach (yr)	Manual Recommended Minimum Remaining Life/ Exact Approach Minimum Remaining Life
5	34	31	1.11
10	33	30	1.10
15	33	30	1.10
20	32	30	1.09
25	32	29	1.07
30	30	29	1.03
35	31	29	1.07
40	31	29	1.08
45	31	29	1.06
50	28	29	0.98

Table 17. Example 1—comparison of Manual recommended approximation and exact solution Equation 20 for $g = 0.08$.

a (yr)	Minimum Remaining Life Using Manual Recommended Approach (yr)	Minimum Remaining Life Using Exact Approach (yr)	Manual Recommended Minimum Remaining Life/ Exact Approach Minimum Remaining Life
10	21	26	0.82
15	20	26	0.78
20	18	26	0.71
25	17	25	0.66
30	15	25	0.60
35	14	25	0.55
40	13	25	0.51
45	12	25	0.46
50	9	25	0.37

Table 18. Example 2—comparison of Manual recommended approximation and exact solution Equation 20 for $g = 0.02$.

a (yr)	Minimum Remaining Life Using Manual Recommended Approach (yr)	Minimum Remaining Life Using Exact Approach (yr)	Manual Recommended Minimum Remaining Life/ Exact Approach Minimum Remaining Life
5	37	35	1.08
10	34	32	1.06
15	32	30	1.04
20	28	28	1.00
25	26	26	0.98
30	22	25	0.89
35	17	23	0.75
40	14	21	0.65
45	10	20	0.50
50	5	19	0.26

Table 19. Example 2—comparison of Manual recommended approximation and exact solution Equation 20 for $g = 0.04$.

a (yr)	Minimum Remaining Life Using Manual Recommended Approach (yr)	Minimum Remaining Life Using Exact Approach (yr)	Manual Recommended Minimum Remaining Life/ Exact Approach Minimum Remaining Life
5	27	27	0.98
10	24	26	0.93
15	22	25	0.88
20	20	24	0.82
25	18	23	0.77
30	15	23	0.67
35	13	22	0.60
40	11	21	0.51
45	9	21	0.42
50	5	21	0.24

Table 20. Example 2—comparison of Manual recommended approximation and exact solution Equation 20 for $g = 0.06$.

a (yr)	Minimum Remaining Life Using Manual Recommended Approach (yr)	Minimum Remaining Life Using Exact Approach (yr)	Manual Recommended Minimum Remaining Life/ Exact Approach Minimum Remaining Life
5	18	23	0.78
10	15	22	0.69
15	13	22	0.60
20	11	21	0.50
25	8	21	0.39
30	5	20	0.26
35	4	20	0.18
40	2	20	0.08
45	-1	20	-0.03
50	-4	20	-0.21

using the closed form solution as the reference. It is seen in Tables 18 and 19 for $g = 0.02$ and 0.04 that the Manual recommended approach may produce over- and underestimates, respectively, with values larger and smaller than 1.0. The maximum is 1.08 (8% over estimate) and the minimum is 0.24 (78% under-estimate). Tables 20 and 21 continue the comparison for $g = 0.06$ and 0.08, where negative values are seen in the last column, indicating that the Manual recommended approximate approach produces negative remaining life, but not the closed form solution Equation 20. Due to the change of sign for the ratio in the last column, these values should be so interpreted with a negative 1 added. For example, the last row of Table 20 for $a = 50$ years, a ratio value of –0.21 is shown. It should be interpreted as –0.21-1 = –1.21 or 121% under-estimated from the closed form solution of 20 years, resulting in –4 years as the minimum remaining life. Note also that the ratio in the last column is calculated before the remaining lives are rounded so that (–4)/20 is not exactly –0.21. In summary, Tables 18 to 21 show that the Manual recommended approximation may over-estimate by 8% and under-estimate by 183% for this example.

In conclusion, it has been seen that the approximation recommended in the Manual may lead to significant errors. Note also that since the closed form solution in Equation 20 is easy to apply, the fatigue rating engineers can use it for their own comparison and check.

Tack Weld Tests

The tack weld tests involve a pair of lap plates attached to a middle main plate with tack welds attached on the sides. Rivets, simulated by bolts, hold the plates together. The assembly is subjected to a range of constant amplitude longitudinal tensile stress to examine the fatigue susceptibility of the tack welds. An important part of the test procedure

Table 21. Example 2—comparison of Manual recommended approximation and exact solution Equation 20 for $g = 0.08$.

a (yr)	Minimum Remaining Life Using Manual Recommended Approach (yr)	Minimum Remaining Life Using Exact Approach (yr)	Manual Recommended Minimum Remaining Life/ Exact Approach Minimum Remaining Life
10	8	20	0.42
15	6	19	0.29
20	2	19	0.12
25	0	19	-0.02
30	-4	19	-0.19
35	-6	18	-0.35
40	-9	18	-0.50
45	-12	18	-0.65
50	-15	18	-0.83

Figure 31. Skidmore-Wilhelm bolt load indicator.

Figure 32. Turn-of-nut calibration.

involves determining how much the bolts need to be tightened in order to have the same clamping effect as a rivet.

Bolt Tightening Procedure

Need for Developing Procedures

Tack welds have been used frequently in bridge structures to temporarily hold members in place before riveting. Some bridge structures can have hundreds of such tack welds that have been left in place. Most of these riveted bridges have already accumulated a significant fatigue life. Since riveting is a procedure that is rarely performed nowadays, bolts were used instead of rivets for the tack weld tests. In order to have the same effect as a rivet, it is essential to emulate the clamping force that a rivet would develop upon placement and subsequent cooling. A bolt tightening procedure was developed for this purpose.

Photographs and Descriptions of Calibration Methodology

The turn-of-nut method of tightening bolts, together with a Skidmore-Wilhelm bolt load indicator, was used to develop the bolt tightening procedure. The Skidmore-Wilhelm bolt load indicator is shown in Figure 31. A bolt has been fitted into the center of the indicator and made snug-tight. The dial gage at the top of the indicator displays the measured bolt tension in pounds. The bolt head is held in position in a wedge present on the opposite side of the indicator. Since the length of the bolt used is less than four times the diameter of the bolt, the bolt has to be turned up to ⅓ of a turn or 120 degrees in order to fully tighten the bolt as per the AISC Steel Construction Manual (AISC 2010). After snug-tightening the bolt, angular lines were marked on the bolt load indicator as shown in the figure, such that the angle in between adjacent lines is approximately 1/12 of a turn or 30 degrees.

The snap-on torqometer shown in Figure 32 was used to measure the torque needed while turning the bolt. The torque is measured in foot-pounds. Three ASTM A325 ⅞-in. diameter bolts were tested. The bolts were initially made snug-tight by manually tightening them using a hand wrench. The bolts were then tightened using the torqometer in increments of 1/12 of a turn (30 degrees) up to ⅓ of a turn (120 degrees) in order to achieve the minimum bolt pretension of 39 kips for a ⅞-in.

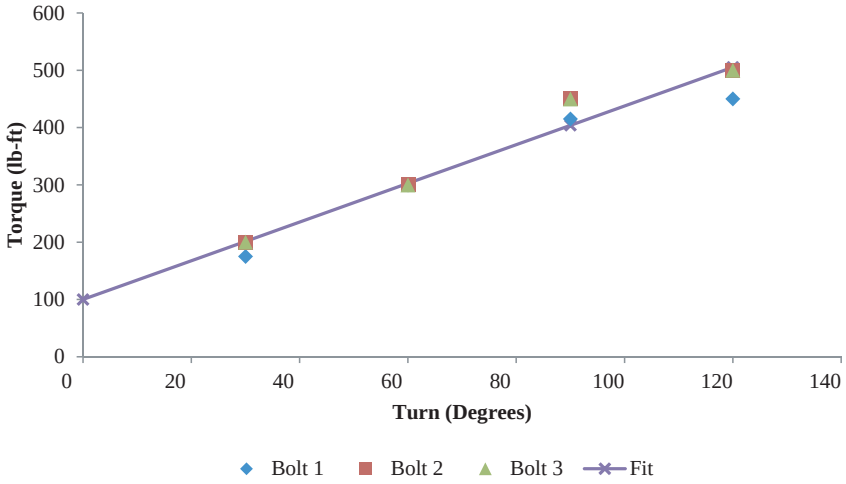

Figure 33. Torque required vs. turn-of-nut.

diameter A325 bolt. The turn angle, bolt pretension, and torque needed were recorded for different turns of each bolt.

Results of Calibration

The measured values for turn angle, bolt pretension, and torque were plotted, and straight lines were fitted for the various plots. Figure 33 shows the plot of the torque needed for turning the bolt against the turn of the nut. Figure 34 shows the plot of the torque vs. the bolt tension, as measured by the Skidmore-Wilhelm bolt load indicator. Lastly, Figure 35 shows the plot of bolt tension vs. turn-of-nut.

It can be seen that all the bolts tested gave very consistent values of torque and tension for a given turn-of-nut. The bolt tension, torque required, and the turn-of-nut all have linear relationships with respect to each other. The bolt pretension for snug-tight varied from about 5 to 8 kip force in these tests. From the plot of tension against turn, it can be seen that the pretension in the bolt exceeds the minimum required pretension of 39 kips for a ⅓ turn of the nut.

Zhou (1994) tested nine specimens with rivets to examine the magnitude of residual clamping stress. The specimens had been cut from riveted girders removed from demolished bridges that were about sixty years old. The measured clamping stress varied from 5 to 24 ksi, with an average of about 12 ksi with a standard deviation of 6 ksi.

The force corresponding to the average clamping stress of 12 ksi stress for a ⅞-in. diameter bolt is 7.2 kips. It can be seen from the plot of tension against turn that this force can be easily achieved by simply snug-tightening the bolt with an ordinary wrench. Hence, the bolts on all specimens were simply snug-tightened to simulate the clamping stress of a rivet, except for the specimens with fully tightened bolts.

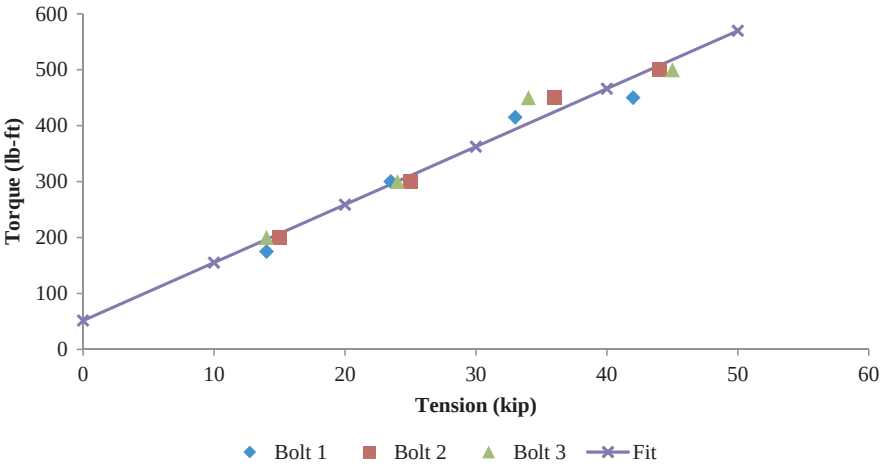

Figure 34. Torque required vs. bolt tension.

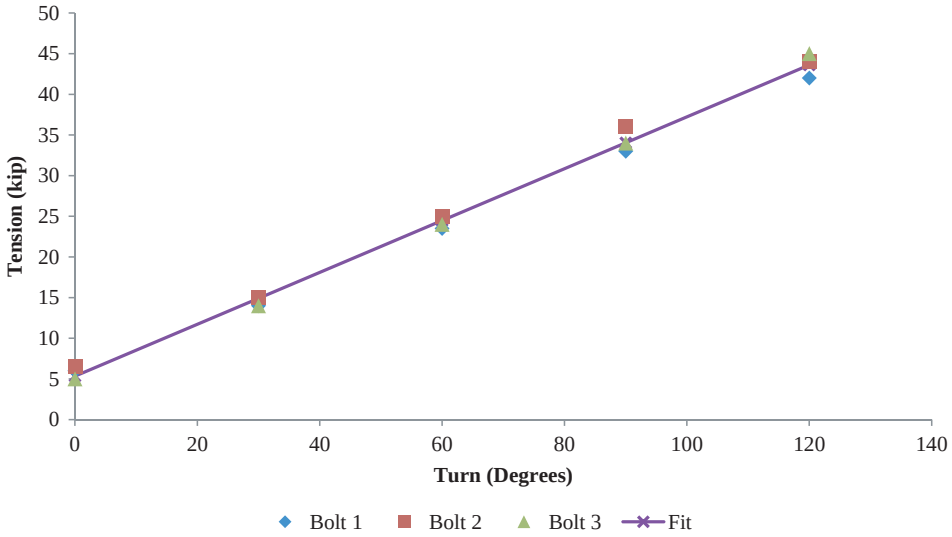

Figure 35. Bolt tension vs. turn-of-nut.

Finite Element Analysis of Tack Weld Specimen

Motivation for Analysis

It is important to know how the stress will flow in the tack weld specimen. Knowledge of the stress distribution is useful for finding the locations where stress concentration occurs during the cyclic loading. The points at which stress concentration occurs will be where the fatigue cracks are most likely to initiate in the tack weld specimen. In order to determine the stress flow in the tack weld specimen, a non-linear three dimensional finite element model of the tack weld specimen was developed. This model was used to examine the effect of various parameters, such as the number and position of the tack welds or different stress ranges on the stress distribution in the tack weld specimen.

Description of Model Parameters and Load Conditions

The finite element model of the tack weld specimen is shown in Figure 36. The finite element model simulates friction contact between the plates. The friction coefficient has been taken as 0.35. The tack welds have a yield strength of 70 ksi while the plates are 36 ksi. The model also incorporates the pretension force in the bolts and the normal contact between the bolt shanks and plates. The model was analyzed for 12 and 20 ksi stress ranges on the net section using an R ratio of 0.1 and for configurations with three, two, and zero tack welds along each side of the splice plate as shown in Figure 37. The stress range distributions at points along two sections, which are shown in Figure 38, were determined.

Results of Analysis

The measured stress ranges are compared in Figures 39 and 40. Figure 39 shows the measured stress ranges through the net section. Note that since the net section passes through the bolt holes, no stress range can be measured where the bolt holes are located. Figure 40 shows the measured stress ranges through the gross section. It was observed that the stress ranges in the net section of the splice plates are lesser than intended. For example, when loads required for producing a nominal 12 ksi stress range in the net section were imposed on the model with 3 tack welds on each side of the splice plate, the calculated average stress range in the net section was found to be of a lower value of 9 ksi. This calculated average stress range of 9 ksi across the net section was obtained by summing up the force across small discrete cross-sectional areas, obtained from the stress ranges shown in Figure 39, and then dividing it by the total

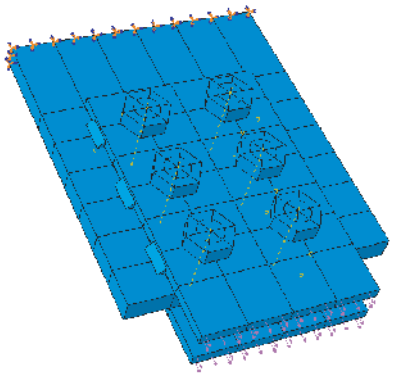

Figure 36. Finite element model of the tack weld specimen.

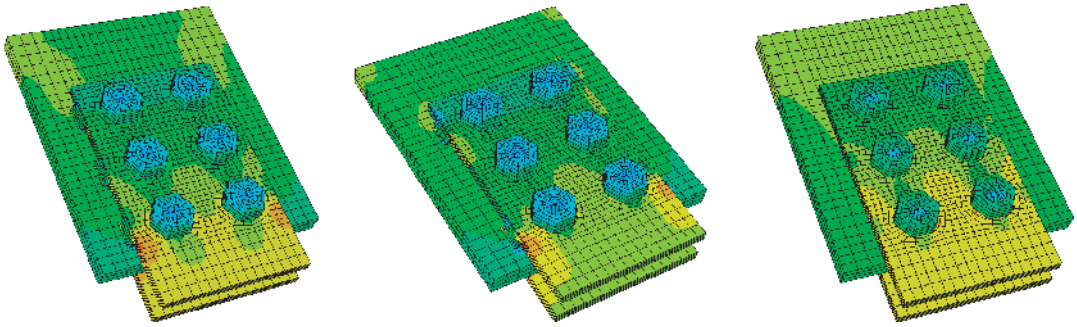

Figure 37. Stress distribution in specimen for 3, 2 and 0 tack welds, respectively.

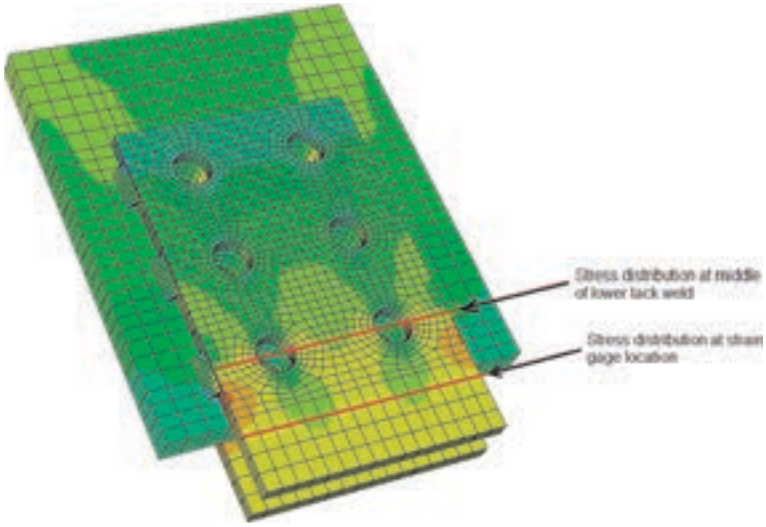

Figure 38. Sections along which stresses are measured.

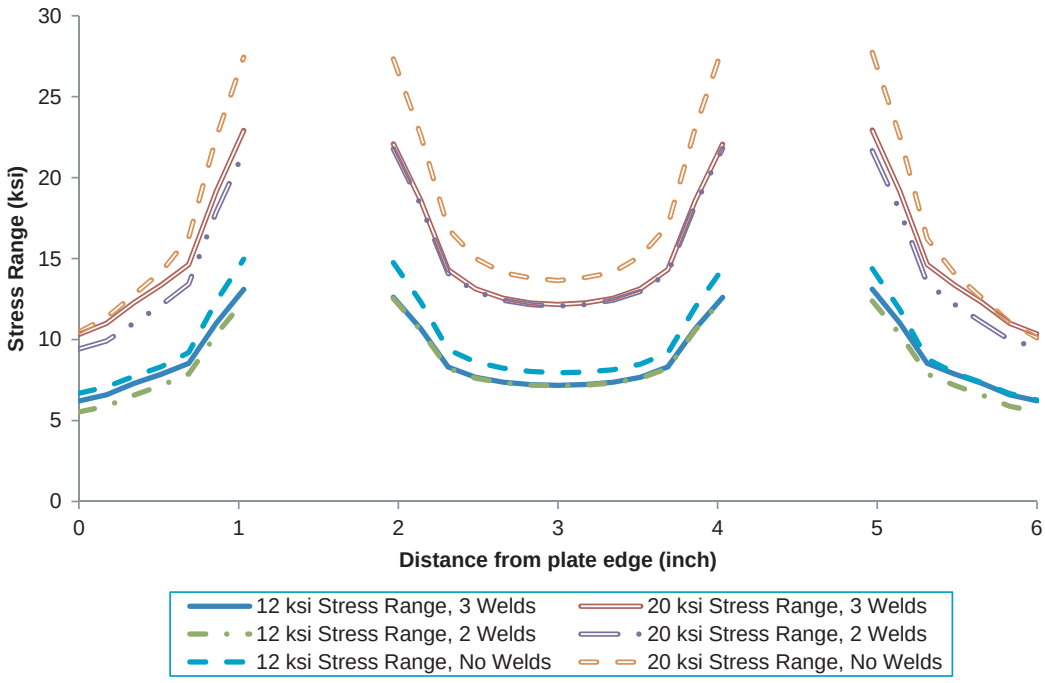

Figure 39. Stress range across section through center of lower tack weld.

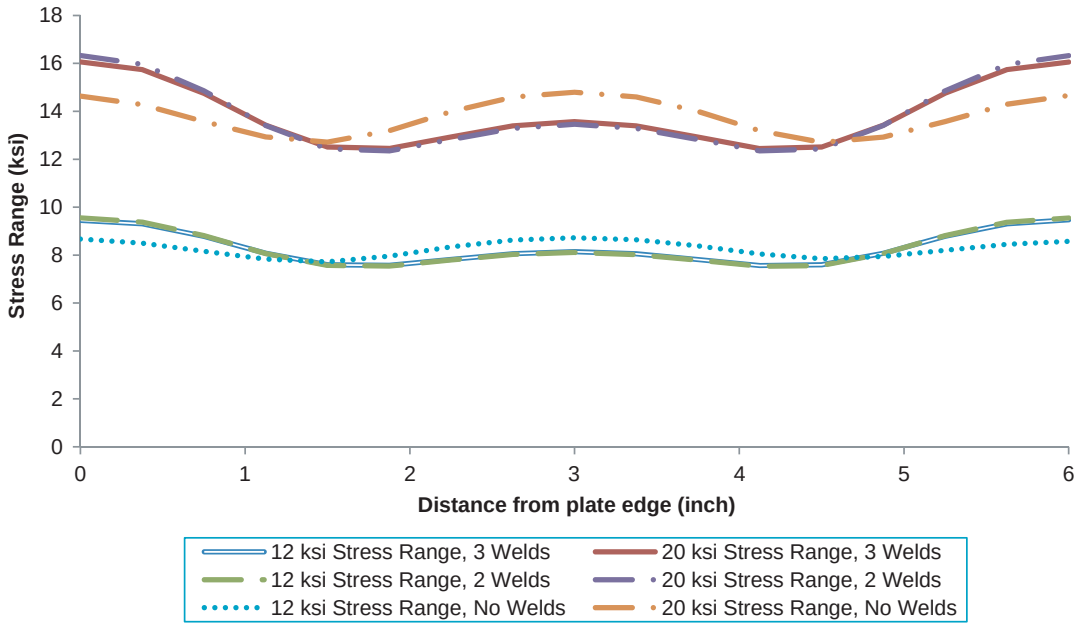

Figure 40. Stress range across section at level of strain gages.

area of the net section. The reduced 9 ksi stress range in the net section indicates that some of the stress range has been transferred into the base plate through the tack weld toes which lie ahead of the net section. However, the stress range distribution in the gross section of the splice plates is comparatively more uniform, as seen in Figure 40, and the calculated average stress range of 8.25 ksi is comparable with the corresponding expected gross section stress value of 8 ksi.

An analysis was also performed to observe the effect on the stress distribution after removing the leading line of tack welds with the specimen having three tack welds along each side of the splice plate. It was found that the stress at the toe of the weld in the direction of the applied load reduced from 4.2 ksi at the toe of the leading line of tack welds to 3.1 ksi at the toe of the second line of tack welds after the leading line of tack welds was removed.

Conclusions

The difference between the nominal stress range on the net section and the stress ranges determined by analysis occurs because of the bolts and the tack welds. A portion of the stress, however, flows through the tack welds, which are much stiffer than the bolts. This can be seen in the stress contours on the model in the figures. As a result, the actual stress flowing through the net section of the splice plates is lower. Hence, during the fatigue testing, it is expected that the most probable location where fatigue cracking will initiate is the toe of the lower tack welds. It can also be observed that there is not much change in the stress range distribution when the number of tack welds is reduced from three to two, as the first line of tack welds, which are mainly responsible for the change in stress flow, still remain in place. There is an appreciable increase in the stress range when all the tack welds are removed. Hence, the number of tack welds probably does not appreciably affect the stress range at the weld toe of the first line of welds, and hence should not appreciably affect the fatigue life of the tack welds. Also, although the stress at the toe of the tack welds does reduce after the leading line of tack welds is removed, this is not enough to conclusively state that the second line of tack welds will not be susceptible to fatigue cracking after the leading line of tack welds is removed.

Test Results

A total of seventeen specimens were tested. Typically, cracks initiated at the toes of the lower tack welds spread laterally across the splice plates. Every specimen of the tack weld tests was run continuously at least until 5 million cycles were completed or until failure had occurred. In this case, failure is defined as the point at which a crack beginning at the toe of a tack weld spreads laterally across the splice plate into the adjacent bolt hole.

Other than the specimens tested at a stress range of 20 ksi, most of the specimens were run well beyond 5 million cycles, mostly averaging about 7 million cycles. There were a total of 6 “run-outs” or specimens that did not show any evidence of fatigue cracking when the cyclic testing was stopped.

Figure 41. Typical tack weld cracks.

Most of the specimens which experienced fatigue cracks had only one weld which cracked. Some specimens experienced crack initiation at multiple tack welds and simultaneous crack growth. Typical fatigue cracks that occurred in the specimens are shown in Figure 41. All fatigue cracks that occurred initiated at the toe of the lower line of tack welds, the location of maximum stress concentration as predicted by the finite element analysis. The cracks then propagated through the splice plates laterally into the adjacent bolt hole depending on how long the crack was allowed to grow. Details of the tack weld specimens, weld parameters, and test results as well as photographs of fatigue cracks for all tack weld specimens are provided in Appendix C.

Comparison of Test Results

Table 22 shows the number of loading cycles at the end of testing for all 17 test specimens and the different parameters for the specimens. An asterisk after the cyclic life indicates a runout test with the number of cycles applied to the specimen when cyclic loading was halted.

The net section stress range across the center of the bolt holes versus the number of cycles was plotted for the specimens. The net section stress was selected because it is commonly used for riveted connections. The results were compared to the AASHTO mean fatigue curves for categories B, C, and D. As can be seen from Figure 42, the test results clearly lie above the category D mean curve and near

Table 22. Cycles at end of testing (* indicates runout).

No. of Tack Welds	Tack Weld Position	Tack Weld Length	No. of Specimens Tested at S_r Value (S_r on net section)		
			20 ksi	12 ksi	12 ksi
2	L	<1-in		8,324,000 8,259,000	
3	L	<1-in	1,066,000 843,000 1,294,000	5,253,000* 5,103,000* 6,316,000	7,667,000* (FT) 7,546,000* (FT)
2	L	<1-in		7,061,000 (MP) 6,507,000 (MP) 7,400,000 (MP)	
2	T	<1-in		5,513,000 7,570,000*	
3	L	>1-in		6,223,000* 6,243,000	

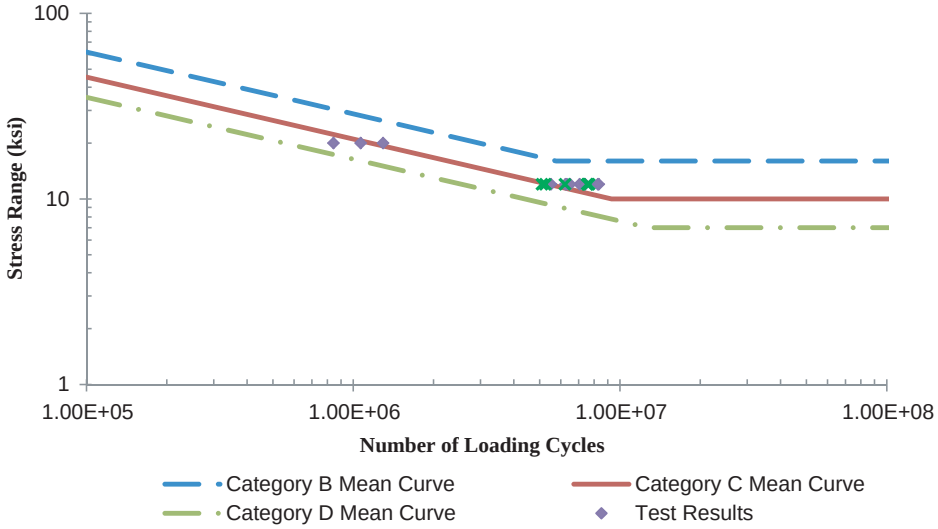

Figure 42. Comparison of test results with AASHTO mean fatigue curves (for Net Section Stress).

the category C mean curve. When comparing the test results with the AASHTO Design Fatigue Curves in Figure 43, it is evident that all the test results lie above the Category C curve.

Distortion-Induced Fatigue Tests

A number of cyclic tests were conducted to provide additional information and understanding of the behavior and performance of retrofits used to mitigate distortion-induced fatigue cracking. The purpose of the testing was to study the effectiveness of retrofit geometrical parameters in slowing or halting distortion-induced fatigue cracking. Finite element modeling was used to evaluate the response of retrofit elements as well as full connection models of bridge structures. The results of the finite element models and the experimental test results are summarized in the following sections.

Finite Element Analysis for Distortion-Induced Fatigue Tests

Finite Element Analysis of Retrofit Behavior Under Applied Loads in Distortion-Induced Fatigue Tests

WT-, single-, and double-angle retrofit elements were evaluated in the distortion-induced fatigue tests. As noted

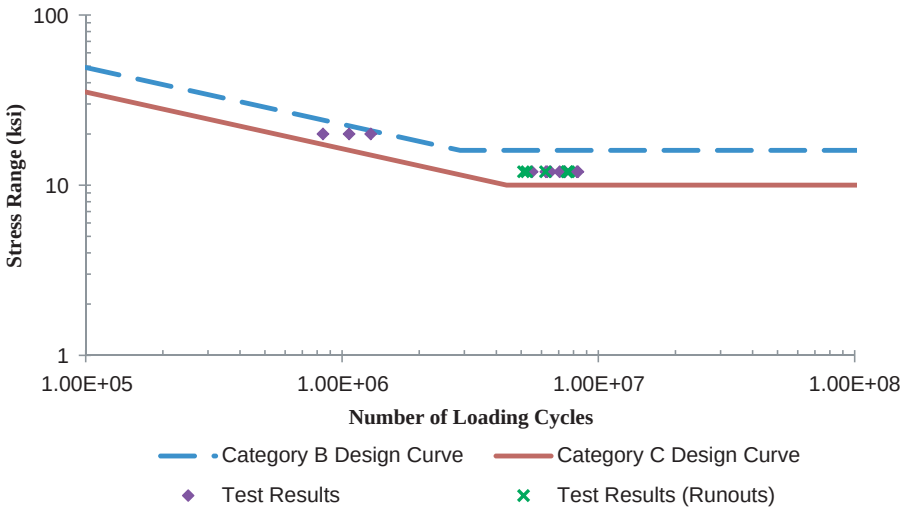

Figure 43. Comparison of test results with AASHTO design fatigue curves (for Net Section Stress).

earlier, Connor and Fisher (2006) describe a situation where a retrofit detail with a small thickness was not fully effective in preventing further crack growth at a detail with distortion-induced fatigue cracking, while a thicker detail used elsewhere on the same bridge was effective in halting further crack growth. Clearly, the stiffness of the detail is quite important. Finite element analysis was carried out for the WT retrofit in order to determine the relative influence of flange thickness and web thickness on the stiffness of the retrofit.

In this finite element analysis, the retrofit was modeled with restraint conditions similar to what it will have when attached to the stiffener plate and girder flange. The analysis was carried out for different combinations of the flange and web thickness of the retrofit to evaluate the load deformation behavior of the various retrofits. The thicknesses of the web and flange used are shown in Table 23. A total of 20 possible combinations of the web and flange thicknesses were used in the analysis.

A typical finite element retrofit model is shown in Figure 44. The model has four 0.9375-in. diameter bolt holes in both the flange and the web, the standard hole size to accommodate ⅞-in diameter bolts. The length of the web is 6.625 in., and the length of the flange is 12 in. The bolt hole spacing is shown in Figure 45. The retrofit was fixed on the inner surface of the bolt holes in the flange, while the load was applied on the web as a pressure load on the upper semicircular areas of the inner bolt hole surfaces. The deformation of the retrofit is measured as the vertical deflection of the corner of the web of the retrofit. The restraint conditions and load applied on the model are shown in Figure 46.

The results obtained from the finite element analysis are shown in Figures 47 through 55. Figures 47 through 51 are plotted such that the flange thickness remains constant, while Figures 52 through 55 show the effect of variation of flange thickness when the web thickness is kept constant. The plots show the variation in maximum load capacity before failure and the type of failure of the retrofit for different web-flange thickness combinations.

Table 23. Thicknesses of flange and web of retrofit detail.

Flange Thickness (in.)	Web Thickness (in.)
3/8	3/8
1/2	1/2
5/8	5/8
3/4	3/4
1	

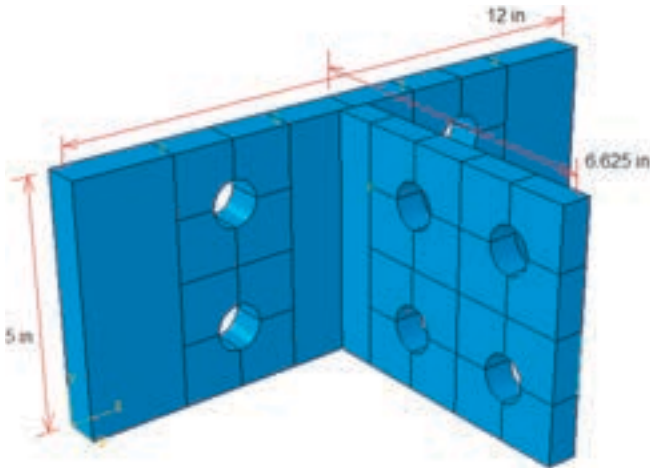

Figure 44. Dimensions of retrofit model.

It was observed that the retrofit exhibits two different failure modes—failure in shear and failure in flexure. Shear failure is primarily observed when the flange thickness is much larger than the web thickness, while flexural failure occurs when flange and web are of comparable thicknesses or if the web thickness exceeds the flange thickness. A shear failure and flexural failure are shown in Figures 56 and 57, respectively. A shear failure can also be pinpointed from the load deformation plots. Wherever the plot has a sharp corner and the deformation suddenly increases very rapidly with the load, that thickness combination has had a shear failure. When the curve slopes gradually and smoothly toward the plastic region, the failure for that particular thickness combination is a flexural failure.

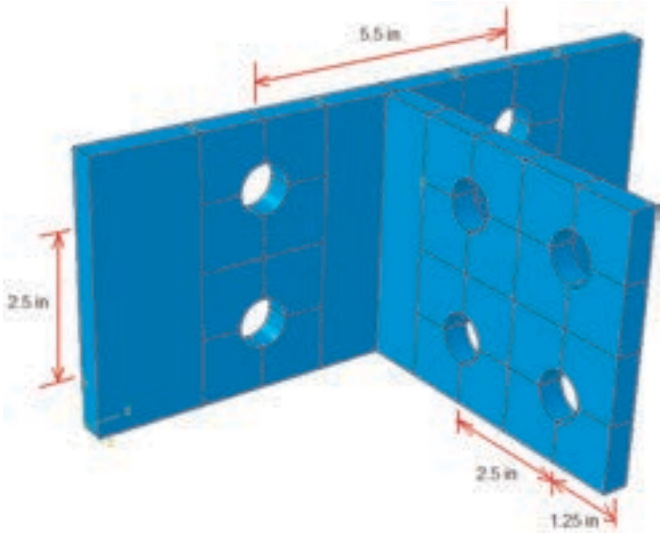

Figure 45. Spacing of bolt holes.

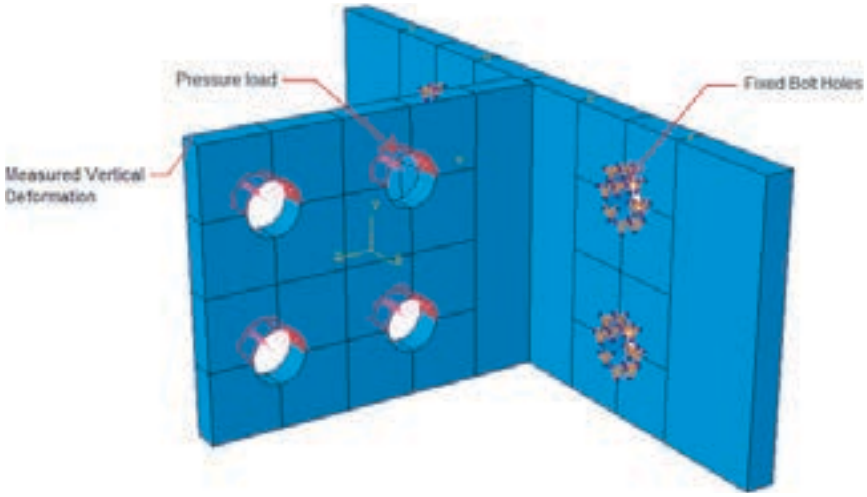

Figure 46. Restraints and loading on retrofit model.

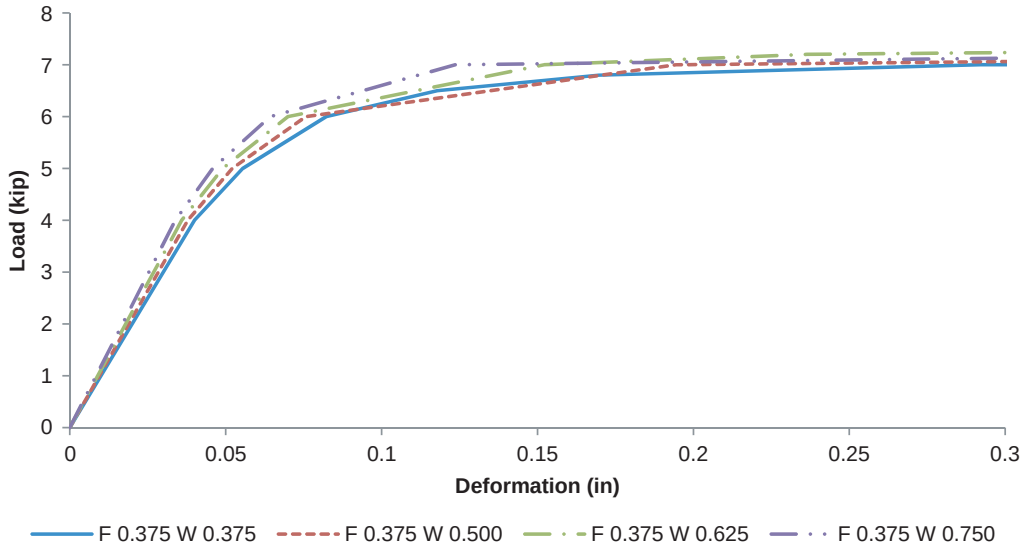

Figure 47. Load vs. deformation for constant ⅜" flange thickness.

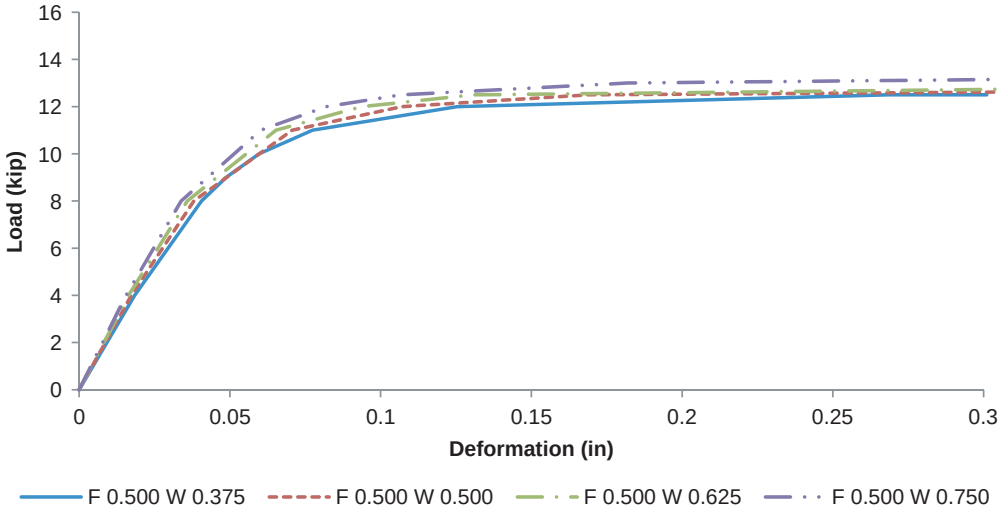

Figure 48. Load vs. deformation for constant ½" flange thickness.

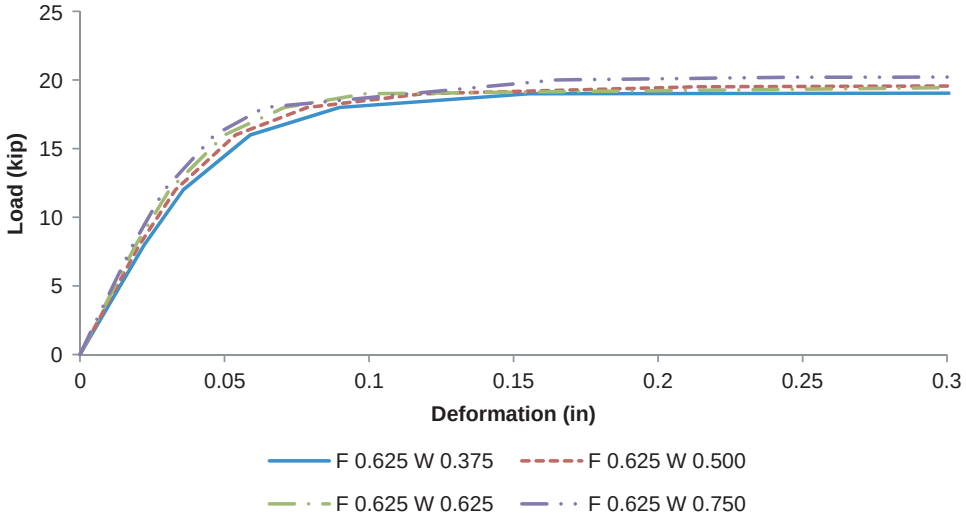

Figure 49. Load vs. deformation for constant ⅝" flange thickness.

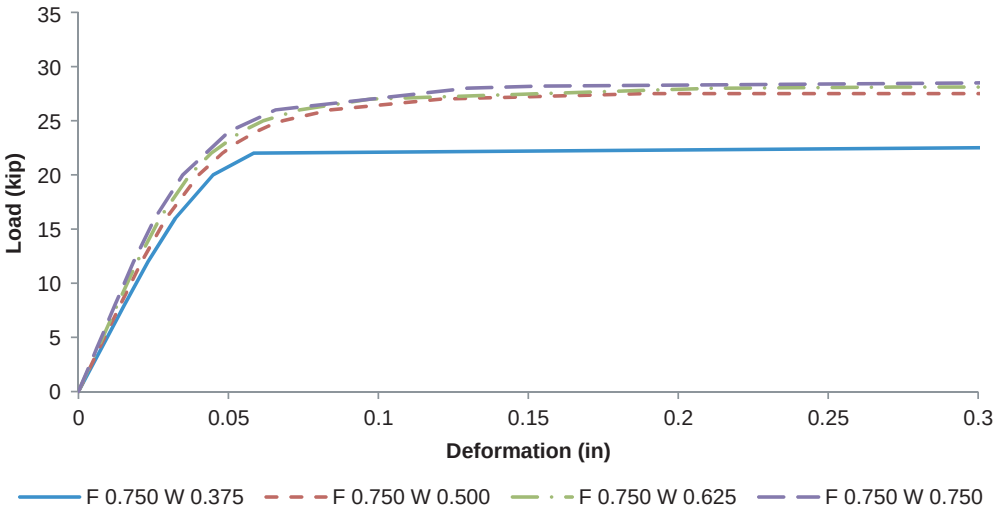

Figure 50. Load vs. deformation for constant ¾" flange thickness.

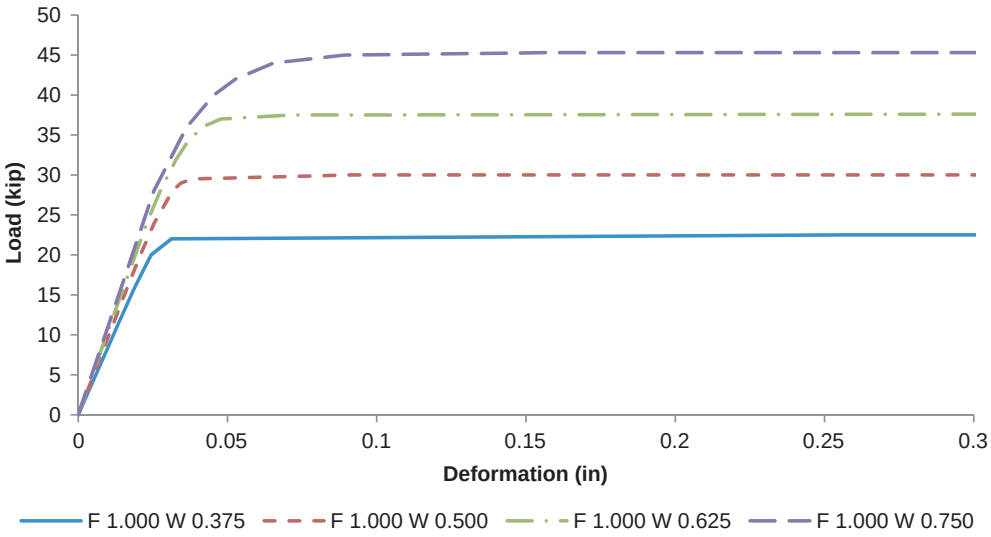

Figure 51. Load vs. deformation for constant 1" flange thickness.

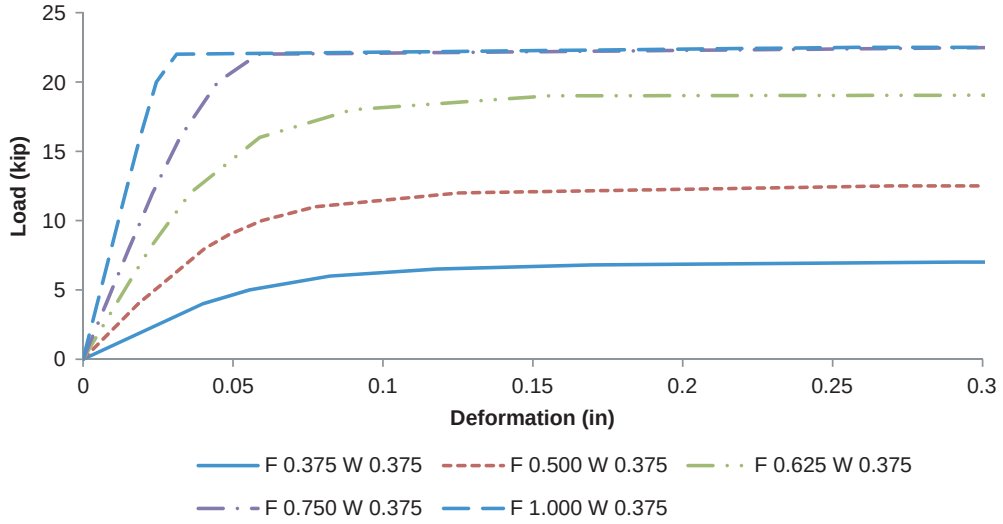

Figure 52. Load vs. deformation for constant ⅜" web thickness.

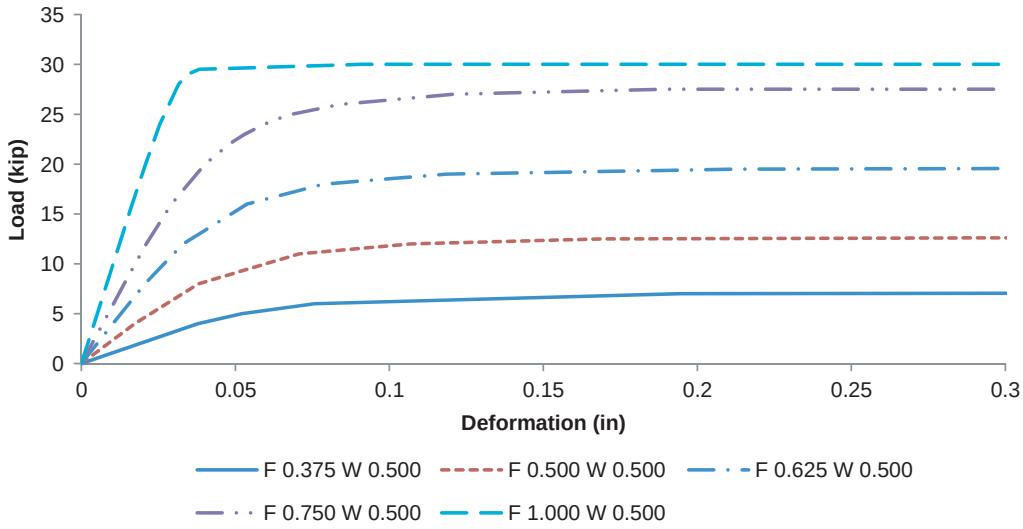

Figure 53. Load vs. deformation for constant ½" web thickness.

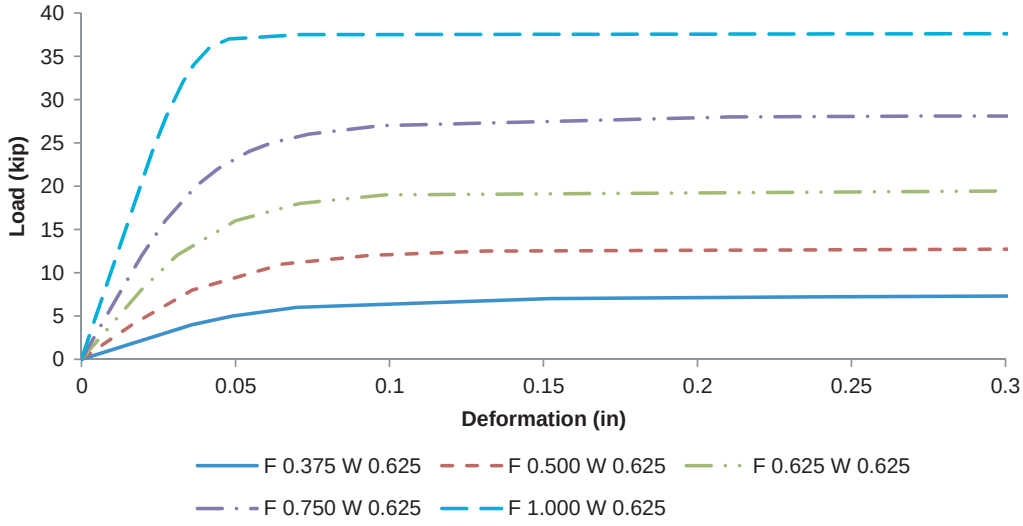

Figure 54. Load vs. deformation for constant ⅝" web thickness.

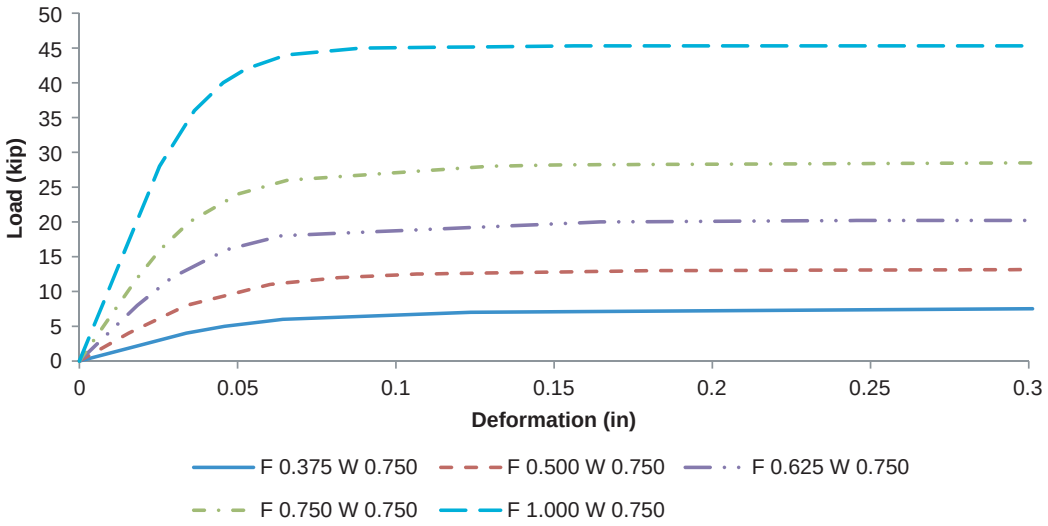

Figure 55. Load vs. deformation for constant ¾" web thickness.

It can be observed from these plots that in general, as both web and flange thicknesses are increased, the maximum load capacity of the retrofit before failure increases. From the plots where the flange thickness of the retrofit is kept constant, it can be seen that changing the web thickness has comparatively little effect on the maximum load capacity of the retrofit as well as the stiffness of the retrofit which is given by the elastic slope of the load vs. deformation plots. However, as the flange thickness becomes much greater than the web thickness, the effect of the web thickness starts becoming evident. Thinner webs fail in shear, while as the web gets thicker, the retrofit starts transitioning to failure in flexure, which causes changes in the load capacity of the retrofit. This can be seen in Figures 50 and 51.

When the web thickness is kept constant, and the flange thickness is varied, the flange thickness has a significant effect on the load capacity of the retrofit as well as the stiffness of the WT retrofit. Generally, as the flange thickness is increased, the load capacity and the stiffness of the retrofit increases; however, when the flange becomes too thick, the retrofit starts failing in shear after which a further increase in flange thickness has little effect on the load capacity of the retrofit. This can be seen in Figures 52 through 55.

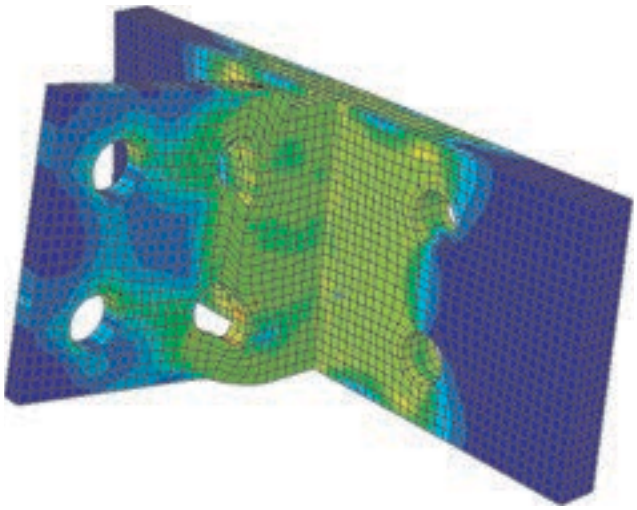

Figure 56. Shear failure of retrofit (deformations are exaggerated).

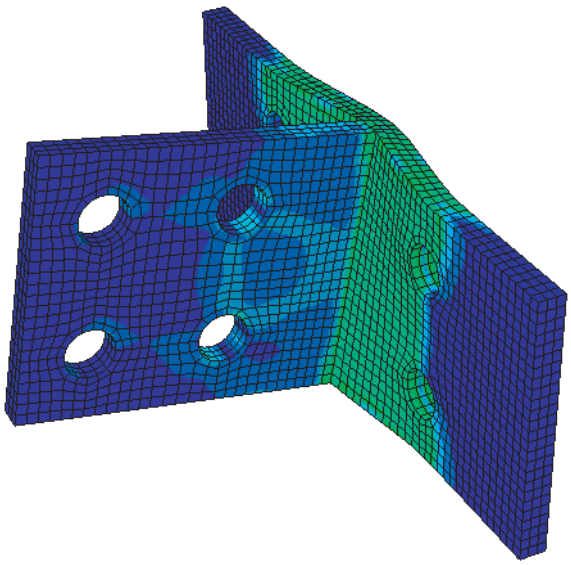

Figure 57. Flexural failure of retrofit (deformations are exaggerated).

Clearly from the previous analysis, the flange thickness is a governing variable influencing the stiffness as well as the maximum load carrying capacity for the WT retrofit. Hence for the WT retrofits, the primary variable that will be changed for observing the behavior of the retrofit will be the flange thickness.

Finite Element Analysis for Determining Typical Web Gap Distortions and Member Forces Before and After Retrofit

A finite element model of a few typical bridges with cross frames was created from available bridge design plans. One bridge (Bridge A) is a continuous composite plate girder built in 1969 over SR 31 in St. Joseph County, Indiana. The bridge has X-type cross frames. Another bridge (Bridge B) has K-type cross frames and is a continuous welded steel plate girder and continuous steel beam bridge built in 1972 over SR 63 in Vigo County, Indiana. It should be noted that these structures were selected for typical sizes and dimensions for the girders and cross frames. They were then analyzed to examine cross frame behavior before and after retrofit. However, neither bridge was retrofitted as noted herein.

A finite element model of one entire bridge span of Bridge B was created, as shown in Figure 58. The ends of the girders were simply supported. The large model was used to estimate the amount of relative distortion that occurs between bridge girders when an HS20 truck is placed over the midspan of the bridge. This distortion was then used to estimate the increase in the force applied by the cross frames on the stiffener, perpendicular to the girder web, before and after the stiffener detail was retrofitted.

To evaluate an upper bound behavior, the full weight of 72 kips of an HS20 Truck was applied as a single concentrated load on one interior girder at the center of the span. The deflections of the girders were measured, and the maximum inter-girder displacement was found to be about 0.2 in. In reality, the girders will be continuous over the supports instead of simply supported. Also, an HS15 fatigue truck load would be applied with corresponding distributed axle weights and not as a single concentrated load. The bridge deck was not modeled which would have redistributed the HS15 fatigue truck load to adjacent girders. Hence, the model created here will overestimate the real distortions of the bridge and thus provide an approximate upper bound. This means that for this bridge, inter-girder vertical displacement will most likely not exceed 0.2 inches.

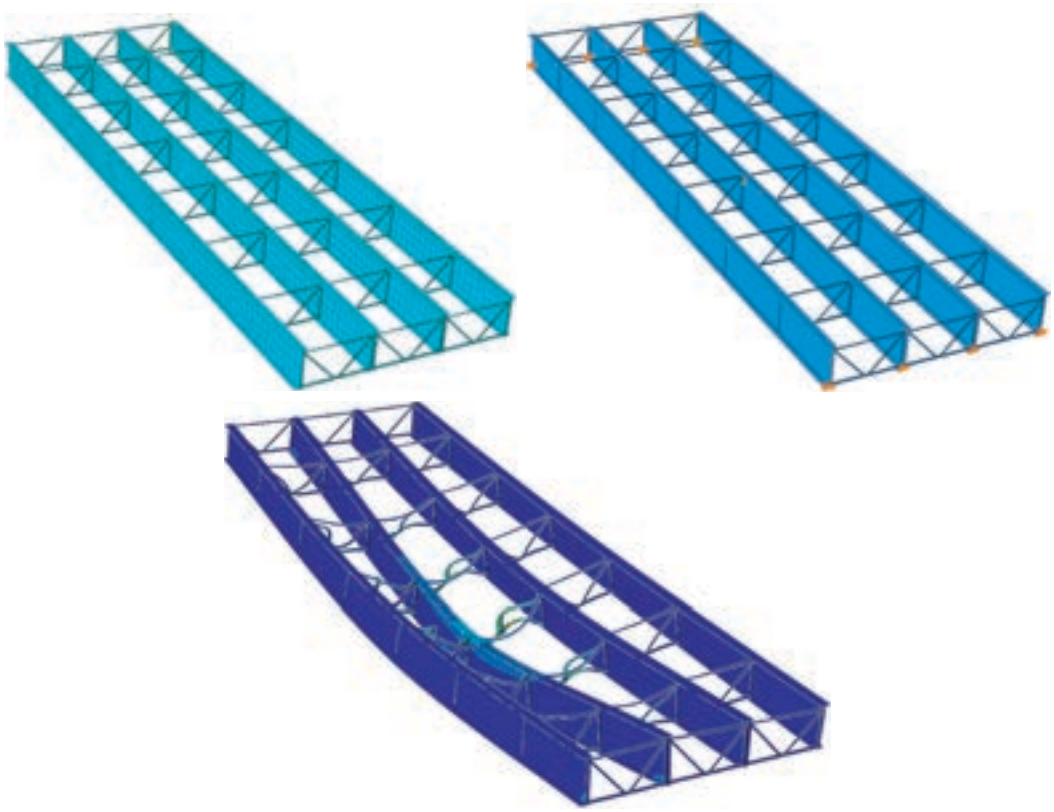

Figure 58. Bridge B—finite element model of single span with exaggerated displacements.

Figure 59. Bridge B—K-type cross frame.

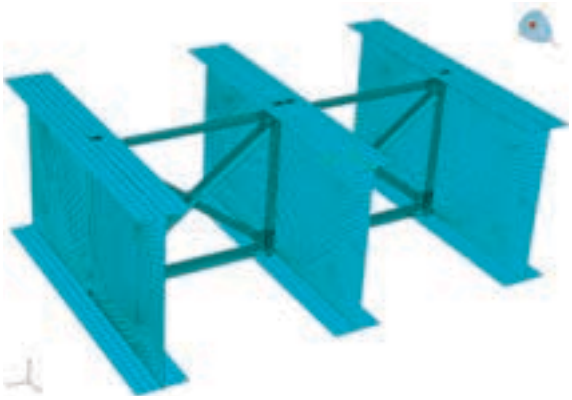

Figure 60. Bridge A—X cross frame.

For the Bridge B and Bridge A models shown in Figures 59 and 60, the upper flanges of the exterior girders were fixed in place while the middle girder was displaced downward. The web gap distortion was measured. The forces in the angles of the cross frames were calculated and components taken to calculate the horizontal force exerted by the angles on the stiffener near the top flange of the exterior girder. This was done again for the model after retrofitting the stiffener connections with WT sections with flange and web thicknesses of 0.75-in. Two web gaps between the stiffener and the girder flange in the bridge models were used: 0.5 in. and 1.75 in. Also, the angle thickness in the cross bracing was varied from 0.5 in. to 0.75 in. The force and web gap distortions were measured before and after retrofitting. The stress distribution in the two bridge models is shown in Figures 61 and 62, and the results of the analysis are given in Tables 24 through 27.

From the results obtained, it can be seen that the web gap distortion decreases significantly after the retrofit is in place while the force applied on the stiffener by the cross braces increases. The distortions after retrofit reduce by a factor that ranged from 6 to 64. Generally, larger displacements of the middle girder produced larger reductions in the web gap distortion after retrofitting. This is primarily because of the increase in the web gap distortion before retrofit with increase in the girder displacement.

A thickness increase in cross-brace angles produced a greater jump in cross-brace force after retrofit. Similarly, a greater reduction in web gap distortion after retrofit was

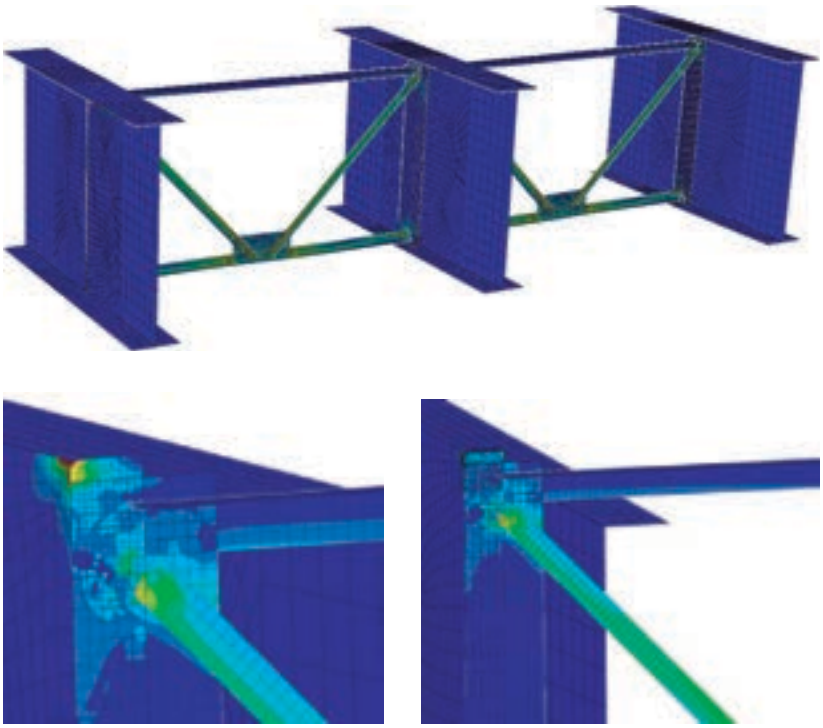

Figure 61. Bridge B—stress distribution before and after retrofit.

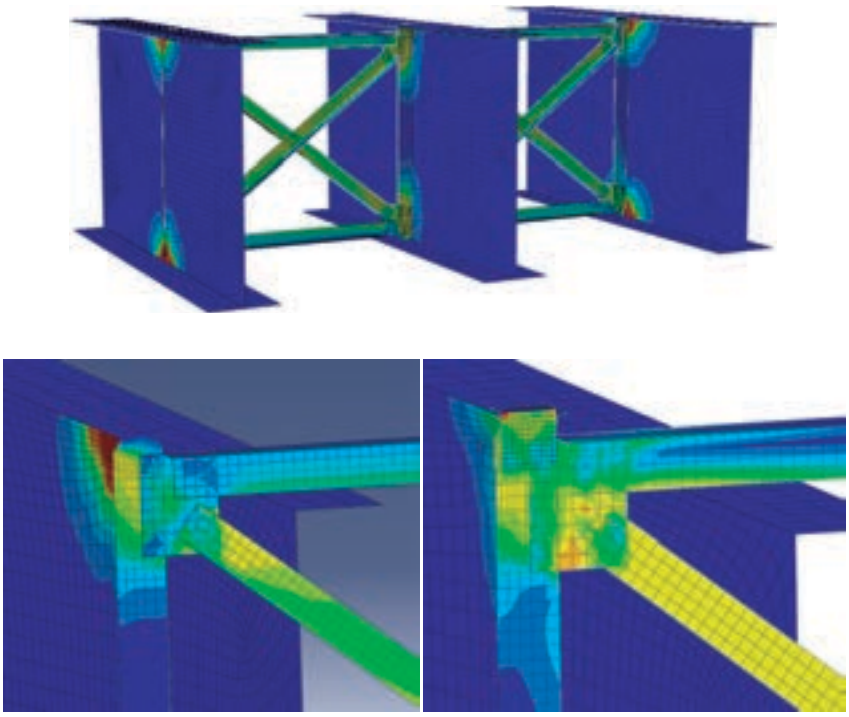

Figure 62. Bridge A—stress distribution before and after retrofit.

Table 24. Bridge B web gap distortions before and after retrofit.

Web Gap - 0.5"	Angles - 0.5"	
Displacement 0.5	Distortion (inch)	Before/After Ratio
Before Retrofit	0.00340	6.1
After Retrofit	0.00056	
Displacement 1.0	Distortion (inch)	Before/After Ratio
Before Retrofit	0.00415	6.8
After Retrofit	0.00061	
Displacement 1.5	Distortion (inch)	Before/After Ratio
Before Retrofit	0.00448	7.3
After Retrofit	0.00062	

Web Gap - 0.5"	Angles - 0.75"	
Displacement 0.5	Distortion (inch)	Before/After Ratio
Before Retrofit	0.00488	5.9
After Retrofit	0.00083	
Displacement 1.0	Distortion (inch)	Before/After Ratio
Before Retrofit	0.00662	7.0
After Retrofit	0.00095	
Displacement 1.5	Distortion (inch)	Before/After Ratio
Before Retrofit	0.00744	7.6
After Retrofit	0.00098	

Web Gap - 1.75"	Angles - 0.5"	
Displacement 0.5	Distortion (inch)	Before/After Ratio
Before Retrofit	0.01642	14.7
After Retrofit	0.00111	
Displacement 1.0	Distortion (inch)	Before/After Ratio
Before Retrofit	0.02111	19.9
After Retrofit	0.00106	
Displacement 1.5	Distortion (inch)	Before/After Ratio
Before Retrofit	0.02333	25.7
After Retrofit	0.00091	

Web Gap - 1.75"	Angles - 0.75"	
Displacement 0.5	Distortion (inch)	Before/After Ratio
Before Retrofit	0.02309	13.3
After Retrofit	0.00173	
Displacement 1.0	Distortion (inch)	Before/After Ratio
Before Retrofit	0.03211	17.8
After Retrofit	0.00181	
Displacement 1.5	Distortion (inch)	Before/After Ratio
Before Retrofit	0.03620	20.9
After Retrofit	0.00173	

Table 25. Bridge B forces before and after retrofit.

Web Gap - 0.5" Angles - 0.5"		
Displacement 0.5	Force (kip)	After/Before Ratio
Before Retrofit	15.4	1.2
After Retrofit	18.0	
Displacement 1.0	Force (kip)	After/Before Ratio
Before Retrofit	16.5	1.2
After Retrofit	19.6	
Displacement 1.5	Force (kip)	After/Before Ratio
Before Retrofit	16.2	1.2
After Retrofit	19.2	

Web Gap - 0.5" Angles - 0.75"		
Displacement 0.5	Force (kip)	After/Before Ratio
Before Retrofit	18.2	1.4
After Retrofit	25.0	
Displacement 1.0	Force (kip)	After/Before Ratio
Before Retrofit	17.9	1.5
After Retrofit	26.6	
Displacement 1.5	Force (kip)	After/Before Ratio
Before Retrofit	15.8	1.6
After Retrofit	24.9	

Web Gap - 1.75" Angles - 0.5"		
Displacement 0.5	Force (kip)	After/Before Ratio
Before Retrofit	11.5	1.6
After Retrofit	18.0	
Displacement 1.0	Force (kip)	After/Before Ratio
Before Retrofit	11.8	1.7
After Retrofit	19.5	
Displacement 1.5	Force (kip)	After/Before Ratio
Before Retrofit	11.0	1.7
After Retrofit	19.1	

Web Gap - 1.75" Angles - 0.75"		
Displacement 0.5	Force (kip)	After/Before Ratio
Before Retrofit	12.1	2.1
After Retrofit	24.9	
Displacement 1.0	Force (kip)	After/Before Ratio
Before Retrofit	10.6	2.5
After Retrofit	26.5	
Displacement 1.5	Force (kip)	After/Before Ratio
Before Retrofit	8.0	3.1
After Retrofit	24.8	

Table 26. Bridge A web gap distortions before and after retrofit.

Web Gap - 0.5" Angles - 0.5"		
Displacement 0.5	Distortion (inch)	Before/After Ratio
Before Retrofit	0.00827	10.1
After Retrofit	0.00082	
Displacement 1.0	Distortion (inch)	Before/After Ratio
Before Retrofit	0.01155	13.9
After Retrofit	0.00083	
Displacement 1.5	Distortion (inch)	Before/After Ratio
Before Retrofit	0.01518	18.2
After Retrofit	0.00083	

Web Gap - 0.5" Angles - 0.75"		
Displacement 0.5	Distortion (inch)	Before/After Ratio
Before Retrofit	0.01071	12.1
After Retrofit	0.00088	
Displacement 1.0	Distortion (inch)	Before/After Ratio
Before Retrofit	0.01942	21.0
After Retrofit	0.00093	
Displacement 1.5	Distortion (inch)	Before/After Ratio
Before Retrofit	0.02813	29.8
After Retrofit	0.00094	

Web Gap - 1.75" Angles - 0.5"		
Displacement 0.5	Distortion (inch)	Before/After Ratio
Before Retrofit	0.04368	17.7
After Retrofit	0.00247	
Displacement 1.0	Distortion (inch)	Before/After Ratio
Before Retrofit	0.07184	32.0
After Retrofit	0.00225	
Displacement 1.5	Distortion (inch)	Before/After Ratio
Before Retrofit	0.09857	44.1
After Retrofit	0.00223	

Web Gap - 1.75" Angles - 0.75"		
Displacement 0.5	Distortion (inch)	Before/After Ratio
Before Retrofit	0.05609	21.7
After Retrofit	0.00259	
Displacement 1.0	Distortion (inch)	Before/After Ratio
Before Retrofit	0.11279	41.7
After Retrofit	0.00270	
Displacement 1.5	Distortion (inch)	Before/After Ratio
Before Retrofit	0.17132	64.3
After Retrofit	0.00266	

Table 27. Bridge A forces before and after retrofit.

Web Gap - 0.5" Angles - 0.5"		
Displacement 0.5	Force (kip)	After/Before Ratio
Before Retrofit	16.9	2.7
After Retrofit	46.1	
Displacement 1.0	Force (kip)	After/Before Ratio
Before Retrofit	20.9	2.4
After Retrofit	49.2	
Displacement 1.5	Force (kip)	After/Before Ratio
Before Retrofit	23.7	2.1
After Retrofit	50.5	

Web Gap - 0.5" Angles - 0.75"		
Displacement 0.5	Force (kip)	After/Before Ratio
Before Retrofit	15.9	3.0
After Retrofit	48.3	
Displacement 1.0	Force (kip)	After/Before Ratio
Before Retrofit	19.1	2.7
After Retrofit	51.3	
Displacement 1.5	Force (kip)	After/Before Ratio
Before Retrofit	20.9	2.6
After Retrofit	54.3	

Web Gap - 1.75" Angles - 0.5"		
Displacement 0.5	Force (kip)	After/Before Ratio
Before Retrofit	8.9	4.7
After Retrofit	42.0	
Displacement 1.0	Force (kip)	After/Before Ratio
Before Retrofit	12.2	3.5
After Retrofit	42.4	
Displacement 1.5	Force (kip)	After/Before Ratio
Before Retrofit	14.5	3.0
After Retrofit	43.5	

Web Gap - 1.75" Angles - 0.75"		
Displacement 0.5	Force (kip)	After/Before Ratio
Before Retrofit	7.2	6.1
After Retrofit	43.7	
Displacement 1.0	Force (kip)	After/Before Ratio
Before Retrofit	10.0	4. 7
After Retrofit	46.6	
Displacement 1.5	Force (kip)	After/Before Ratio
Before Retrofit	11.6	4.0
After Retrofit	46.8	

observed for larger web gaps. Also, the cross frame forces increase by greater amounts after retrofit for larger web gaps.

Another factor is the type of cross frame. Larger distortion reductions and greater bracing forces were observed for X-type braces than for K-type braces. For K-type braces, the distortions reduce by a factor of 6 to 26, while the force jumps by a factor of 1.2 to 3.1. For the X-type braces, the distortions reduce by a factor of 10 to 64, while the force jumps by a factor of 2.1 to 4.7. This shows that the type of cross frame influences the web gap distortions and cross frame forces before and after retrofitting. However, in the analysis, the girders are rigidly held, and the connections are all pinned over the overlapping surfaces. Hence, the amount of rigidity in the models is larger than what it should be. Also the models are not able to simulate the effects of the presence of an existing fatigue crack at the stiffener ends. An existing fatigue crack would result in a more flexible girder web, which should increase the web gap distortion and reduce the forces in the cross bracings after retrofit.

The displacements and forces for the two bridges when the displacement of the middle girder is 0.2 in. were also calculated. The results are shown in Table 28. It can be seen here too that the web gap distortion reduces by a factor of about 10 and the force in the cross frames increases by a factor of 1.8 to 8.3, depending upon cross frame type.

Based upon finite element analysis of the two bridge models, it can be observed that a wide range of angle bracing forces were developed before and after retrofit. Variations occur due to changes in the cross frame type, angle bracing thickness and web gap size. No single value will be representative of the variation in brace force before and after retrofit. Nevertheless, a factor of two was selected as the multiplier for the force to be applied after retrofitting the test specimens compared to the initial force needed for pre-cracking the specimen. This value is at the lower end of the force ratio noted previously, but it is probably realistic when considering the softening effect of the web gap crack and associated drilled retrofit hole which was not considered in the analysis.

To verify if the load factor of two is also applicable to angle retrofits, finite element analysis was again performed for Bridge A that has an X-type bracing. The middle girder in the model was pushed downward, as shown in Figure 63, and the horizontal load in the cross bracings was measured. Three displacements of 0.5 in., 1.0 in., and 1.5 in. were induced in the middle girder. Also, two different web gap sizes of 0.5 in.

Table 28. Bridge A and B distortions and forces before and after retrofit for 0.2 inch displacement.

Bridge B

Web Gap - 1.75" Angles - 0.75"		
Displacement 0.2	Distortion (inch)	Before/After Ratio
Before Retrofit After Retrofit	0.00869 0.00080	10.9
Displacement 0.2	Force (kip)	After/Before Ratio
Before Retrofit After Retrofit	6.3 11.3	1.8

Bridge A

Web Gap - 1.75" Angles - 0.75"		
Displacement 0.2	Distortion (inch)	Before/After Ratio
Before Retrofit After Retrofit	0.02609 0.00256	10.2
Displacement 0.2	Force (kip)	After/Before Ratio
Before Retrofit After Retrofit	4.8 39.9	8.3

and 1.75 in. were used, and two different cross bracing thicknesses of 0.5 in. and 0.75 in. were used. A single-angle retrofit of thickness 0.75 in. was used in the analysis. The results are given in Table 29. The factor for the forces varies from 2.1 to 5.2. Similar to the previous finite element model for the WTs, the current finite element model also has a greater stiffness than will be actually present. Hence, the factor of two that was used earlier for the WTs can also be used for the angle retrofits.

Test Results

As stated earlier, the purpose of the cyclic retrofit testing was to evaluate the effectiveness of the retrofit elements to mitigate distortion-induced fatigue cracking. The testing protocol involved application of a cyclic out-of-plane distortion to pre-crack the specimen, followed by installation of the retrofit. After retrofit, the specimen was subjected to a constant amplitude load for 5,000,000 cycles minimum to evaluate the ability of the retrofit to halt or significantly decrease further growth of the distortion-induced fatigue cracks.

After the retrofit is installed, it behaves like a fixed end for the stiffener. It was found that after the retrofit is installed, a force larger than 40 kips cannot be applied to the specimen as it results in fatigue cracking occurring in the stiffener itself after about 2.5 million cycles of loading. Hence, in order to evaluate the fatigue behavior of the retrofit, and not the stiffener connection, the load that can be applied on the

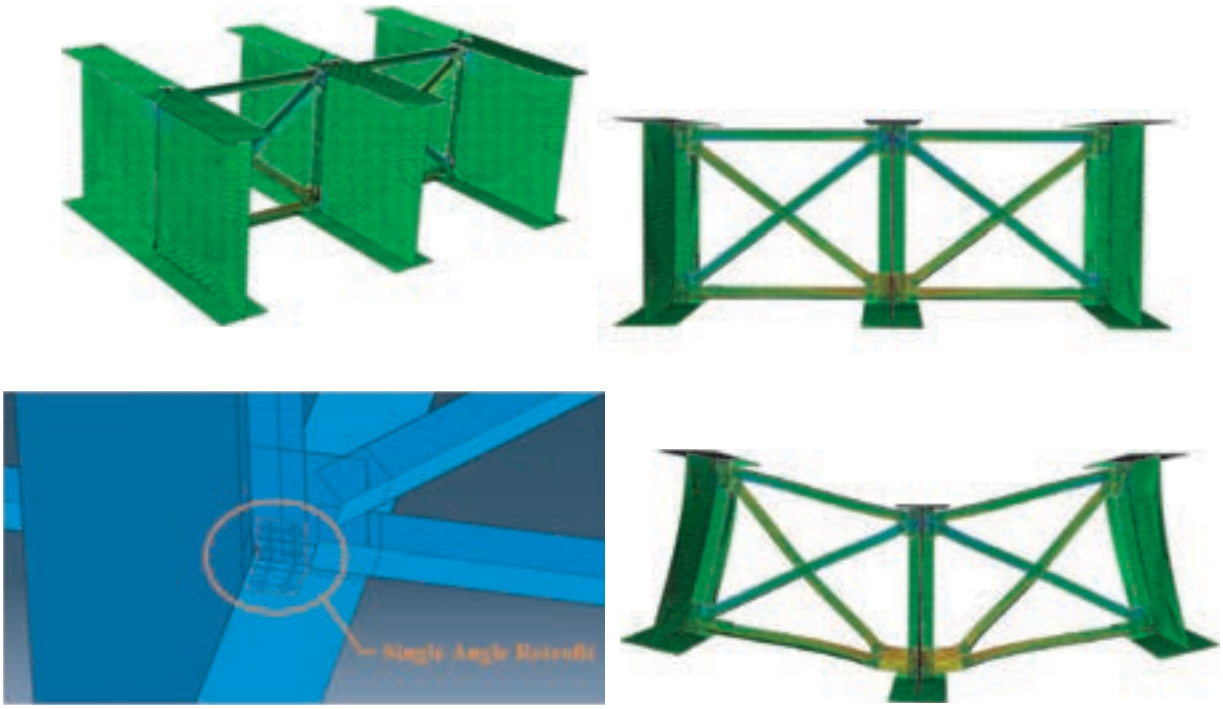

Figure 63. X-brace type bridge A finite element model retrofitted with single-angle retrofit.

Table 29. Cross bracing forces for bridge A (single-angle retrofit).

Web Gap - 0.5" Bracings - 0.5"			Web Gap - 0.5" Bracings - 0.75"		
Displacement 0.5	Force (kip)	After/Before Ratio	Displacement 0.5	Force (kip)	After/Before Ratio
Before Retrofit After Retrofit	15.7 39.2	2.5	Before Retrofit After Retrofit	14.7 39.6	2.7
Displacement 1.0	Force (kip)	After/Before Ratio	Displacement 1.0	Force (kip)	After/Before Ratio
Before Retrofit After Retrofit	19.1 43.4	2.3	Before Retrofit After Retrofit	17.2 44.0	2. 6
Displacement 1.5	Force (kip)	After/Before Ratio	Displacement 1.5	Force (kip)	After/Before Ratio
Before Retrofit After Retrofit	21.3 44.7	2.1	Before Retrofit After Retrofit	18.6 47.1	2.5

Web Gap - 1.75" Bracings - 0.5"			Web Gap - 1.75" Bracings - 0.75"		
Displacement 0.5	Force (kip)	After/Before Ratio	Displacement 0.5	Force (kip)	After/Before Ratio
Before Retrofit After Retrofit	8.8 38.0	4.3	Before Retrofit After Retrofit	7.3 38.1	5.2
Displacement 1.0	Force (kip)	After/Before Ratio	Displacement 1.0	Force (kip)	After/Before Ratio
Before Retrofit After Retrofit	11.4 42.3	3.7	Before Retrofit After Retrofit	9.4 42.4	4.5
Displacement 1.5	Force (kip)	After/Before Ratio	Displacement 1.5	Force (kip)	After/Before Ratio
Before Retrofit After Retrofit	13.2 43.8	3.3	Before Retrofit After Retrofit	10.7 45.5	4.3

specimen after the retrofit was subject to a maximum limit of about 40 kips.

A total of thirteen test specimens were tested. Table 30 shows the specimen parameters, loading force, and distortion values and results of the experimental testing for all thirteen specimens. Note that the pre-cracking force shown for every specimen in the Table is only the initial pre-cracking force needed at the beginning of cycling. As fatigue cracks develop in the specimen, the force needed to maintain a constant distortion starts reducing due to the increasing flexibility of the cracked specimen. A more detailed description of the specimen tests, web gap distortions, and cyclic loads used before and after retrofit, along with photographs of retrofits and fatigue cracks are found in Appendix D. None of the WT retrofits experienced any fatigue cracking. Double-angle retrofits also did not experience any fatigue cracking. However, fatigue cracks did develop in the single-angle retrofits, except for the 1-in.-thick, single-angle retrofits.

It is important to note that in all the tests performed, no retrofit holes were drilled to remove the crack tip after pre-cracking, except in case of the "RH" specimens. This was done to simulate the worst possible condition for the retrofit. Ideally, a retrofit hole would also be drilled if a fatigue crack is present along with installing the retrofit. Since no retrofit holes were drilled for most of the specimens, more load was transferred to the retrofit from the specimen web as the distortion-induced fatigue cracks grew. This would effectively test the retrofit in the worst condition. Also, it allowed the research team to observe whether or not the retrofit was stiff enough to halt or notably slow fatigue crack growth. This was considered to be an indirect measure of the effectiveness of the retrofit.

Most of the WT retrofits were installed with four bolts in the web and four bolts in the flange of the retrofit as shown in Figure 64. For one subassembly, retrofit holes of 1 in. diameter were drilled to remove the crack tip. For another subassembly, the WT retrofits were installed with only two bolts in the web and the flange of the retrofit to examine the influence of the reduced stiffness of the retrofit on the fatigue strength. These retrofits are shown in Figure 65.

Figure 66 shows typical double-angle and single-angle retrofits installed. None of the double-angle retrofits showed any indications of fatigue cracking. Single-angle retrofits, on the other hand, did experience fatigue cracking as shown in Figure 67. Three of the four ¾-in.-thick, single-angle retrofits tested experienced fatigue cracks. However, none of the 1-in.-thick, single-angle retrofits tested experienced any fatigue cracking. Fatigue cracks in single-angle retrofits tended to

Table 30. Distortion-induced fatigue test results.

Specimen	Web Gap Length (inch)	Distortion (inch)	Pre-cracking Force (kip)	No. of Cycles for Pre-cracking	Loading Force (kip)	No. of Cycles after Retrofit	Retrofit Type	Retrofit Thickness (inch)	Damage
1	1.5	0.01	9.6	3,066,000	20	10,479,000	WT	0.75	No new cracks or crack growth
2	1.5	0.01	13.1	2,395,000	20	5,356,000	WT	0.5	No new cracks or crack growth
3	1.5	0.02	24.7	710,000	40	5,129,000	WT	0.75	No new cracks, Little crack growth
4	1.5	0.02	24.9	970,000	40	5,049,000	WT	0.5	No new cracks, Little crack growth
5	1.5	0.01	8.75	3,770,000	20	5,039,000	WT (RH)	0.75	No new cracks or crack growth
6	0.75	0.01	20.4	1,996,000	40	5,113,000	WT	0.75	No new cracks, Little crack growth
7	1.5	0.01	9.8	3,403,000	20	10,327,000	WT (B)	0.75	No new cracks or crack growth
8	0.75	0.0075	14.7	12,676,000	30	5,254,000	DA	0.625	No new cracks or crack growth
9	0.75	0.01	29.6	5,955,000	40	4,345,000	DA	0.625	New crack initiation and growth in web-to-flange welds
10	0.75	0.0075	14.9	5,034,400	30	5,179,000	DA	0.75	No new cracks or crack growth
11	0.75	0.01	30	1,178,000	40	5,308,000	SA	0.75	New crack initiation in web-to-flange welds and crack in SA retrofit
12	0.75	0.0075	18.9	8,960,000	30	10,235,000	SA	0.75	New crack initiation and growth in web-to-flange welds and cracks in both SA retrofits
13	0.75	0.0075	27	925,000	30	5,153,000	SA	1	No new cracks or crack growth

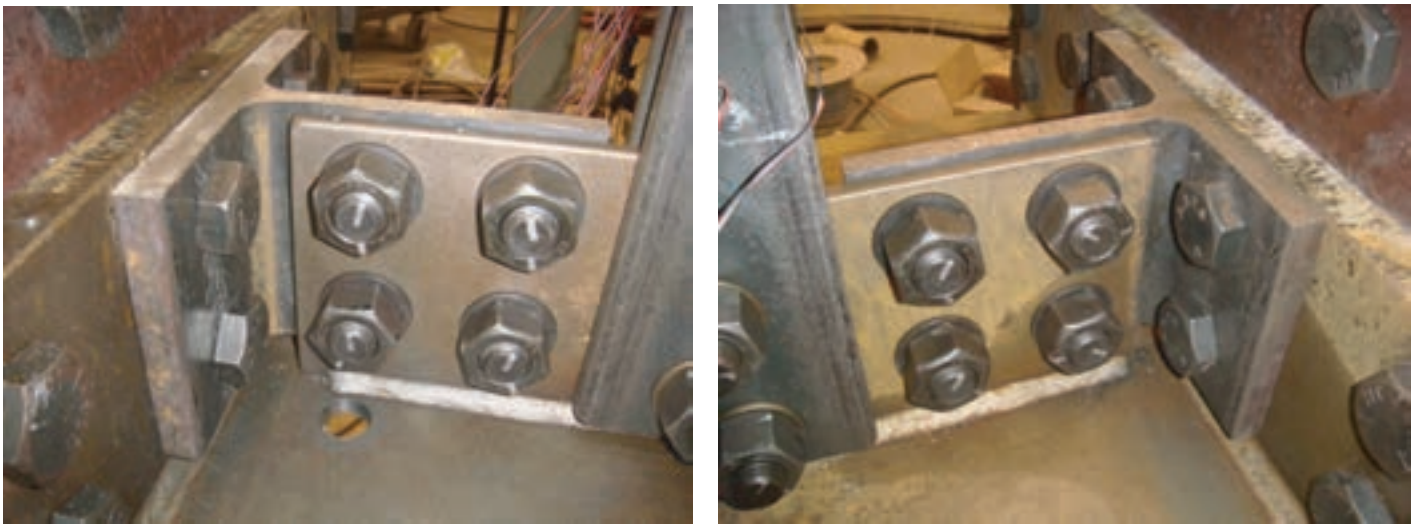

Figure 64. Typical WT retrofits installed with and without retrofit hole.

Figure 65. WT retrofit installed with reduced number of bolts.

initiate on the top side of the flange of the retrofit away from the web of the specimen. The cracks traveled downwards and into the junction of the web and flange of the single angle. The fatigue cracks were initiated due to high stresses generated at the retrofit flange due to the asymmetry of the single-angle retrofit, which resulted in noticeable out-of-plane bending of the retrofit. Also, since the single-angle retrofit is considerably less stiff than a comparable double-angle or WT retrofit, the end of the stiffener plate at which the single-angle retrofit is installed behaves more like a pinned end connection than a fixed end connection. Hence, most of the tension force gets transferred from the stiffener into the retrofit through the top side of the retrofit, resulting in fatigue cracking at the top of the retrofit instead of what would be expected at the bottom side in the case of a fixed end connection.

Figure 66. Typical double-angle and single-angle retrofits.

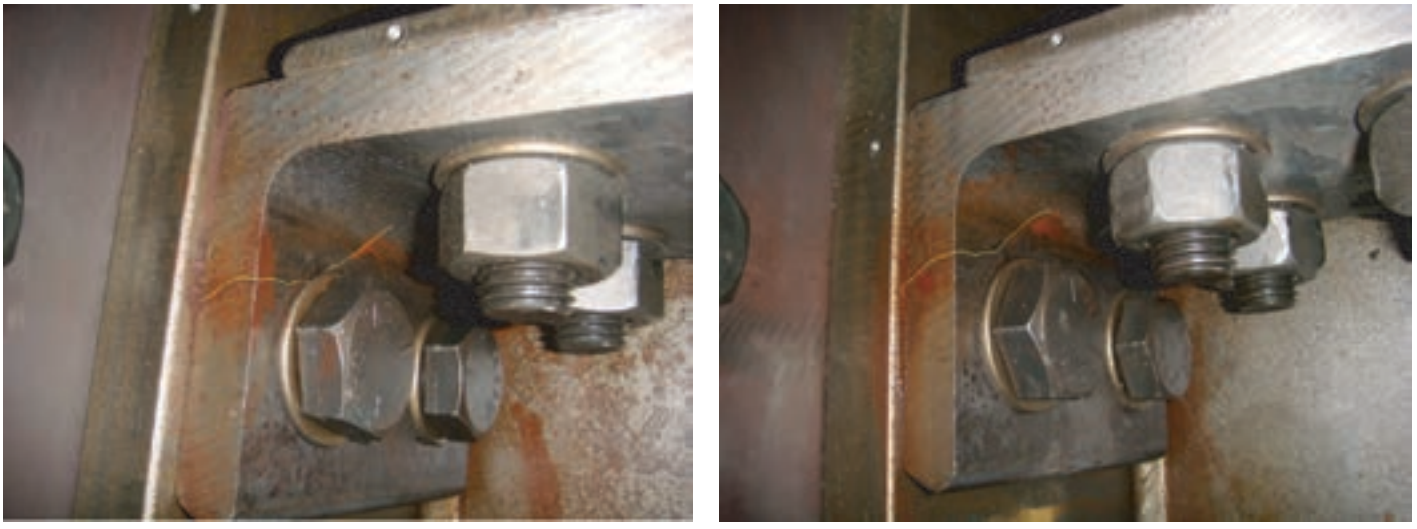

Figure 67. Typical fatigue cracks in single-angle retrofits (cracks marked with line).

CHAPTER 4

Conclusions

The conclusions and suggestions in this chapter are based upon an analysis and evaluation of data gathered in experimental laboratory studies and of truck data gathered previously by various state transportation agencies. Also, an evaluation of existing fatigue analysis procedures was conducted and recommendations for modifying those procedures were developed through the incorporation of recent research results by others and the observations developed in this study.

- Finite fatigue life predictions based upon the use of a curve to approximate the lifetime average ADTT based upon the present single-lane ADTT were found to lead to inconsistencies and errors in the prediction of the remaining fatigue life. The use of a closed form solution for the effect of traffic growth developed in NCHRP Project 12-51 by Fu et al. (2003) is recommended for inclusion in the updated version of Section 7.
- The resistance factor for the finite fatigue life was found to be well correlated with the 95th percentile for the minimum life. The values for R_R were correspondingly recalculated for the Evaluation Life and the mean life levels and are suggested for inclusion in the revised Section 7 provisions.
- Presence of multiple trucks was found to have some influence on the loading used for fatigue evaluation. The primary factors involved were the ADTT level, the number of lanes available, and the bridge span length. WIM data with a high-resolution time stamp of 0.01 seconds from four different states and for different bridge configurations were used to study the effect of multiple trucks on various bridge structures. It was found that an equation involving the three predominant variables could be used to reasonably model multiple truck presence.
- Remaining fatigue life was found to have an undesirable connotation and it was believed that a new methodology to evaluate fatigue serviceability would be useful. Hence, a non-dimensional parameter, named the fatigue serviceability index (FSI), was developed to evaluate the condition and the assessment outcome with respect to fatigue. The method uses bridge age, predicted fatigue life, structural configuration, and bridge importance to determine the fatigue evaluation.
- When the bridge age exceeds the predicted fatigue life of a given bridge detail then the remaining life predicted in the current MBE Section 7 provisions gives a negative fatigue life. A method was developed to recalculate the cumulative frequency distribution based upon satisfactory performance with no observed fatigue cracking so that a positive remaining life would be produced at all times. The new method utilizes a modified frequency distribution with the same reliability factor as the original estimate.
- An experimental study was conducted to evaluate the fatigue strength of members with tack welds. A number of existing bridge structures, especially older riveted structures, have tack welds that were used for fit-up during construction and which were simply left in place.
  - Finite element analysis indicated that the weld toe of the first line of tack welds experiences the maximum stress. Hence, it was expected that the weld toe of the first tack weld would be the critical location for fatigue due to the stress concentration at that location. This was confirmed through fatigue testing, as all of the fatigue cracks that formed were observed to initiate at the weld toe of the first tack weld.
  - Variations in the number of tack welds, length of tack welds, position of the tack weld relative to the fastener hole, and orientation of the tack welds relative to the load were all studied. The number, length, and orientation of the tack welds were not observed to significantly affect the fatigue strength of the tack welds.
  - Based upon the results of 17 cyclic tests, it was found that the cyclic strength of the tack welds all exceeded the mean value of the Category D curve, were closest to the mean fatigue strength for the Category C curve, and exceeded the design fatigue strength for Category C.

Hence, it was concluded that the fatigue strength can be adequately modeled using a Category C design life as given per the LRFD Bridge Design Specification.

- Distortion-induced fatigue cracking of steel bridge web gap details was studied. Both analytical modeling and experimental testing were used to evaluate the behavior of retrofits used to stiffen the connection and mitigate distortion-induced fatigue cracking.
  - Results of a survey conducted to evaluate current fatigue inspection and evaluation procedures revealed that distortion-induced fatigue cracking is the most frequently encountered type of fatigue distress observed among various state transportation agencies. Both softening and stiffening, in addition to hole drilling, were reported as methods being used to retrofit distortion-induced cracking.
  - Finite element analysis was used to study the stiffness and response of WT sections used for retrofit elements to mitigate distortion-induced cracking. It was found that increasing the thickness of the flange of the WT section is more effective in controlling out-of-plane distortions than increasing the web thickness.
  - Finite element analysis was conducted to analytical study forces developed in cross frame angle members of representative bridges since they frequently provide the out-of-plane forces that cause distortion of the girder web. It was found that out-of-plane deformations decreased significantly after a retrofit was installed, but the force in the brace was found to increase notably, often two-fold or more for a given differential girder displacement. Predicting the out-of-plane force in the retrofit is quite difficult because it was found to be influenced by several different factors, including the differential deflection of adjacent girders, the size and length of the cross-brace members, the size of the girder web gap, the thickness of the girder web, and the geometry of the retrofit detail. These factors must be accounted for through refined analysis or field measurement if the retrofit forces are to be accurately assessed. Otherwise, a sufficiently stiff retrofit must be installed to minimize the distortion and transfer the out-of-plane force to the girder flange.
  - Experimental testing was used to evaluate the cyclic performance of three retrofit details bolted to the girder flange and the vertical connection plate: WT sections, double angles, and single angles. Thirteen test specimens were used with variations in the retrofit thicknesses and web gap dimensions. It was observed that fatigue cracking initiated very quickly for all girder sections tested when subjected to out-of-plane distortions. Although the cracks initiated quickly, growth slowed considerably as it propagated away from the web gap region due to softening of the connection. (After the retrofit, the fatigue cracks were not removed by hole drilling to permit evaluation while still in this most critical condition.) No subsequent fatigue cracks were observed to occur for any of the WT or double-angle retrofit details which were installed. The fatigue cracks left intact were observed to not grow further or to only grow by a small amount. A number of single-angle retrofits were observed to develop active fatigue cracks, but none of them failed after at least 5,000,000 additional loading cycles after retrofit. The cracking is believed to be due to a lack of symmetry and greater flexibility of the single-angle retrofit.
  - If a stiffening retrofit is used, it is recommended that either a WT section or a pair of angles should be used if possible. Thicknesses greater than ½-in should be utilized to provide sufficient connection stiffness with at least four bolts used to connect the retrofit to the web and flanges. If single angles are used for the retrofit, then a relatively thick angle should be used. Also, retrofit holes should always be drilled to remove the crack tip of the distortion-induced fatigue cracks that have been detected.

Proposed Revisions to MBE Section 7

A number of revisions have been proposed to the provisions in Section 7 of the Manual of Bridge Evaluation. The suggested revisions are shown with a strike out through deletions to existing provisions and new underlining shown for new provisions.

The new proposed provisions for Section 7 of the MBE are shown in Appendix E of this document. Moreover, examples to illustrate use of the proposed Section 7 provisions are provided in Appendix F.

Options for Design Consideration

Based upon the results of this study for the evaluation of fatigue serviceability, a number of options for inclusion in the LRFD Bridge Design Specification may wish to be considered. These are noted below.

- Presence of multiple trucks, either side-by-side in adjacent lanes or back-to-back in the same lane, may cause increased stresses that are not considered when a single lane of loading only is used for fatigue design. For most common bridge applications this factor is not very dominant and the single truck for a Fatigue II loading is quite adequate. However, for certain structures, such as two-girder bridges or trusses that support multiple lanes and with long span lengths and a high ADTT volume, then a multiple lane loading stress range amplification factor can

become quite important. A multiple presence factor was developed for inclusion in MBE Section 7 to model this loading situation.

- Tack welds are classified as Category E in the LRFD Bridge Design Specification. A number of fatigue tests were conducted in conjunction with this study and it was found that the cyclic lives were most closely aligned with the Category C mean fatigue strength. Although the Category E classification may be partially to discourage the practice of leaving tack welds in place after fabrication, it appears that the classification can be improved to be no worse than Category D.
- The finite fatigue life is based on an approximation when accounting for the growth of traffic volume by estimating the ADTT in a single lane of traffic averaged over the design life. The LRFD commentary indicates that it may be best to consult with a traffic engineer. However, a closed form solution for incorporating traffic growth into the finite fatigue life equation was developed in conjunction with NCHRP Study 12-51 for existing bridges, and perhaps a procedure similar in approach should be developed for inclusion in the finite-life equation directly in Chapter 6 or the single lane ADTT expression in Chapter 3.

References

AASHTO. (1990). *Guide Specifications for Fatigue Evaluation of Existing Steel Bridges.* American Association of State Highway and Transportation Officials, Washington, D.C.

AASHTO. (1994). *Manual for Condition Evaluation of Bridges.* Second Edition, American Association of State Highway and Transportation Officials, Washington, D.C.

AASHTO. (2003). *Guide Manual for Condition Evaluation and Load and Resistance Factor Rating (LRFR) of Highway Bridges.* American Association of State Highway and Transportation Officials, Washington, D.C.

AASHTO. (2010). *LRFD Bridge Design Specifications.* Fifth Edition, American Association of State Highway and Transportation Officials, Washington, D.C.

AASHTO. (2011). *Manual for Bridge Evaluation.* Second Edition, American Association of State Highway and Transportation Officials, Washington, D.C.

AISC. (2010). *Steel Construction Manual.* 14th Edition, American Institute of Steel Construction, Chicago.

BridgeTech, Tennessee Technological University, and Mertz, D. (2007). *NCHRP Report 592: Simplified Live Load Distribution Factor Equations.* Transportation Research Board, Washington, D.C.

Cohen, H., Fu, G., Dekelbab, W., and Moses, F. (2003). "Predicting Truck Weight Spectra under Weight Limit Changes and Its Application to Steel Bridge Fatigue Assessment." *Journal of Bridge Engineering,* ASCE, Vol. 8, No. 5, p. 312–322.

Connor, R. J. and Fisher, J. W. (2006). "Identifying Effective and Ineffective Retrofits for Distortion Induced Fatigue Cracking in Steel Bridges using Field Instrumentation." *Journal of Bridge Engineering,* ASCE, 11(6), pp. 745–752.

Council of Standards Australia. (2004a). AS5100.6-2004 Bridge Design Part 6: Steel and Composite Construction.

Council of Standards Australia. (2004b). AS5100.7-2004 Bridge Design Part 6: Rating of Existing Bridges.

Eurocode: EN 1993—1–9: 2005 Eurocode 3: Design of Steel Structures—Part 1–9: Fatigue, 2005.

Fisher, J. W., Frank, K. H., Hirt, M. A., and McNamee, B. M. (1970). *NCHRP Report 102: Effects of Weldments on the Fatigue Strength of Steel Beams.* Transportation Research Board, Washington, D.C.

Fisher, J. W., Albrecht, P. A., Yen, B. T., Klingerman, D. J. and McNamee, B. M. (1974). *NCHRP Report 147: Fatigue Strength of Steel Beams with Welded Stiffeners and Attachments.* Transportation Research Board, Washington, D.C.

Fisher, J. W., Hausammann, H., Sullivan, M. D., and Pense, A. W. (1979). *NCHRP Report 206: Detection and Repair of Fatigue Damage in Welded Highway Bridges.* Transportation Research Board, Washington, D.C.

Fisher, J. W., Berthelemy, B. M., Mertz, D. R., and Edinger, J. A. (1980). *NCHRP Report 227: Fatigue Behavior of Full-Scale Welded Bridge Attachments.* Transportation Research Board, Washington, D.C.

Fisher, J. W., Jin, J., Wagner, D. C., and Yen, B. T. (1990). *NCHRP Report 336: Distortion-Induced Fatigue Cracking in Steel Bridges.* Transportation Research Board, Washington, D.C.

Fisher, J. W., Nussbaumer, A., Keating, P. B., and Yen, B. T. (1993). *NCHRP Report 354: Resistance of Welded Details under Variable Amplitude Long-Life Fatigue Loading.* Transportation Research Board, Washington, D.C.

Fu, G. and Tang, J. (1995). "Risk Based Proof Load Requirements for Bridge Evaluation." *Journal of Structural Engineering,* ASCE, 121(3), pp. 542.

Fu, G., Feng, J., Dekelbab, W., Moses, F., Cohen, H., Mertz, D., and Thompson, P. (2003). *NCHRP Report 495: Effect of Truck Weight on Bridge Network Costs.* Department of Civil and Environmental Engineering, Wayne State University.

Keating, P. B. and Fisher, J. W. (1986). *NCHRP Report 286: Evaluation of Fatigue Tests and Design Criteria on Welded Details.* Transportation Research Board, Washington, D.C.

Moses, F., Schilling, C. G., and Raju, K. S. (1987). *NCHRP Report 299: Fatigue Evaluation Procedures for Steel Bridges.* Transportation Research Board, Washington, D.C.

Zhou, Y. (1994). "Fatigue Strength Evaluation of Riveted Bridge Members." Doctoral Dissertation, Lehigh University, Bethlehem, Pennsylvania.

Zokaie, T., Osterkamp, T. A., and lmbsen, R. A. (1991). "Distribution of Wheel Loads on Highway Bridges." Final Report to NCHRP for Project 12-26.

APPENDICES A THROUGH D

Appendices A through D are not published herein, but they are available on the *NCHRP Report 721* summary webpage at http://www.trb.org/Main/Blurbs/167233.aspx

APPENDIX E

PROPOSED SECTION 7 OF MBE

E.1 SECTION 7 (STRIKE-OUT FORMAT)

SECTION 7

7.1—LOAD-INDUCED VERSUS DISTORTION-INDUCED FATIGUE

Fatigue damage has been traditionally categorized as either ~~due to~~ load-induced or distortion-induced fatigue damage.

Load-induced fatigue is that due to the in-plane stresses in the steel plates that comprise bridge member cross-sections. These in-plane stresses are those typically calculated by designers during bridge design or evaluation.

Distortion-induced fatigue is that due to secondary stresses in the steel plates that comprise bridge member cross-sections. These stresses, which are typically caused by out-of-plane forces, can only be calculated with very refined methods of analysis, far beyond the scope of a typical bridge design or evaluation. These secondary stresses are minimized through proper detailing.

C7.1

The previous most comprehensive codification of fatigue evaluation of steel bridges, the *Guide Specifications for Fatigue Evaluation of Existing Steel Bridges* (AASHTO, 1990), explicitly considered only load-induced fatigue damage. The Guide Specifications referenced NCHRP Report 299 for considering "fatigue due to secondary bending stresses that are not normally calculated," NCHRP (1987).

These "plates" may be the individual plates which comprise a built-up welded, bolted, or riveted plate girder, or may be the flanges, webs, or other elements of rolled shapes.

The traditional approximate methods of analysis utilizing lateral live-load distribution factors have encouraged bridge designers to discount the secondary stresses induced in bridge members due to the interaction of longitudinal and transverse members, both main and secondary members.

Detailing to minimize the potential for distortion-induced fatigue, such as connecting transverse connection plates for diaphragms and floorbeams to both the compression and tension flanges of girders, is specified in LRFD Design Article 6.6.1.3.

7.2—LOAD-INDUCED FATIGUE -DAMAGE EVALUATION

7.2.1—Application

~~Article 7.2 includes t~~Two levels of fatigue evaluation are specified for load-induced fatigue: the infinite-life check of Article 7.2.4 and the finite-life calculations of Article 7.2.5. Only bridge details which fail the infinite-life check are subject to the more complex finite-life fatigue evaluation.

~~Cumulative fatigue damage of uncracked members subject to load-induced stresses shall be assessed according to the provisions of Article 7.2.~~ Except for the case of riveted connections and tack weld details specified below, the list of detail categories to be considered for load-induced fatigue-damage evaluation, and illustrative examples of these categories are shown in LRFD Design Table 6.6.1.2.3-1 ~~and Figure 6.6.1.2.3-1~~.

The base metal at net sections of riveted connections shall be evaluated based upon the requirements of Category C, given in LRFD Design Table 6.6.1.2.3-1, instead of ~~the~~ Category D as specified for new designs. The exception is for riveted members of poor physical condition, such as with missing rivets or indications of punched holes, in which case Category D shall be used.

C7.2.1

The initial infinite-life check should be made with the simplest, least refined stress-range estimate. If the detail passes the check, no further refinement is required. The stress-range estimate for the infinite-life check should be refined before the more complex procedures of the finite-life fatigue evaluation are considered.

For new design, the base metal at net sections of riveted connections is specified to be Category D. This represents the first cracking of a riveted member, which is highly redundant internally. Category C more accurately represents cracking that has propagated to a critical size. This increase in fatigue life for evaluation purposes is appropriate due to the redundancy of riveted members.

Tack welds may be evaluated based upon the requirements of Category C, given in LRFD Design Table 6.6.1.2.3-1.

Tack welds were frequently left in place in riveted connections. The tack welds were used to hold the members in place initially prior to placement of the rivets. Tack welds in this context are typically less than 2-in in length. The strength of tack welds was found to conform to fatigue Category C based on laboratory testing.

As uncertainty is ~~removed~~ reduced from the evaluation by more refined analysis or site-specific data, the increased certainty is reflected in lower partial load factors, summarized in Table 7.2.2.1-1 and described in Articles 7.2.2.1 and 7.2.2.2.

~~If cracks have already been visually detected, a more complex fracture mechanics approach for load-induced fatigue damage evaluation is required instead of the procedure specified herein. Further, the expense and trouble of a fracture mechanics analysis may not be warranted. Generally, upon visual detection of fatigue cracking, the majority of the fatigue life has been exhausted and retrofitting measures should be initiated.~~ If cracks have been visually detected then the fatigue life evaluation procedure specified herein should be used with caution. Generally, upon visual detection of load-induced fatigue cracking, the majority of the fatigue life has been exhausted and retrofitting measures should be initiated. Alternatively, a fracture mechanics approach can be used to evaluate the fatigue crack damage.

The partial load factors specified in Article 7.2 were adapted from the *Guide Specifications for Fatigue Evaluation of Existing Steel Bridges* (AASHTO, 1990).

7.2.2—Estimating Stress Ranges

C7.2.2

The effective stress range shall be estimated as:

$$\text{~~}(\Delta f)_{eff} = R_s \Delta f\text{~~} \quad (\Delta f)_{eff} = R_p R_s \Delta f \qquad (7.2.2\text{-}1)$$

where:

R_p = The multiple presence factor, calculated as described in Article 7.2.2.1 for calculated stress ranges, or 1.0 for measured stress ranges

R_s = The stress-range estimate partial load factor, calculated as $R_{sa}R_{st}$, unless otherwise specified, summarized in Table 7.2.2.1-1, and

Δf = Measured effective stress range; or ~~75 percent of the~~factored calculated stress range due to the passage of the fatigue truck as specified in LRFD Design Article 3.6.1.4 for Fatigue II Load Combination, or the calculated stress range due to a fatigue truck determined by a truck survey or weigh-in-motion study

The calculated stress range~~, either measured or calculated,~~ is ~~the stress range~~ due to a single truck in a single lane on the bridge.

~~The 0.75 applied to the calculated stress range due to the passage of the LRFD fatigue truck represents the load factor for live load specified for the fatigue limit state in LRFD Design Table 3.4.1-1.~~

The multiple presence factor takes into account the effect of trucks present simultaneously in multiple lanes instead of a single lane loading. When using measured stress ranges, the multiple presence factor should not be used in the equation, as the effects of multiple presence are already reflected in the measured stress ranges.

The load factor is 0.75 for live load specified for the Fatigue II limit state (finite load-induced fatigue life) in LRFD Design Table 3.4.1-1.

7.2.2.1—Calculating Estimated Stress Ranges

The multiple presence factor R_p shall be calculated

as:

$R_p = 0.988 + 6.87x10^{-5} (L) + 4.01x10^{-6} [ADTT]_{PRESENT} + 0.0107/(n_L)$
≥ 1.0 (7.2.2.1-1)

where

L = span length in feet,

$[ADTT]_{PRESENT}$ = Present average number of trucks per day for all directions of truck traffic including all lanes on the bridge, and

n_L = number of lanes.

Two sources of uncertainty are present in the calculation of effective stress range at a particular fatigue detail:

- Uncertainty associated with analysis, represented by the analysis partial load factor, R_{sa}, and
- Uncertainty associated with assumed effective truck weight, represented by the truck-weight partial load factor, R_{st}.

The limits used in developing the equation are noted as follows: $2 \leq n_L \leq 4$; $[ADTT]_{PRESENT} < 8{,}000$ for $n_L=2$; 11,000 for $n_L=3$, and 13,000 for $n_L=4$, and 30 ft < L < 220 ft. These are the ranges used in the analysis, based on the WIM data available. Use of these equations may be justified outside of these ranges, but are not based on experimental evidence. The multiple presence factor is applicable to longitudinal parallel members only. For transverse members, use $R_P = 1.0$.

Table 7.2.2.1-1—Partial Load Factors: R_{sa}, R_{st}, and R_s

Fatigue-Life Evaluation Methods	Analysis Partial Load Factor, R_{sa}	Truck-Weight Partial Load Factor, R_{st}	Stress-Range Estimate Partial Load Factor, R_s[a]
For Evaluation or Minimum Fatigue Life			
Stress range by simplified analysis, and truck weight per LRFD Design Article 3.6.1.4	1.0	1.0	1.0
Stress range by simplified analysis, and truck weight estimated through weigh-in-motion study	1.0	0.95	0.95
Stress range by refined analysis, and truck weight per LRFD Design Article 3.6.1.4	0.95	1.0	0.95
Stress range by refined analysis, and truck weight by weigh-in-motion study	0.95	0.95	0.90
Stress range by field-measured strains	N/A	N/A	0.85
For Mean Fatigue Life			
All methods	N/A	N/A	1.00

[a] In general, $R_s = R_{sa}R_{st}$

7.2.2.1.1—For ~~the~~ Determination of Evaluation or Minimum Fatigue Life

In the calculation of effective stress range for the determination of evaluation or minimum fatigue life, the stress-range estimate partial load factor shall be taken as the product of the analysis partial load factor and the truck-weight partial load factor:

$$R_s = R_{sa}R_{st} \qquad (7.2.2.1.1\text{-}1)$$

If the effective stress range is calculated through refined methods of analysis, as defined in LRFD Design Article 4.6.3:

$$R_{sa} = 0.95 \qquad (7.2.2.1.1\text{-}2)$$

otherwise:

$$R_{sa} = 1.0 \qquad (7.2.2.1.1\text{-}3)$$

If the effective truck weight is estimated through a weight-in-motion study at, or near, the bridge:

$$R_{st} = 0.95 \qquad (7.2.2.1.1\text{-}4)$$

otherwise:

$$R_{st} = 1.0 \qquad (7.2.2.1.1\text{-}5)$$

7.2.2.1.2—For ~~the~~ Determination of Mean Fatigue Life

In the calculation of effective stress range for the determination of mean fatigue life, the stress-range estimate partial load factor shall be taken as 1.0.

7.2.2.2—Measuring Estimated Stress Ranges

The effective stress range may be estimated through field measurements of strains at the fatigue-prone detail under consideration under typical traffic conditions. The effective stress range shall be ~~taken~~ computed as the cube root of the weighted sum of the cubes of the measured stress ranges, as given in:

$$(\Delta f)_{eff} = R_s \left(\Sigma \gamma_i \Delta f_i^3\right)^{\frac{1}{3}} \quad (7.2.2.2\text{-}1)$$

where:

γ_i = Percentage of cycles at a particular stress range and

Δf_i = The particular stress range in a measured stress range histogram of magnitude greater than one half of the constant-amplitude-fatigue-threshold of the fatigue prone detail under consideration, i.e. > $\Delta F_{TH}/2$.

7.2.2.2.1—For ~~the~~ Determination of Evaluation or Minimum Fatigue Life

Where field-measured strains are used to generate an effective stress range, R_s, for the determination of evaluation or minimum fatigue life, the stress-range estimate partial load factor shall be taken as 0.85.

7.2.2.2.2—For ~~the~~ Determination of Mean Fatigue Life

Where field-measured strains are used to generate an effective stress range, R_s, for the determination of mean fatigue life, the stress-range estimate partial load factor shall be taken as 1.0.

7.2.3—Determining Fatigue-Prone Details

Bridge details are only considered prone to load-induced fatigue damage if they experience a net tensile stress. Thus, fatigue damage need only be evaluated if, at the detail under evaluation:

C7.2.2.2

Field measurements of strains represent the most accurate means to estimate effective stress ranges at fatigue-prone details.

The *AASHTO LRFD Bridge Design Specifications* assume that the maximum stress range is twice the effective stress range. It is unlikely that the maximum stress range during the service life of the bridge will be captured during a limited field ~~testing~~ measurement session; therefore means to extrapolate from the measured ~~effective~~ stress range histogram to the maximum stress range must be used.

~~The *AASHTO LRFD Bridge Design Specifications* assume that the maximum stress range is twice the effective stress range. If the effective truck weight is significantly less than 54 kips, a multiplier more than two should be considered. Similarly, for a measured effective truck weight greater than 54 kips a multiplier less than two would be appropriate.~~

The lower portion of field measured stress range histograms must be truncated in order to avoid underestimating the effective stress range.

C7.2.3

The multiplier of two in the equation represents the assumed relationship between maximum stress range and effective stress range, as specified in the *AASHTO LRFD Bridge Design Specifications*.

~~$2R_s(\Delta f)_{tension} > f_{dead\text{-}load\ compression}$~~

$$2(\Delta f)_{tension} > f_{dead\text{-}load\ compression} \quad (7.2.3\text{-}1)$$

When measured stress ranges are used to evaluate fatigue life, the multiplier of two in the equation should be reconsidered based upon the discussion of Article C7.2.2.2.

If the effective truck weight is significantly less than 54 kips, a multiplier more than two should be considered. Similarly, for a measured effective truck weight greater than 54 kips a multiplier less than two would be appropriate.

where:

~~R_s = The stress range estimate partial load factor, specified in Article 7.2.2 and summarized in Table 7.2.2.1-1~~

$(\Delta f)_{tension}$ = ~~Factored t~~Tensile portion of the effective stress range ~~due to the passage of a fatigue truck~~ as specified in Article 7.2.2, and

$f_{dead\text{-}load\ compression}$ = Unfactored compressive stress at the detail due to dead load

7.2.4—Infinite-Life Check

C7.2.4

If:

$$(\Delta f)_{max} \le (\Delta F)_{TH} \quad (7.2.4\text{-}1)$$

Theoretically, a fatigue-prone detail will experience infinite life if all of the stress ranges are less than the constant amplitude fatigue threshold; in other words, if the maximum stress range is less than the threshold.

When measured stress ranges are used to evaluate fatigue life, the multiplier of two in the equation for $(\Delta f)_{max}$ should be reconsidered based upon the discussion of Article C7.2.2.2.

then:

$$Y = \infty \quad (7.2.4\text{-}2)$$

where:

$(\Delta f)_{max}$ = The maximum stress range expected at the fatigue-prone detail, which may be taken as:

- R_p times the factored calculated stress range due to the passage of the fatigue truck as specified in LRFD Design Article 3.6.1.4 for Fatigue I Load Combination

The load factor is 1.50 for live load specified for the Fatigue I limit state (infinite load-induced fatigue life) in LRFD Design Table 3.4.1-1.

- $2.0(\Delta f)_{eff}$ *; for calculated stress range due to a fatigue truck determined by a truck survey or weigh-in-motion study with* $R_{S=1.0}$

- Larger of maximum (Δf_i), $2.0(\Delta f)_{eff}$, or other suitable value; for measured stress ranges *with* $R_{S=1.0}$

When measured stress ranges are used to evaluate fatigue life, the maximum stress range should be taken as the larger value of two times field measured effective stress range or the field measured maximum stress range, unless another suitable value is justified.

$(\Delta F)_{TH}$ = The constant-amplitude fatigue threshold given in LRFD Design Table 6.6.1.2.5-3

Otherwise, the total fatigue life shall be estimated as specified in Article 7.2.5.

7.2.5—Estimating Finite Fatigue Life

7.2.5.1—General

~~Three~~ Four levels of finite fatigue life may be estimated:

- The minimum expected fatigue life (which equals the conservative design fatigue life),
- Evaluation 1 fatigue life (which is a somewhat less conservative fatigue life for evaluation),
- ~~The e~~Evaluation 2 fatigue life (which equals a more conservative fatigue life for evaluation), and
- The mean fatigue life (which equals the statistically most likely fatigue life).

The total finite fatigue life of a fatigue-prone detail, in years, shall be determined as:

$$Y = \frac{R_R A}{365 n \left(ADTT\right)_{SL} \left[\left(\Delta f\right)_{eff}\right]^3}$$

$$Y = \frac{\log\left[\frac{R_R A}{365 n \left[(ADTT)_{SL}\right]_{PRESENT} \left[(\Delta f)_{eff}\right]^3} g(1+g)^{a-1} + 1\right]}{\log(1+g)} \quad (7.2.5.1\text{-}1)$$

C7.2.5.1

Much scatter, or variability, exists in experimentally derived fatigue lives. For design, a conservative fatigue resistance two standard deviations shifted below the mean fatigue resistance or life is assumed. This corresponds to the minimum expected finite fatigue life of this Article. Limiting actual usable fatigue life to this design fatigue life is very conservative and can be costly. As such, means of estimating the two evaluation fatigue ~~life~~ lives and the mean finite fatigue life are also included to aid the evaluator in the decision making.

~~Figure C7.2.5.5-1 may be used to estimate the average number of trucks per day in a single lane averaged over the fatigue life, $(ADTT)_{SL}$, from the present average number of trucks per day in a single lane, $[(ADTT)_{SL}]_{present}$, the present age of the bridge, a, and the estimated annual traffic volume growth rates, g.~~

Recent research has made it possible to obtain a closed-form solution for the total finite fatigue life using an estimated traffic growth rate and the present $(ADTT)_{SL}$. For cases with zero traffic growth, a very small value of g should be selected (less than 0.01%) for use in the expression for Y.

where:

R_R = Resistance factor specified for evaluation, minimum, or mean fatigue life as given in Table 7.2.5.~~2~~1-1

A = Detail-category constant given in LRFD Design Table 6.6.1.2.5-1

n = Number of stress-range cycles per truck passage estimated according to Article 7.2.5.2

g = Estimated annual traffic-volume growth rate in percentage

a = Present age of the detail in years

$[(ADTT)_{SL}]_{PRESENT}$

= Present ~~Average~~ average number of trucks per day in a single lane~~ averaged over the fatigue life as specified in LRFD Design Article 3.6.1.4.2~~

$(\Delta f)_{eff}$ = The effective stress range as specified in Article 7.2.2

The resistance factors for fatigue life, specified in Table 7.2.5.~~2~~1-1, represent the variability of the fatigue life of the various detail categories, A through E′. The minimum life, evaluation 1 life and evaluation 2 life fatigue-life curves are shifted from the mean fatigue-life S-N curves in log-log space. Scatter of the fatigue lives at given stress range values from controlled laboratory testing provides statistical information on fatigue behavior of bridge details under cyclic loading. Accordingly, the probability of failure associated with each level of fatigue life, approaches 2 percent, 16 percent, 33 percent and 50 percent for the minimum, evaluation 1, evaluation 2 and mean fatigue lives, respectively. Typically, the minimum life or evaluation 1 life is used to evaluate the fatigue serviceability. If concerns are encountered regarding the computed fatigue serviceability, then the serviceability index can be revised according to Article 7.2.7.2.~~As the stress range estimate grows closer and closer to the actual value of stress range, the probability of failure associated with each level of fatigue life approaches two percent, 16 percent, and 50 percent for the minimum, evaluation, and mean fatigue lives, respectively. The minimum and evaluation fatigue life curves are two and one standard deviations off of the mean fatigue life S-N curves in log-log space, respectively. Thus, the partial resistance factors for mean and evaluation fatigue life are calculated as raised to the power of twice and one times the standard deviation of the log of experimental fatigue life for each detail category, respectively.~~

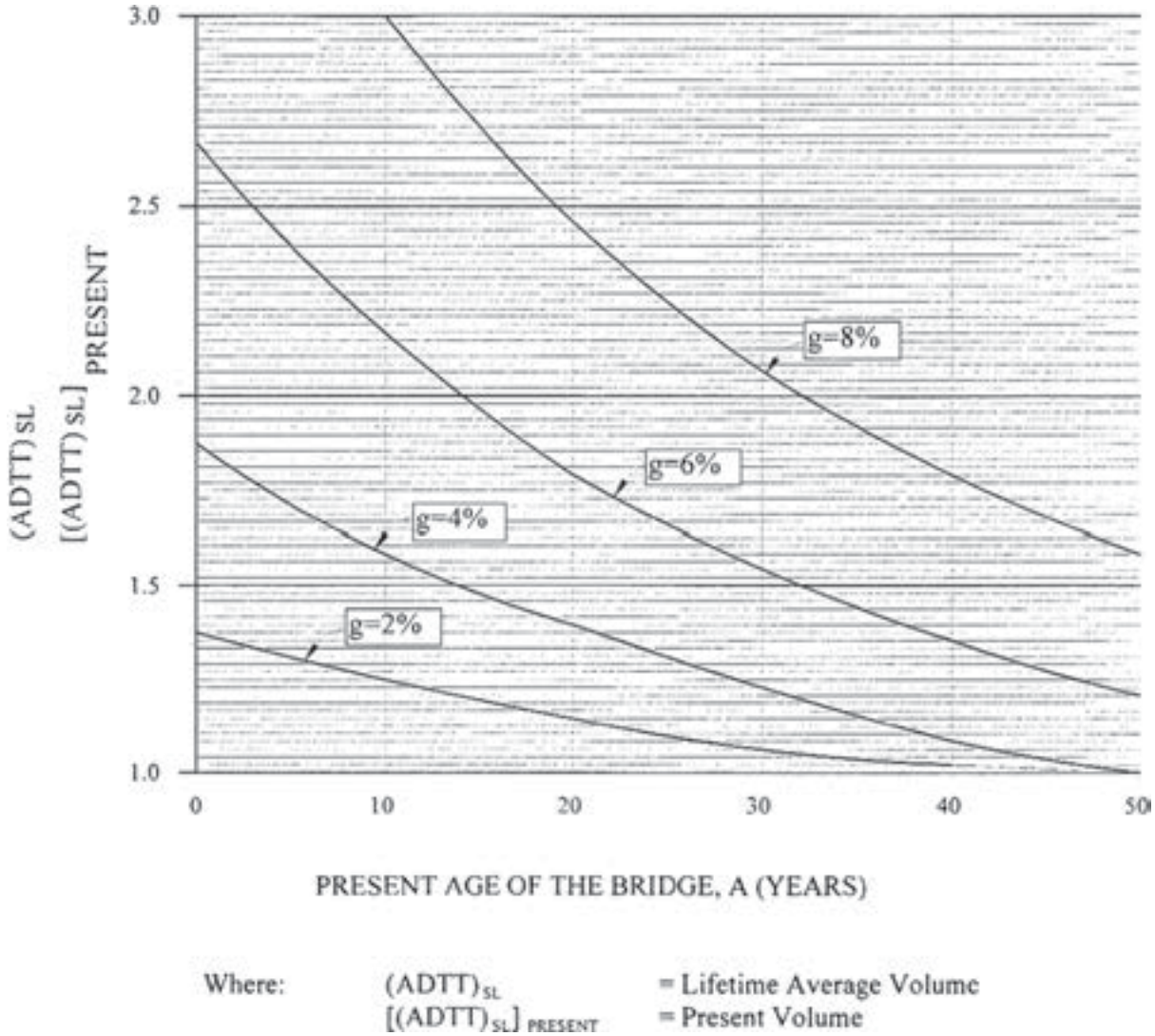

Figure C7.2.5.1-1—Lifetime Average Truck Volume for an Existing Bridge

Table 7.2.5.1-1 Resistance Factor for Evaluation, Minimum or Mean Fatigue Life, R_R

Detail Category (from Table 6.6.1.2.5-1 of the *LRFD Specifications*)	R_R			
	Minimum Life	Evaluation 1 Life	Evaluation 2 Life	Mean Life
A	1.0	1.5	2.2	2.9
B	1.0	1.3	1.7	2.0
B’	1.0	1.3	1.6	1.9
C	1.0	1.3	1.7	2.1
C’	1.0	1.3	1.7	2.1
D	1.0	1.3	1.7	2.0
E	1.0	1.2	1.4	1.6
E’	1.0	1.3	1.6	1.9

7.2.5.2—Estimating the Number of Cycles per Truck Passage

The number of stress-range cycles per truck passage may be estimated (in order of increasing apparent accuracy and complexity):

~~**Table 7.2.5.2-1—Resistance Factor for Evaluation, Minimum, or Mean Fatigue Life, R_R**~~

~~Detail Category~~[a]	~~R_R~~		
	~~Evaluation Life~~	~~Minimum Life~~	~~Mean Life~~
~~A~~	~~1.7~~	~~1.0~~	~~2.8~~
~~B~~	~~1.4~~	~~1.0~~	~~2.0~~
~~B′~~	~~1.5~~	~~1.0~~	~~2.4~~
~~C~~	~~1.2~~	~~1.0~~	~~1.3~~
~~C′~~	~~1.2~~	~~1.0~~	~~1.3~~
~~D~~	~~1.3~~	~~1.0~~	~~1.6~~
~~E~~	~~1.3~~	~~1.0~~	~~1.6~~
~~E′~~	~~1.6~~	~~1.0~~	~~2.5~~

~~[a] From LRFD Design Table 6.6.1.2.3-1 and Figure 6.6.1.2.3-1~~

- Through the use of LRFD Design Table 6.6.1.2.5-2,
- Through the use of influence lines, or
- By field measurements.

~~7.2.6 Acceptable Remaining Fatigue Life~~

~~The remaining fatigue life of a fatigue prone detail is the total fatigue life, as determined through Article 7.2.5, minus the present age of the bridge.~~

7.2.6 Fatigue Serviceability Index

7.2.6.1 Calculating the Fatigue Serviceability Index

The fatigue serviceability index shall be calculated as:

$$Q = \left(\frac{Y - a}{N}\right) GRI \qquad (7.2.6.1\text{-}1)$$

where:

N = Greater of Y or 100 years
G = Load Path Factor, as given in Table 7.2.6.1-1
R = Redundancy Factor, as given in Table 7.2.6.1-2
I = Importance Factor, as given in Table 7.2.6.1-3

Table 7.2.6.1-1 Load Path Factor G

Number of Load Path Members	G
1 or 2 members	0.8
3 members	0.9
4 or more members	1

Table 7.2.6.1-2 Redundancy Factor R

Type of Span	R
Simple	0.9
Continuous	1

C7.2.6

The fatigue serviceability index is a dimensionless relative measure of the performance of a structural detail, at a particular location in the structure, with respect to the overall fatigue resistance of the member.

The load path, redundancy and importance factors are risk factors that modify the fatigue serviceability index. They reduce the index from its base value, i.e. based on fatigue resistance alone, to a reduced value that reflects greater consequences from the lack of ability to redistribute the load (load path factor), lack of redundancy (redundancy factor), or use of the structure (importance factor). The net effect of a reduction in the index will be to move the composite index value to a lower value that may initiate a lower fatigue rating. These risk factors are similar to the ductility, redundancy and operational classification factors in the *AASHTO LRFD Bridge Design Specifications*. Improved quantification with time will possibly modify these factors.

The number of members that carry load when a fatigue truck is placed on the bridge is used to select the load path factor; e.g., two members for a two-girder bridge and for a typical truss structure; four or more members for a multi-beam or multi-girder bridge; etc. For diaphragms and secondary members, use G = 1.

Table 7.2.6.1-3 Importance Factor I

Structure or Location	Importance Factor, I
Interstate Highway Main Arterial State Route Other Critical Route	0.90
Secondary Arterial Urban Areas	0.95
Rural Roads Low ADTT routes	1.00

7.2.6.2 Recommended Actions Based on Fatigue Serviceability Index

The fatigue ratings and assessment outcomes as given in Table 7.2.6.2-1 are recommended as a guideline for actions that may be undertaken based on the obtained value for the fatigue serviceability index. A better fatigue rating may be assumed for Q values at the boundary of two ranges.

In the recommended actions provided, it is expected that based upon increasing risk, the inspection frequency of the bridge shall be increased on a case-by-case assessment by the bridge owner.

Table 7.2.6.2-1 Fatigue Rating and Assessment Outcomes

Fatigue Serviceability Index, Q	Fatigue Rating	Assessment Outcome
1.00 to 0.50	Excellent	Continue Regular Inspection
0.50 to 0.35	Good	Continue Regular Inspection
0.35 to 0.20	Moderate	Continue Regular Inspection
0.20 to 0.10	Fair	Increase Inspection Frequency
0.10 to 0.00	Poor	Assess Frequently
< 0.00	Critical	Consider Retrofit, Replacement or Reassessment

7.2.7—Strategies to Increase ~~Remaining~~ Fatigue ~~Life~~Serviceability Index

7.2.7.1—General

If the ~~remaining~~ fatigue serviceability index ~~life~~ is deemed unacceptable, the strategies of Articles 7.2.7.2 and 7.2.7.3 may be applied to enhance the fatigue ~~life~~serviceability index.

C7.2.7.1

Retrofit or load-restriction decisions should be made based upon the evaluation fatigue life unless the physical condition or fabrication quality of the bridge is poor. In general, it is uneconomical to limit the useful fatigue life of in-service bridges to the minimum (design) fatigue life.

If the estimated ~~remaining~~ fatigue serviceability index ~~life~~ based upon the evaluation fatigue life is deemed unacceptable, a fatigue life approaching the mean fatigue life can be used for evaluation purposes if the additional risk of fatigue cracking is acceptable.

7.2.7.2—Recalculate ~~the~~ Fatigue ~~Life~~ Serviceability Index

7.2.7.2.1—Through Accepting Greater Risk

In general, ~~the~~ evaluation 1 life of Article 7.2.5 is used in determining the ~~remaining~~ fatigue serviceability index ~~life~~ of a bridge detail according to Article 7.2.6. If the evaluator is willing to accept greater risk of fatigue cracking due to:

- Long satisfactory cyclic performance~~fatigue life~~ of the detail to date,
- A high degree of redundancy, and/or
- Increased inspection effort, e.g., decreased inspection interval, ~~or~~
- **Some combination of the above**

the ~~remaining~~ fatigue serviceability index~~life~~ may be determined using a fatigue life approaching the mean fatigue life of Article 7.2.5.

7.2.7.2.2—Through More Accurate Data

The calculated fatigue ~~life~~ serviceability index may be ~~enhanced~~ refined by using more accurate data as input to the fatigue-life estimate. Sources of improvement of the estimate include:

- Field measurement of stress ranges at the fatigue prone detail under construction
- 3-D finite element analysis for stresses at the fatigue prone detail under consideration
- Weigh-in-motion data of truck weights at or near the bridge site,
- Site-specific data on average daily truck traffic (ADTT) at or near the bridge site
- ~~Effective stress range or effective truck weight,~~
- ~~The average daily truck traffic (ADTT), or~~
- ~~The number of cycles per truck passage.~~

This strategy is based upon achieving a better estimate of the ~~actual~~ fatigue life.

7.2.7.2.3 Through Truncated Fatigue Life Distribution

When a negative fatigue serviceability index is obtained according to Article 7.2.6, the detail's fatigue serviceability index may be updated using equations below for mean, evaluation and minimum lives, provided a field inspection finds no evidence of fatigue cracking at the detail.

C7.2.7.2.3

The fatigue life of a structural detail is modeled using a lognormally distributed random variable, as shown in the figure C7.2.7.2.3-1. When the estimated life using Article 7.2.5 is smaller than the present age, the remaining life becomes negative as illustrated.

In this situation, if field inspection finds no

$$Y'_{mean} = 2.19 Y_{mean} e^{0.73\Phi^{-1}[0.18(1-P)+P]-0.27} \quad (7.2.7.2.3-1)$$

$$Y'_{eval\,2} = 2.19 Y_{mean} e^{0.73\Phi^{-1}[0.12(1-P)+P]-0.27} \quad (7.2.7.2.3-2)$$

$$Y'_{eval\,1} = 2.19 Y_{mean} e^{0.73\Phi^{-1}[0.074(1-P)+P]-0.27} \quad (7.2.7.2.3-3)$$

$$Y'_{minimum} = 2.19 Y_{mean} e^{0.73\Phi^{-1}[0.039(1-P)+P]-0.27} \quad (7.2.7.2.3-4)$$

where

Y'_{mean} = Updated mean life in years

Y_{mean} = Mean life in years without updating based on no detection of cracking at detail in question

Y'_{eval1} = Updated evaluation 1 life in years

Y'_{eval2} = Updated evaluation 2 life in years

$Y'_{minimum}$ = Updated minimum life in years

Φ^{-1} = Inverse of the standard normal variable's cumulative probability function (Table 7.2.7.2-1)

P = Probability of fatigue life being shorter than current age before updating based on no crack found

$$= \Phi\left[\frac{Ln\left(\frac{a}{2.19 Y_{mean}}\right)+0.27}{0.73}\right] \quad (7.2.7.2.3-5)$$

where a = Present age in years

Φ = Standard normal variable's cumulative probability function (Table 7.2.7.2-1)

evidence of cracking, the estimated life is an overly-conservative estimate. The low tail of the total life distribution is truncated up to the present life. The eliminated probability P is computed, and the resulting probability density function is divided by (1 – P) to ensure that the total probability under the distribution curve is still 1.0 as shown in Figure C7.2.7.2.3-2. Then the updated life is determined to maintain the same reliability level for fatigue life distribution. Functions Φ (.) and Φ^{-1}(.) are commonly available in commercial spreadsheet programs.

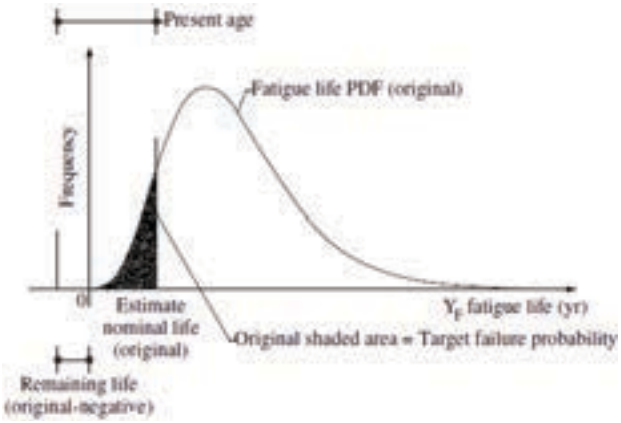

Fig C7.2.7.2.3-1 Probability Density Function of Fatigue Life and Estimated Life as a Value on Horizontal Axis

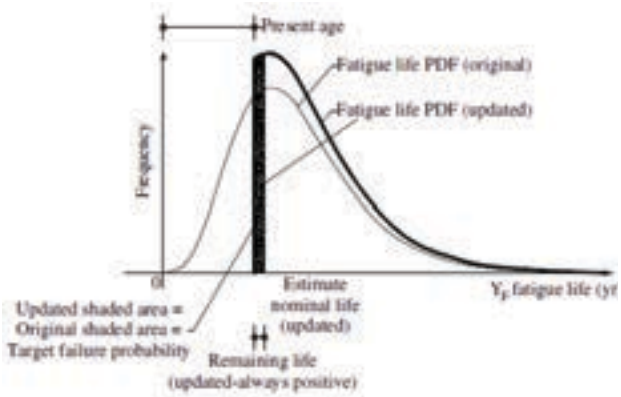

Fig C7.2.7.2.3-2 Truncated Probability Density Function of Fatigue Life and Updated Life as a value on the Horizontal Axis

Table 7.2.7.2-1 Cumulative Distribution Function Φ(x) for Standard Normal Variable x

x	0.00	0.01	0.02	0.03	0.04	0.05	0.06	0.07	0.08	0.09
0.0	0.5000	0.5040	0.5080	0.5120	0.5160	0.5199	0.5239	0.5279	0.5319	0.5359
0.1	0.5398	0.5438	0.5478	0.5517	0.5557	0.5596	0.5636	0.5675	0.5714	0.5753
0.2	0.5793	0.5832	0.5871	0.5910	0.5948	0.5987	0.6026	0.6064	0.6103	0.6141
0.3	0.6179	0.6217	0.6255	0.6293	0.6331	0.6368	0.6406	0.6443	0.6480	0.6517
0.4	0.6554	0.6591	0.6628	0.6664	0.6700	0.6736	0.6772	0.6808	0.6844	0.6879
0.5	0.6915	0.6950	0.6985	0.7019	0.7054	0.7088	0.7123	0.7157	0.7190	0.7224
0.6	0.7257	0.7291	0.7324	0.7357	0.7389	0.7422	0.7454	0.7486	0.7517	0.7549
0.7	0.7580	0.7611	0.7642	0.7673	0.7704	0.7734	0.7764	0.7794	0.7823	0.7852
0.8	0.7881	0.7910	0.7939	0.7967	0.7995	0.8023	0.8051	0.8078	0.8106	0.8133
0.9	0.8159	0.8186	0.8212	0.8238	0.8264	0.8289	0.8315	0.8340	0.8365	0.8389
1.0	0.8413	0.8438	0.8461	0.8485	0.8508	0.8531	0.8554	0.8577	0.8599	0.8621
1.1	0.8643	0.8665	0.8686	0.8708	0.8729	0.8749	0.8770	0.8790	0.8810	0.8830
1.2	0.8849	0.8869	0.8888	0.8907	0.8925	0.8944	0.8962	0.8980	0.8997	0.9015
1.3	0.9032	0.9049	0.9066	0.9082	0.9099	0.9115	0.9131	0.9147	0.9162	0.9177
1.4	0.9192	0.9207	0.9222	0.9236	0.9251	0.9265	0.9279	0.9292	0.9306	0.9319
1.5	0.9332	0.9345	0.9357	0.9370	0.9382	0.9394	0.9406	0.9418	0.9429	0.9441
1.6	0.9452	0.9463	0.9474	0.9484	0.9495	0.9505	0.9515	0.9525	0.9535	0.9545
1.7	0.9554	0.9564	0.9573	0.9582	0.9591	0.9599	0.9608	0.9616	0.9625	0.9633
1.8	0.9641	0.9649	0.9656	0.9664	0.9671	0.9678	0.9686	0.9693	0.9699	0.9706
1.9	0.9713	0.9719	0.9726	0.9732	0.9738	0.9744	0.9750	0.9756	0.9761	0.9767
2.0	0.9772	0.9778	0.9783	0.9788	0.9793	0.9798	0.9803	0.9808	0.9812	0.9817
2.1	0.9821	0.9826	0.9830	0.9834	0.9838	0.9842	0.9846	0.9850	0.9854	0.9857

7.2.7.3—Retrofit ~~The Bridge~~

If the recalculated fatigue ~~life~~ serviceability index is not ultimately acceptable, the actual fatigue ~~life~~ serviceability index may be increased by retrofitting the critical details to ~~change~~ improve the detail category and thus increase the ~~life~~fatigue serviceability index. This strategy increases the actual ~~life~~ fatigue serviceability index when further enhancement of the calculated ~~life~~fatigue serviceability index, through improved input, is no longer possible or practical.

C7.2.7.3

In certain cases, Owners may wish to institute more intensive inspections, in lieu of more costly retrofits, to assure adequate safety. Restricting traffic to ~~extend~~ increase the fatigue ~~life~~ serviceability index is generally not considered cost effective. If the ~~remaining fatigue life~~fatigue serviceability index is deemed inadequate, the appropriate option to ~~extend~~ increase the ~~life~~ fatigue serviceability index should be determined based upon the economics of the particular situation.

7.3—DISTORTION-INDUCED FATIGUE EVALUATION

C7.3

Distortion-induced fatigue is typically caused by out-of-plane deformation of the web plate that results in fatigue crack formation at details prone to such cracking under cyclic loading. The cracks tend to form in the member web at locations where there is a geometrical discontinuity, such as a vertical gap between a stiffener or connection plate and the girder flange or a horizontal gap between a gusset plate and a connection plate.~~a low-cycle fatigue phenomenon. In other words, relatively few stress-range cycles are required to initiate cracking at distortion-induced fatigue-prone details.~~ Distortion-induced fatigue is a stiffness problem (more precisely the lack thereof) versus a load problem.

Often, distortion-induced fatigue cracks initiate after

Existing bridges should not be assumed to be insensitive to distortion-induced cracking if fatigue cracks do not appear after a short period of time. Experience has shown that in some cases cracking may not be evident for 10 years after the beginning of service.~~Distortion-induced cracks have even been discovered on bridges prior to being opened to traffic.~~

relatively few stress-range cycles at fatigue-prone details. However, depending upon the magnitude of the out-of-plane distortion and the geometry of the web gap detail, the crack growth may be slow and a significant period of time may be required before they become large enough to be detected visually.~~As such, existing bridges which have experienced many truck passages, if uncracked, may be deemed insensitive to distortion-induced cracking, even under heavier permit loads.~~

7.3.1 Methods to Assess Distortion-Induced Cracking

Out-of-plane distortions caused by truck loading must be accommodated by the regions that contain unsupported web gaps. Even very small distortions can cause high local stresses that may induce fatigue cracking. Often, the fatigue cracks grow in a plane that is parallel to the primary stresses of the member and will slow down or even stop as the web gap becomes more flexible due to the presence of the crack. However, it is possible that the crack may turn and become perpendicular to the primary stress of the member, leading to more rapid crack growth. Therefore, distortion-induced fatigue cracks should be repaired.

C7.3.1

Typically, smaller web gaps are subject to higher distortion-induced stresses than larger web gaps provided the same demand for the out-of-plane distortion. The demand for out-of-plane distortion is determined by the global behavior of the structural system. Accurate quantification of the stress field in an unsupported web gap detail can be very difficult, even for finite element modeling or field measurement of strains and/or local deformations. This is especially the case when the dimension of the web gap is comparable to the thicknesses of the surrounding plates and the sizes of the connecting welds, resulting in high stress gradients across the web gap.

7.3.2 Retrofit Options for Distortion-Induced Fatigue Cracking

Retrofit should be considered if distortion-induced cracking has been detected. Two primary retrofit methods are available: softening or stiffening. The softening approach is used to increase the overall flexibility of the detail in question to accommodate the out-of-plane deformations without further cracking. The stiffening approach is used to minimize the local distortion by providing a positive load path for the forces that tend to cause the distortion. In either case, a hole should be drilled at the tip of each crack.

C7.3.2

In the softening retrofit, the flexibility of the detail in question is increased. Drilling holes to eliminate the tip of distortion-induced fatigue cracks will typically increase the local flexibility somewhat. However, the primary method used to increase the flexibility is to increase the size of the web gap. This can be effective since the out-of-plane bending stresses are related to the inverse of the square of the web gap length. One critical issue for this approach is to avoid an excessive increase of out-of-plane deformation resulting from the web gap enlargement. Removal of portions of a stiffener or other plate to increase the size of the web gap will also require removal of the connecting weld in those regions to provide a smooth, flush surface. Non-destructive inspection should be conducted to ensure that no undesirable gouges, notches or discontinuities remain.

In the stiffening retrofit, the stiffness of the detail in question is increased to minimize the out-of-plane distortion. Commonly, this will require the addition of a WT section, or a double or single angle section. Drilling retrofit holes to eliminate the tip of any distortion-induced fatigue cracks should be done prior to installation of the retrofit connection element. Typically, the installation of a retrofit element will increase the stiffness and significantly decrease the out-of-plane deformation at the detail. However, the force effect of the retrofit on the primary and secondary members

should be considered. One critical issue for this approach is to size the retrofit connection of sufficient thickness and strength for the loading forces to be generated at the new connection.

7.4—FRACTURE-CONTROL FOR OLDER BRIDGES

Bridges fabricated prior to the adoption of AASHTO's *Guide Specifications for Fracture-Critical Nonredundant Steel Bridge Members* (1978) may have lower fracture toughness levels than are currently deemed acceptable. Destructive material testing of bridges fabricated prior to 1978 to ascertain actual toughness levels may be justified. Decisions on fatigue evaluations of a bridge can be made based upon the information from these tests. ~~Without destructive material testing of bridges fabricated prior to 1978 to ascertain toughness levels, a fatigue life estimate greater than the minimum expected fatigue life is questionable. An even lower value of fatigue life, to guard against fracture, may be appropriate.~~

C7.4

The fatigue life of a steel bridge detail generally consists of crack initiation and stable crack propagation. The propagation stage continues until the crack reaches a critical length associated with unstable, rapid crack extension, namely fracture. An exception is constraint-induced fracture, where very little or no crack growth occurs prior to fracture.

Fracture toughness reflects the tolerance of the steel for a crack prior to fracture. Fracture of steel bridges is governed by the total stress, including the dead load stress, and not just the live load stress range as is the case with fatigue. Older bridges with satisfactory performance histories likely have adequate fracture toughness for the maximum total stresses that they have experienced. ~~probably have demonstrated that their fracture toughness is adequate for their total stresses, i.e., the dead load stress plus the stress range due to the heaviest truck that has crossed the bridge.~~ However, propagating fatigue cracks in bridges of questionable fracture toughness ~~are~~ is very serious, and may warrant immediate bridge closure. ~~A rehabilitation of a bridge of unknown fracture toughness which may increase the dead load stress must be avoided.~~

7.5 ALTERNATE ANALYSIS METHODS

Alternative analysis techniques, such as fracture mechanics and hot-spot stress analysis, may be used to predict the finite fatigue life of a detail. The estimate for finite life obtained from these methods should be used in place of Y in Article 7.2.6 to determine the fatigue serviceability index.

C7.5

These analyses may be helpful in assessing cases where S-N test data from appropriately sized connections are not available. Hot-spot stress fatigue design has been used in certain industries to evaluate structures with complex geometries where nominal stress is not easily defined and where weld toe cracking is the most likely mode of failure. Fracture mechanics, on the other hand, has also been used in certain industries for a "fitness for purpose" type of assessment to establish a suitable design life for members with certain known flaw sizes. Efforts should be made to use a level of safety comparable with those levels prescribed in Article 7.2.6 for minimum, evaluation, or mean fatigue life.

~~7.5~~7.6—REFERENCES

AASHTO. 1978. *Guide Specifications for Fracture-Critical Nonredundant Steel Bridge Members*. American Association of State Highway and Transportation Officials, Washington, DC.

AASHTO. 1990. *Guide Specifications for Fatigue Evaluation of Existing Steel Bridges*. American Association of State Highway and Transportation Officials, Washington, DC.

AASHTO. ~~2007~~2010. *AASHTO LRFD Bridge Design Specifications, ~~Fourth~~ Fifth Edition~~, LRFDUS-4-M or LRFDSI-4~~*. American Association of State Highway and Transportation Officials, Washington, DC.

Moses, F., C. G. Schilling, and K. S. Raju. 1987. *Fatigue Evaluation Procedures for Steel Bridges*, NCHRP Report 299. Transportation Research Board, National Research Council, Washington, DC

E.2 Section 7 (Incorporating Recommended Changes)

SECTION 7

FATIGUE EVALUATION OF STEEL BRIDGES

7.1 LOAD-INDUCED VERSUS DISTORTION-INDUCED FATIGUE

Fatigue damage has been traditionally categorized as either load-induced or distortion-induced.

Load-induced fatigue is that due to the in-plane stresses in the steel plates that comprise bridge member cross-sections. These in-plane stresses are those typically calculated by designers during bridge design or evaluation.

Distortion-induced fatigue is that due to secondary stresses in the steel plates that comprise bridge member cross sections. These stresses, which are typically caused by out-of-plane forces, can only be calculated with very refined methods of analysis, far beyond the scope of a typical bridge design or evaluation. These secondary stresses are minimized through proper detailing.

C7.1

The previous most comprehensive codification of fatigue evaluation of steel bridges, the *Guide Specifications for Fatigue Evaluation of Existing Steel Bridges*, AASHTO (1990), explicitly considered only load-induced fatigue damage. The Guide Specifications referenced *NCHRP Report 299* for considering "fatigue due to secondary bending stresses that are not normally calculated," NCHRP (1987).

These "plates" may be the individual plates which comprise a built-up welded, bolted or riveted plate girder, or may be the flanges, webs, or other elements of rolled shapes.

The traditional approximate methods of analysis utilizing lateral live-load distribution factors have encouraged bridge designers to discount the secondary stresses induced in bridge members due to the interaction of longitudinal and transverse members, both main and secondary members.

Detailing to minimize the potential for distortion-induced fatigue, such as connecting transverse connection plates for diaphragms and floor beams to both the compression and tension flanges of girders, is specified in LRFD Design Article 6.6.1.3.

7.2 LOAD-INDUCED FATIGUE DAMAGE EVALUATION

7.2.1 Application

Two levels of fatigue evaluation are specified for load-induced fatigue: the infinite-life check of Article 7.2.4 and the finite-life calculations of Article 7.2.5. Only bridge details which fail the infinite-life check are subject to the more complex finite-life fatigue evaluation.

Except for the case of riveted connections and tack weld details specified below, the list of detail categories to be considered for load-induced fatigue-damage evaluation, and illustrative examples of these categories are shown in LRFD Design Table 6.6.1.2.3-1.

C7.2.1

The initial infinite-life check should be made with the simplest, least refined stress-range estimate. If the detail passes the check, no further refinement is required. The stress-range estimate for the infinite-life check should be refined before the more complex procedures of the finite-life fatigue evaluation are considered.

The base metal at net sections of riveted connections shall be evaluated based upon the requirements of Category C, given in LRFD Design Table 6.6.1.2.3-1, instead of Category D as specified for new designs. The exception is for riveted members of poor physical condition, such as with missing rivets or indications of punched holes, in which case Category D shall be used.

Tack welds may be evaluated based upon the requirements of Category C, given in LRFD Design Table 6.6.1.2.3-1.

As uncertainty is reduced from the evaluation by more refined analysis or site-specific data, the increased certainty is reflected in lower partial load factors, summarized in Table 7.2.2.1-1 and described in Articles 7.2.2.1 and 7.2.2.2.

If cracks have been visually detected then the fatigue life evaluation procedure specified herein should be used with caution. Generally, upon visual detection of load-induced fatigue cracking, the majority of the fatigue life has been exhausted and retrofitting measures should be initiated. Alternatively, a fracture mechanics approach can be used to evaluate the fatigue crack damage.

For new design, the base metal at net sections of riveted connections is specified to be Category D. This represents the first cracking of a riveted member, which is highly redundant internally. Category C more accurately represents cracking that has propagated to a critical size. This increase in fatigue life for evaluation purposes is appropriate due to the redundancy of riveted members.

Tack welds were frequently left in place in riveted connections. The tack welds were used to hold the members in place initially prior to placement of the rivets. Tack welds in this context are typically less than 2-in in length. The strength of tack welds was found to conform to fatigue Category C based on laboratory testing.

The partial load factors specified in Article 7.2 were adapted from the *Guide Specifications for Fatigue Evaluation of Existing Steel Bridges*, AASHTO (1990).

7.2.2 Estimating Stress Ranges

The effective stress range shall be estimated as:

$$(\Delta f)_{eff} = R_p R_s \Delta f \qquad (7.2.2\text{-}1)$$

where:

R_p = The multiple presence factor, calculated as described in Article 7.2.2.1 for calculated stress ranges, or 1.0 for measured stress ranges

R_s = The stress-range estimate partial load factor, calculated as $R_{sa}R_{st}$, unless otherwise specified, summarized in Table 7.2.2.1-1, and

Δf = Measured effective stress range; or factored calculated stress range due to the passage of the fatigue truck as specified in LRFD Design Article 3.6.1.4 for Fatigue II Load Combination, or the calculated stress range due to a fatigue truck determined by a truck survey or weigh-in-motion study.

C7.2.2

The calculated stress range is due to a single truck in a single lane on the bridge.

The multiple presence factor takes into account the effect of trucks present simultaneously in multiple lanes instead of a single lane loading. When using measured stress ranges, the multiple presence factor should not be used in the equation, as the effects of multiple presence are already reflected in the measured stress ranges.

The load factor is 0.75 for live load specified for the Fatigue II limit state (finite load-induced fatigue life) in LRFD Design Table 3.4.1-1.

7.2.2.1 Calculating Estimated Stress Ranges

The multiple presence factor R_p shall be calculated as:

$$R_p = 0.988 + 6.87\text{x}10^{-5} (L) + 4.01\text{x}10^{-6} [ADTT]_{PRESENT} + 0.0107 / (n_L) \geq 1.0 \quad (7.2.2.1\text{-}1)$$

where

L = span length in feet,

$[ADTT]_{PRESENT}$ = Present average number of trucks per day for all directions of truck traffic including all lanes on the bridge, and

n_L = number of lanes.

Two sources of uncertainty are present in the calculation of effective stress range at a particular fatigue detail:

- Uncertainty associated with analysis, represented by the analysis partial load factor, R_{sa}, and
- Uncertainty associated with assumed effective truck weight, represented by the truck-weight partial load factor, R_{st}.

The limits used in developing the equation are noted as follows: $2 \leq n_L \leq 4$; $[ADTT]_{PRESENT} < 8{,}000$ for n_L=2; 11,000 for n_L=3, and 13,000 for n_L=4, and 30 ft < L < 220 ft. These are the ranges used in the analysis, based on the WIM data available. Use of these equations may be justified outside of these ranges, but are not based on experimental evidence. The multiple presence factor is applicable to longitudinal parallel members only. For transverse members, use $R_P = 1.0$.

Table 7.2.2.1-1 Partial Load Factors: R_{sa}, R_{st}, and R_s.

Fatigue-Life Evaluation Methods	Analysis Partial Load Factor, R_{sa}	Truck-Weight Partial Load Factor, R_{st}	Stress-Range Estimate Partial Load Factor, R_s[a]
For Evaluation or Minimum Fatigue Life			
Stress range by simplified analysis, and truck weight per Article 3.6.1.4 of the *LRFD Specifications*	1.0	1.0	1.0
Stress range by simplified analysis, and truck weight estimated through weigh-in-motion study	1.0	0.95	0.95
Stress range by refined analysis, and truck weight per Article 3.6.1.4 of the *LRFD Specifications*	0.95	1.0	0.95
Stress range by refined analysis, and truck weight by weigh-in-motion study	0.95	0.95	0.90
Stress range by field-measured strains	NA	NA	0.85
For Mean Fatigue Life			
All methods	NA	NA	1.00

[a] In general, $R_s = R_{sa}R_{st}$

7.2.2.1.1 For Determination of Evaluation or Minimum Fatigue Life

In the calculation of effective stress range for the determination of evaluation or minimum fatigue life, the stress-range estimate partial load factor shall be taken as the product of the analysis partial load factor and the truck-weight partial load factor:

$$R_s = R_{sa}R_{st} \qquad (7.2.2.1.1\text{-}1)$$

If the effective stress range is calculated through refined methods of analysis, as defined in LRFD Design Article 4.6.3,

$$R_{sa} = 0.95 \qquad (7.2.2.1.1\text{-}2)$$

otherwise,

$$R_{sa} = 1.0 \qquad (7.2.2.1.1\text{-}3)$$

If the effective truck weight is estimated through a weigh-in-motion study at, or near, the bridge,

$$R_{st} = 0.95 \qquad (7.2.2.1.1\text{-}4)$$

otherwise,

$$R_{st} = 1.0 \qquad (7.2.2.1.1\text{-}5)$$

7.2.2.1.2 For Determination of Mean Fatigue Life

In the calculation of effective stress range for the determination of mean fatigue life, the stress-range estimate partial load factor shall be taken as 1.0.

7.2.2.2 Measuring Estimated Stress Ranges

The effective stress range may be estimated through field measurements of strains at the fatigue-prone detail under consideration under typical traffic conditions. The effective stress range shall be computed as the cube root of the weighted sum of the cubes of the measured stress ranges, as given in:

$$(\Delta f)_{eff} = R_s\left(\sum \gamma_i \Delta f_i^3\right)^{1/3} \qquad (7.2.2.2-1)$$

where:

γ_i = Percentage of cycles at a particular stress range, and

Δf_i = The particular stress range in a measured stress range histogram of magnitude greater than one half of the constant-amplitude-fatigue-threshold of the fatigue prone detail under consideration, i.e. $> \Delta F_{TH}/2$.

C7.2.2.2

Field measurements of strains represent the most accurate means to estimate effective stress ranges at fatigue-prone details.

The *AASHTO LRFD Bridge Design Specifications* assume that the maximum stress range is twice the effective stress range. It is unlikely that the maximum stress range during the service life of the bridge will be captured during a limited field measurement session; therefore means to extrapolate from the measured stress range histogram to the maximum stress range must be used.

The lower portion of field measured stress range histograms must be truncated in order to avoid underestimating the effective stress range.

7.2.2.2.1 For Determination of Evaluation or Minimum Fatigue Life

Where field-measured strains are used to generate an effective stress range, R_s, for the determination of evaluation or minimum fatigue life, the stress-range estimate partial load factor, shall be taken as 0.85

7.2.2.2.2 For Determination of Mean Fatigue Life

Where field-measured strains are used to generate an effective stress range, R_s, for the determination of mean fatigue life, the stress-range estimate partial load factor, shall be taken as 1.0.

7.2.3 Determining Fatigue-Prone Details

Bridge details are only considered prone to load-induced fatigue damage if they experience a net tensile stress. Thus, fatigue damage need only be evaluated if, at the detail under evaluation,

$$2(\Delta f)_{tension} > f_{dead\text{-}load\ compression} \qquad (7.2.3\text{-}1)$$

where:

$(\Delta f)_{tension}$ = Tensile portion of the effective stress range as specified in Article 7.2.2, and

$f_{dead\text{-}load\ compression}$ = Unfactored compressive stress at the detail due to dead load.

C7.2.3

The multiplier of two in the equation represents the assumed relationship between maximum stress range and effective stress range, as specified in the *AASHTO LRFD Bridge Design Specifications.*

When measured stress ranges are used to evaluate fatigue life, the multiplier of two in the equation should be reconsidered based upon the discussion of Article C7.2.2.2.

If the effective truck weight is significantly less than 54 kips, a multiplier more than two should be considered. Similarly, for a measured effective truck weight greater than 54 kips a multiplier less than two would be appropriate.

7.2.4 Infinite-Life Check

If:

$$(\Delta f)_{max} \le (\Delta F)_{TH}, \qquad (7.2.4\text{-}1)$$

then:

$$Y = \infty, \qquad (7.2.4\text{-}2)$$

where:

$(\Delta f)_{max}$ = The maximum stress range expected at the fatigue-prone detail, which may be taken as:

- R_p times the factored calculated stress range due to the passage of the fatigue truck as specified in LRFD Design Article 3.6.1.4 for Fatigue I Load Combination

C7.2.4

Theoretically, a fatigue-prone detail will experience infinite life if all of the stress ranges are less than the constant amplitude fatigue threshold; in other words, if the maximum stress range is less than the threshold.

The load factor is 1.50 for live load specified for the Fatigue I limit state (infinite load-induced fatigue life) in LRFD Design Table 3.4.1-1.

- $2.0(\Delta f)_{eff}$; for calculated stress range due to a fatigue truck determined by a truck survey or weigh-in-motion study with R_s=1.0
- Larger of maximum (Δf_i), $2(\Delta f)_{eff}$, or other suitable value; for measured stress ranges with R_s=1.0

$(\Delta F)_{TH}$ = The constant-amplitude fatigue threshold given in LRFD Design Table 6.6.1.2.5-3

otherwise, the total fatigue life shall be estimated as specified in Article 7.2.5.

7.2.5 Estimating Finite Fatigue Life

7.2.5.1 General

Four levels of finite fatigue life may be estimated:

- The minimum expected fatigue life (which equals the conservative design fatigue life),
- Evaluation 1 fatigue life (which is a somewhat less conservative fatigue life for evaluation),
- Evaluation 2 fatigue life (which equals a more conservative fatigue life for evaluation), and
- The mean fatigue life (which equals the statistically most likely fatigue life).

The total finite fatigue life of a fatigue-prone detail, in years, shall be determined as:

$$Y = \frac{\log\left[\dfrac{R_R A}{365n\left[(ADTT)_{SL}\right]_{PRESENT}\left[(\Delta f)_{eff}\right]^3} g(1+g)^{a-1}+1\right]}{\log(1+g)} \quad (7.2.5.1\text{-}1)$$

where:

R_R = Resistance factor specified for evaluation, minimum, or mean fatigue life as given in Table 7.2.5.1-1

A = Detail-category constant given in LRFD Design Table 6.6.1.2.5-1

n = Number of stress-range cycles per truck passage estimated according to Article 7.2.5.2

g = Estimated annual traffic-volume growth rate in percentage

a = Present age of the detail in years

$[(ADTT)_{SL}]_{PRESENT}$ = Present average number of trucks per day in a single lane

When measured stress ranges are used to evaluate fatigue life, the maximum stress range should be taken as the larger value of two times field measured effective stress range or the field measured maximum stress range, unless another suitable value is justified.

C7.2.5.1

Much scatter, or variability, exists in experimentally derived fatigue lives. For design, a conservative fatigue resistance two standard deviations shifted below the mean fatigue resistance or life is assumed. This corresponds to the minimum expected finite fatigue life of this Article. Limiting actual usable fatigue life to this design fatigue life is very conservative and can be costly. As such, means of estimating the two evaluation fatigue lives and the mean finite fatigue life are also included to aid the evaluator in the decision making.

Recent research has made it possible to obtain a closed-form solution for the total finite fatigue life using an estimated traffic growth rate and the present $(ADTT)_{SL}$. For cases with zero traffic growth, a very small value of g should be selected for use in the expression for Y.

The resistance factors for fatigue life, specified in Table 7.2.5.1-1, represent the variability of the fatigue life of the various detail categories, A through E'. The minimum life, evaluation 1 life and evaluation 2 life fatigue-life curves are shifted from the mean fatigue-life S-N curves in log-log space. Scatter of the fatigue lives at given stress range values from controlled laboratory testing provides statistical information on fatigue behavior of bridge details under cyclic loading. Accordingly, the probability of failure associated with each level of fatigue life, approaches 2 percent, 16 percent, 33 percent and 50 percent for the minimum, evaluation 1, evaluation 2 and mean fatigue lives, respectively. Typically, the minimum life or evaluation 1 life is used to evaluate the fatigue serviceability. If concerns are encountered regarding the computed fatigue serviceability, then the serviceability index can be revised according to Article 7.2.7.2.

$(\Delta f)_{eff}$ = The effective stress range as specified in Article 7.2.2

Table 7.2.5.1-1 Resistance Factor for Evaluation, Minimum or Mean Fatigue Life, R_R

Detail Category (from Table 6.6.1.2.5-1 of the *LRFD Specifications*)	R_R			
	Minimum Life	Evaluation 1 Life	Evaluation 2 Life	Mean Life
A	1.0	1.5	2.2	2.9
B	1.0	1.3	1.7	2.0
B’	1.0	1.3	1.6	1.9
C	1.0	1.3	1.7	2.1
C’	1.0	1.3	1.7	2.1
D	1.0	1.3	1.7	2.0
E	1.0	1.2	1.4	1.6
E’	1.0	1.3	1.6	1.9

7.2.5.2 Estimating the Number of Cycles per Truck Passage

The number of stress-range cycles per truck passage may be estimated (in order of increasing apparent accuracy and complexity):

- Through the use of LRFD Design Table 6.6.1.2.5-2,
- Through the use of influence lines, or
- By field measurements.

7.2.6 Fatigue Serviceability Index

7.2.6.1 Calculating the Fatigue Serviceability Index

The fatigue serviceability index shall be calculated as:

$$Q = \left(\frac{Y-a}{N}\right)GRI \qquad (7.2.6.1\text{-}1)$$

where:

N = Greater of Y or 100 years
G = Load Path Factor, as given in Table 7.2.6.1-1
R = Redundancy Factor, as given in Table 7.2.6.1-2
I = Importance Factor, as given in Table 7.2.6.1-3

C7.2.6

The fatigue serviceability index is a dimensionless relative measure of the performance of a structural detail, at a particular location in the structure, with respect to the overall fatigue resistance of the member.

The load path, redundancy and importance factors are risk factors that modify the fatigue serviceability index. They reduce the index from its base value, i.e. based on fatigue resistance alone, to a reduced value that reflects greater consequences from the lack of ability to redistribute the load (load path factor), lack of redundancy (redundancy factor), or use of the structure (importance factor). The net effect of a reduction in the index will be to move the composite index value to a lower value that may initiate a lower fatigue rating. These risk factors are similar to the ductility, redundancy and operational classification factors in the *AASHTO LRFD Bridge Design Specifications*. Improved quantification with time will possibly modify these factors.

Table 7.2.6.1-1 Load Path Factor G

Number of Load Path Members	G
1 or 2 members	0.8
3 members	0.9
4 or more members	1

The number of members that carry load when a fatigue truck is placed on the bridge is used to select the load path factor; e.g., two members for a two-girder bridge and for a typical truss structure; four or more members for a multi-beam or multi-girder bridge; etc. For diaphragms and secondary members, use G = 1.

Table 7.2.6.1-2 Redundancy Factor R

Type of Span	R
Simple	0.9
Continuous	1

Table 7.2.6.1-3 Importance Factor I

Structure or Location	Importance Factor, I
Interstate Highway Main Arterial State Route Other Critical Route	0.90
Secondary Arterial Urban Areas	0.95
Rural Roads Low ADTT routes	1.00

7.2.6.2 Recommended Actions Based on Fatigue Serviceability Index

The fatigue ratings and assessment outcomes as given in Table 7.2.6.2-1 are recommended as a guideline for actions that may be undertaken based on the obtained value for the fatigue serviceability index. A better fatigue rating may be assumed for Q values at the boundary of two ranges.

In the recommended actions provided, it is expected that based upon increasing risk, the inspection frequency of the bridge shall be increased on a case-by-case assessment by the bridge owner.

Table 7.2.6.2-1 Fatigue Rating and Assessment Outcomes

Fatigue Serviceability Index, Q	Fatigue Rating	Assessment Outcome
1.00 to 0.50	Excellent	Continue Regular Inspection
0.50 to 0.35	Good	Continue Regular Inspection
0.35 to 0.20	Moderate	Continue Regular Inspection
0.20 to 0.10	Fair	Increase Inspection Frequency
0.10 to 0.00	Poor	Assess Frequently
< 0.00	Critical	Consider Retrofit, Replacement or Reassessment

7.2.7 Strategies to Increase Fatigue Serviceability Index

7.2.7.1 General

If the fatigue serviceability index is deemed unacceptable, the strategies of Articles 7.2.7.2 and 7.2.7.3 may be applied to enhance the fatigue serviceability index.

C7.2.7.1

Retrofit or load-restriction decisions should be made based upon the evaluation fatigue life unless the physical condition or fabrication quality of the bridge is poor. In general, it is uneconomical to limit the useful fatigue life of in-service bridges to the minimum (design) fatigue life.

If the estimated fatigue serviceability index based upon the evaluation fatigue life is deemed unacceptable, a fatigue life approaching the mean fatigue life can be used for evaluation purposes if additional risk of fatigue cracking is acceptable.

7.2.7.2 Recalculate Fatigue Serviceability Index

7.2.7.2.1 Through Accepting Greater Risk

In general, evaluation 1 life of Article 7.2.5 is used in determining the fatigue serviceability index of a bridge detail according to Article 7.2.6. If the evaluator is willing to accept greater risk of fatigue cracking due to:

- Long satisfactory cyclic performance of the detail to date,
- A high degree of redundancy, and/or
- Increased inspection effort, e.g., decreased inspection interval,
- Some combination of the above

the fatigue serviceability index may be determined using a fatigue life approaching the mean fatigue life of Article 7.2.5.

7.2.7.2.2 Through More Accurate Data

The calculated fatigue serviceability index may be refined by using more accurate data as input to the fatigue-life estimate. Sources of improvement of the estimate include:

- Field measurement of stress ranges at the fatigue prone detail under construction
- 3-D finite element analysis for stresses at the fatigue prone detail under consideration
- Weigh-in-motion data of truck weights at or near the bridge site,
- Site-specific data on average daily truck traffic (ADTT) at or near the bridge site

This strategy is based upon achieving a better estimate of the fatigue life.

7.2.7.2.3 Through Truncated Fatigue Life Distribution

When a negative fatigue serviceability index is obtained according to Article 7.2.6, the detail's fatigue serviceability index may be updated using equations below for mean, evaluation and minimum lives, provided a field inspection finds no evidence of fatigue cracking at the detail.

$$Y'_{mean} = 2.19 Y_{mean} e^{0.73\Phi^{-1}[0.18(1-P)+P]-0.27} \quad (7.2.7.2.3-1)$$

$$Y'_{eval\,2} = 2.19 Y_{mean} e^{0.73\Phi^{-1}[0.12(1-P)+P]-0.27} \quad (7.2.7.2.3-2)$$

$$Y'_{eval1} = 2.19 Y_{mean} e^{0.73\Phi^{-1}[0.074(1-P)+P]-0.27} \quad (7.2.7.2.3-3)$$

$$Y'_{\text{minimum}} = 2.19 Y_{mean} e^{0.73\Phi^{-1}[0.039(1-P)+P]-0.27} \quad (7.2.7.2.3-4)$$

where

Y'_{mean} = Updated mean life in years

Y_{mean} = Mean life in years without updating based on no detection of cracking at detail in question

Y'_{eval1} = Updated evaluation 1 life in years

Y'_{eval2} = Updated evaluation 2 life in years

$Y'_{minimum}$ = Updated minimum life in years

Φ^{-1} = Inverse of the standard normal variable's cumulative probability function (Table 7.2.7.2-1)

P = Probability of fatigue life being shorter than current age before updating based on no crack found

$$= \Phi\left[\frac{Ln\left(\frac{a}{2.19Y_{mean}}\right)+0.27}{0.73}\right] \quad (7.2.7.2.3-5)$$

where a = Present age in years

Φ = Standard normal variable's cumulative probability function (Table 7.2.7.2-1)

C7.2.7.2.3

The fatigue life of a structural detail is modeled using a lognormally distributed random variable, as shown in the figure C7.2.7.2.3-1. When the estimated life using Article 7.2.5 is smaller than the present age, the remaining life becomes negative as illustrated.

In this situation, if field inspection finds no evidence of cracking, the estimated life is an overly-conservative estimate. The low tail of the total life distribution is truncated up to the present life. The eliminated probability P is computed, and the resulting probability density function is divided by (1 – P) to ensure that the total probability under the distribution curve is still 1.0 as shown in Figure C7.2.7.2.3-2. Then the updated life is determined to maintain the same reliability level for fatigue life distribution. Functions Φ (.) and Φ^{-1}(.) are commonly available in commercial spreadsheet programs.

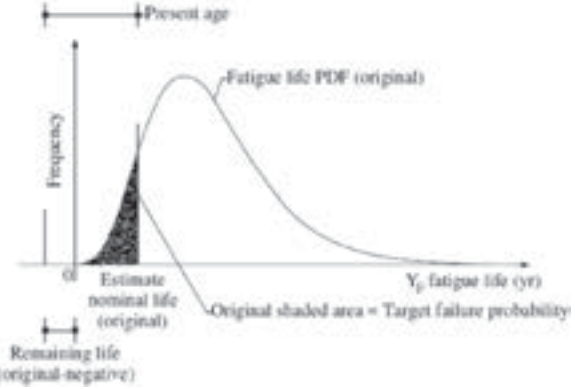

Fig C7.2.7.2.3-1 Probability Density Function of Fatigue Life and Estimated Life as a Value on Horizontal Axis

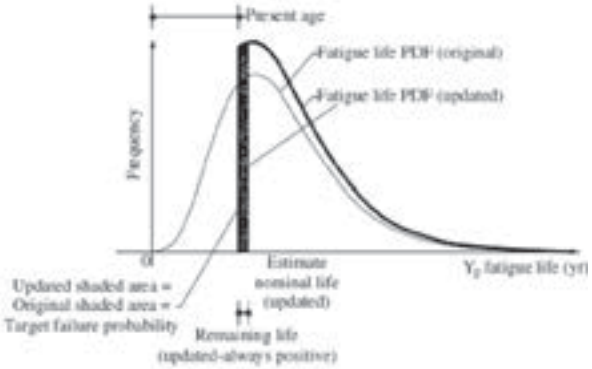

Fig C7.2.7.2.3-2 Truncated Probability Density Function of Fatigue Life and Updated Life as a value on the Horizontal Axis

Table 7.2.7.2-1 Cumulative Distribution Function Φ(x) for Standard Normal Variable x

x	0.00	0.01	0.02	0.03	0.04	0.05	0.06	0.07	0.08	0.09
0.0	0.5000	0.5040	0.5080	0.5120	0.5160	0.5199	0.5239	0.5279	0.5319	0.5359
0.1	0.5398	0.5438	0.5478	0.5517	0.5557	0.5596	0.5636	0.5675	0.5714	0.5753
0.2	0.5793	0.5832	0.5871	0.5910	0.5948	0.5987	0.6026	0.6064	0.6103	0.6141
0.3	0.6179	0.6217	0.6255	0.6293	0.6331	0.6368	0.6406	0.6443	0.6480	0.6517
0.4	0.6554	0.6591	0.6628	0.6664	0.6700	0.6736	0.6772	0.6808	0.6844	0.6879
0.5	0.6915	0.6950	0.6985	0.7019	0.7054	0.7088	0.7123	0.7157	0.7190	0.7224
0.6	0.7257	0.7291	0.7324	0.7357	0.7389	0.7422	0.7454	0.7486	0.7517	0.7549
0.7	0.7580	0.7611	0.7642	0.7673	0.7704	0.7734	0.7764	0.7794	0.7823	0.7852
0.8	0.7881	0.7910	0.7939	0.7967	0.7995	0.8023	0.8051	0.8078	0.8106	0.8133
0.9	0.8159	0.8186	0.8212	0.8238	0.8264	0.8289	0.8315	0.8340	0.8365	0.8389
1.0	0.8413	0.8438	0.8461	0.8485	0.8508	0.8531	0.8554	0.8577	0.8599	0.8621
1.1	0.8643	0.8665	0.8686	0.8708	0.8729	0.8749	0.8770	0.8790	0.8810	0.8830
1.2	0.8849	0.8869	0.8888	0.8907	0.8925	0.8944	0.8962	0.8980	0.8997	0.9015
1.3	0.9032	0.9049	0.9066	0.9082	0.9099	0.9115	0.9131	0.9147	0.9162	0.9177
1.4	0.9192	0.9207	0.9222	0.9236	0.9251	0.9265	0.9279	0.9292	0.9306	0.9319
1.5	0.9332	0.9345	0.9357	0.9370	0.9382	0.9394	0.9406	0.9418	0.9429	0.9441
1.6	0.9452	0.9463	0.9474	0.9484	0.9495	0.9505	0.9515	0.9525	0.9535	0.9545
1.7	0.9554	0.9564	0.9573	0.9582	0.9591	0.9599	0.9608	0.9616	0.9625	0.9633
1.8	0.9641	0.9649	0.9656	0.9664	0.9671	0.9678	0.9686	0.9693	0.9699	0.9706
1.9	0.9713	0.9719	0.9726	0.9732	0.9738	0.9744	0.9750	0.9756	0.9761	0.9767
2.0	0.9772	0.9778	0.9783	0.9788	0.9793	0.9798	0.9803	0.9808	0.9812	0.9817
2.1	0.9821	0.9826	0.9830	0.9834	0.9838	0.9842	0.9846	0.9850	0.9854	0.9857

7.2.7.3 Retrofit

If the recalculated fatigue serviceability index is not ultimately acceptable, the actual fatigue serviceability index may be increased by retrofitting the critical details to improve the detail category and thus increase the fatigue serviceability index. This strategy increases the actual fatigue serviceability index when further enhancement of the calculated fatigue serviceability index, through improved input, is no longer possible or practical.

C7.2.7.3

In certain cases, Owners may wish to institute more intensive inspections, in lieu of more costly retrofits, to assure adequate safety. Restricting traffic to increase the fatigue serviceability index is generally not considered cost effective. If the fatigue serviceability index is deemed inadequate, the appropriate option to increase the fatigue serviceability index should be determined based upon the economics of the particular situation.

7.3 DISTORTION-INDUCED FATIGUE EVALUATION

C7.3

Distortion-induced fatigue is typically caused by out-of-plane deformation of the web plate that results in fatigue crack formation at details prone to such cracking under cyclic loading. The cracks tend to form in the member web at locations where there is a geometrical discontinuity, such as a vertical gap between a stiffener or connection plate and the girder flange or a horizontal gap between a gusset plate and a connection plate. Distortion-induced fatigue is a stiffness problem (more precisely the lack thereof) versus a load problem.

Existing bridges should not be assumed to be insensitive to distortion-induced cracking if fatigue cracks do not appear after a short period of time. Experience has shown that in some cases cracking may not be evident for 10 years after the beginning of service.

Often, distortion-induced fatigue cracks initiate after relatively few stress-range cycles at

fatigue-prone details. However, depending upon the magnitude of the out-of-plane distortion and the geometry of the web gap detail, the crack growth may be slow and a significant period of time may be required before they become large enough to be detected visually.

7.3.1 Methods to Assess Distortion-Induced Cracking

Out-of-plane distortions caused by truck loading must be accommodated by the regions that contain unsupported web gaps. Even very small distortions can cause high local stresses that may induce fatigue cracking. Often, the fatigue cracks grow in a plane that is parallel to the primary stresses of the member and will slow down or even stop as the web gap becomes more flexible due to the presence of the crack. However, it is possible that the crack may turn and become perpendicular to the primary stress of the member, leading to more rapid crack growth. Therefore, distortion-induced fatigue cracks should be repaired.

C7.3.1

Typically, smaller web gaps are subject to higher distortion-induced stresses than larger web gaps provided the same demand for the out-of-plane distortion. The demand for out-of-plane distortion is determined by the global behavior of the structural system. Accurate quantification of the stress field in an unsupported web gap detail can be very difficult, even for finite element modeling or field measurement of strains and/or local deformations. This is especially the case when the dimension of the web gap is comparable to the thicknesses of the surrounding plates and the sizes of the connecting welds, resulting in high stress gradients across the web gap.

7.3.2 Retrofit Options for Distortion-Induced Fatigue Cracking

Retrofit should be considered if distortion-induced cracking has been detected. Two primary retrofit methods are available: softening or stiffening. The softening approach is used to increase the overall flexibility of the detail in question to accommodate the out-of-plane deformations without further cracking. The stiffening approach is used to minimize the local distortion by providing a positive load path for the forces that tend to cause the distortion. In either case, a hole should be drilled at the tip of each crack.

C7.3.2

In the softening retrofit, the flexibility of the detail in question is increased. Drilling holes to eliminate the tip of distortion-induced fatigue cracks will typically increase the local flexibility somewhat. However, the primary method used to increase the flexibility is to increase the size of the web gap. This can be effective since the out-of-plane bending stresses are related to the inverse of the square of the web gap length. One critical issue for this approach is to avoid an excessive increase of out-of-plane deformation resulting from the web gap enlargement. Removal of portions of a stiffener or other plate to increase the size of the web gap will also require removal of the connecting weld in those regions to provide a smooth, flush surface. Non-destructive inspection should be conducted to ensure that no undesirable gouges, notches or discontinuities remain.

In the stiffening retrofit, the stiffness of the detail in question is increased to minimize the out-of-plane distortion. Commonly, this will require the addition of a WT section, or a double or single angle section. Drilling retrofit holes to eliminate the tip of any distortion-induced fatigue cracks should be done

prior to installation of the retrofit connection element. Typically, the installation of a retrofit element will increase the stiffness and significantly decrease the out-of-plane deformation at the detail. However, the force effect of the retrofit on the primary and secondary members should be considered. One critical issue for this approach is to size the retrofit connection of sufficient thickness and strength for the loading forces to be generated at the new connection.

7.4 FRACTURE-CONTROL FOR OLDER BRIDGES

Bridges fabricated prior to the adoption of AASHTO's *Guide Specifications for Fracture-Critical Non-Redundant Steel Bridge Members* (1978) may have lower fracture toughness levels than are currently deemed acceptable. Destructive material testing of bridges fabricated prior to 1978 to ascertain actual toughness levels may be justified. Decisions on fatigue evaluations of a bridge can be made based upon the information from these tests.

C7.4

The fatigue life of a steel bridge detail generally consists of crack initiation and stable crack propagation. The propagation stage continues until the crack reaches a critical length associated with unstable, rapid crack extension, namely fracture. An exception is constraint-induced fracture, where very little or no crack growth occurs prior to fracture.

Fracture toughness reflects the tolerance of the steel for a crack prior to fracture. Fracture of steel bridges is governed by the total stress, including the dead load stress, and not just the live load stress range as is the case with fatigue. Older bridges with satisfactory performance histories likely have adequate fracture toughness for the maximum total stresses that they have experienced. However, propagating fatigue cracks in bridges of questionable fracture toughness is very serious, and may warrant immediate bridge closure.

7.5 ALTERNATE ANALYSIS METHODS

Alternative analysis techniques, such as fracture mechanics and hot-spot stress analysis, may be used to predict the finite fatigue life of a detail. The estimate for finite life obtained from these methods should be used in place of Y in Article 7.2.6 to determine the fatigue serviceability index.

C7.5

These analyses may be helpful in assessing cases where S-N test data from appropriately sized connections are not available. Hot-spot stress fatigue design has been used in certain industries to evaluate structures with complex geometries where nominal stress is not easily defined and where weld toe cracking is the most likely mode of failure. Fracture mechanics, on the other hand, has also been used in certain industries for a "fitness for purpose" type of assessment to establish a suitable design life for members with certain known flaw sizes. Efforts should be made to use a level of safety comparable with those levels prescribed in Article 7.2.6 for minimum, evaluation, or mean fatigue life.

7.6—REFERENCES

AASHTO. 1978. *Guide Specifications for Fracture-Critical Nonredundant Steel Bridge Members*. American Association of State Highway and Transportation Officials, Washington, DC.

AASHTO. 1990. *Guide Specifications for Fatigue Evaluation of Existing Steel Bridges*. American Association of State Highway and Transportation Officials, Washington, DC.

AASHTO. 2010. *AASHTO LRFD Bridge Design Specifications, Fifth Edition*. American Association of State Highway and Transportation Officials, Washington, DC.

Moses, F., C. G. Schilling, and K. S. Raju. 1987. *Fatigue Evaluation Procedures for Steel Bridges*, NCHRP Report 299. Transportation Research Board, National Research Council, Washington, DC.

APPENDIX F

FATIGUE EXAMPLES

NCHRP 12-81

Fatigue Examples

Using

Section 7 – Fatigue Evaluation of Steel Bridges

Example 1:

Note: The example presented below is a modification of the existing example currently in the Section 7 of the Manual for Bridge Evaluation (2011). It is assumed that the bridge structure carries two lanes of traffic in one direction only with a total ADTT of 1000 trucks.

Detail: Welded cover plates on tension flanges (Detail Category E)

Fatigue Load Stress Range

$\Delta f_{LL+IM} = \Delta f = 4.56$ ksi at cover plate weld

Nominal fatigue resistance for infinite life

$(\Delta F)_{TH} = 2.6$ ksi for Detail Category E *LRFD Table 6.6.1.2.5-3*

Infinite-Life Fatigue Check *MBE 7.2.4*

Span Length L = 65 ft

ADTT (One Direction, all lanes) = 1000

Number of lanes $n_L = 2$

$[ADTT]_{PRESENT} = 1000$

$R_p = 0.988 + 6.87 \times 10^{-5} (L) + 4.01 \times 10^{-6} [ADTT]_{PRESENT} + 0.0107 / (n_L)$

$= 0.988 + (6.87 \times 10^{-5}) (65) + (4.01 \times 10^{-6}) (1000) + 0.0107/2$

$= 1.0018$ *MBE 7.2.2.1*

$R_{sa} = 1.0$ *MBE Table 7.2.2.1-1*

$R_{st} = 1.0$

$R_s = R_{sa} \times R_{st} = 1.0$

$(\Delta f)_{eff} = (R_p)(R_s)(\Delta f_{FATIGUE\ II}) = (1.0018)(1.0)(0.75)(4.56) = 3.43$ ksi *MBE 7.2.2*

$(\Delta f)_{max} = (R_p)(\Delta f_{FATIGUE\ I}) = (1.0018)(1.50)(4.56)$

$= 6.85$ ksi > 2.6 ksi *MBE 7.2.4*

Thus, $(\Delta f)_{max} > (\Delta F)_{TH}$.

The detail does not possess infinite fatigue life.

Evaluate fatigue life using procedures given in Section 7 of AASHTO's The Manual for Bridge Evaluation.

CALCULATION OF FATIGUE LIFE

Fatigue life determination will be based upon the finite fatigue life.

$$Y = \frac{\log\left[\frac{R_R A}{365n\left[(ADTT)_{SL}\right]_{PRESENT}[(\Delta f)_{eff}]^3} g(1+g)^{a-1}+1\right]}{\log(1+g)}$$ *MBE 7.2.5.1*

$[ADTT]_{PRESENT}$ (One Direction) = 1000

$[(ADTT)_{SL}]_{PRESENT} = 0.85(1000) = 850$ *LRFD Table 3.6.1.4.2-1*

Traffic Growth Rate g: 2%

Bridge Age a: 43 years

Assume Evaluation 1 Life to be used for bridge assessment.

Hence, $R_R = 1.3$ *MBE Table 7.2.5.1-1*

$(\Delta f)_{eff} = 3.43$ ksi

A = 3.9×10^8 ksi^3 *LRFD Table 6.6.1.2.5-1*

n = 1.0 simple span girders with L > 40 ft. *LRFD Table 6.6.1.2.5-2*

$$Y = \frac{\log\left[\frac{1.3(3.9x10^8)}{365(1)(850)(3.43)^3}(0.02)(1+0.02)^{43-1}+1\right]}{\log(1+0.02)} = 53 \text{ years}$$

CALCULATION OF FATIGUE SERVICEABILITY INDEX

Fatigue Serviceability Index $Q = \left(\frac{Y - a}{N} \right) GRI$ *MBE 7.2.6.1*

No. of load paths (in this case, girders) = 4

G = 1.0 *MBE Table 7.2.6.1-1*

No. of Spans = 1 (Simple Span)

R = 0.90 *MBE Table 7.2.6.1-2*

N = (larger of 100 or Y) = 100

Assuming that the bridge is on an Interstate Highway, I = 0.9 *MBE Table 7.2.6.1-3*

$$Q = \left(\frac{53 - 43}{100} \right)(1.0)(0.9)(0.9) = 0.08$$

The serviceability rating and assessment outcome are provided in MBE Table 7.2.6.2-1 for various ranges of the Fatigue Serviceability Index. In this example, a Q value of 0.08 means that the bridge will be rated as 'Poor' from a fatigue standpoint and the assessment outcome would be 'Assess Frequently'. The bridge owner will need to define how often to increase the inspection frequency based upon the importance of the structure.

Example 2: (Retrofit fatigue evaluation)

In order to improve the fatigue life of the detail given in Example 1, a retrofit option would be to modify the welded cover plate detail by adding a slip-critical bolted end plate connection. In this case, based upon data available in published research, the engineer can re-classify the retrofitted detail as category B.

Detail: Bolted splice for end cover plates on tension flanges (Detail Category B)

Fatigue Load Stress Range

$\Delta f_{LL+IM} = \Delta f$ = 4.56 ksi at cover plate weld

Nominal fatigue resistance for infinite life

$(\Delta F)_{TH}$ = 16 ksi for Detail Category B *LRFD Table 6.6.1.2.5-3*

Infinite-Life Fatigue Check *MBE 7.2.4*

Span Length L = 65 ft

$[ADTT]_{PRESENT}$ (One Direction, all lanes) = 1000

Number of lanes $n_L = 2$

$[ADTT]_{PRESENT}$ = 1000

$R_p = 0.988 + 6.87x10^{-5}(L) + 4.01x10^{-6}\,[ADTT]_{PRESENT} + 0.0107 / (n_L)$

$= 0.988 + (6.87x10^{-5})\,(65) + (4.01x10^{-6})\,(1000) + 0.0107/2$

= 1.0018 *MBE 7.2.2.1*

R_{sa} = 1.0 *MBE Table 7.2.2.1-1*

R_{st} = 1.0

$R_s = R_{sa}$ x R_{st} = 1.0

$(\Delta f)_{eff} = (R_p)(R_s)(\Delta f_{FATIGUE\ II}) = (1.0018)(1.0)(0.75)(4.56)$ = 3.43 ksi *MBE 7.2.2*

$(\Delta f)_{max} = (R_p)(\Delta f_{FATIGUE\ I}) = (1.0018)(1.50)(4.56)$

= 6.85 ksi < 16 ksi *MBE 7.2.4*

Thus, $(\Delta f)_{max} < (\Delta F)_{TH}$.

Hence, the detail possesses infinite fatigue life.

Example 3: (Floorbeam Fatigue)

A two-girder bridge with floorbeams and stringers has welded cover plates attached to the floorbeam flanges. The cover plate detail is investigated for fatigue susceptibility. It can be assumed that the width between girders is 40 ft, the floorbeams spaced at 25 ft centers, and the stringers placed at 8 ft center to center. The bridge, which was built in 1962, has 3 lanes with traffic in one direction and a span length of 100 ft.

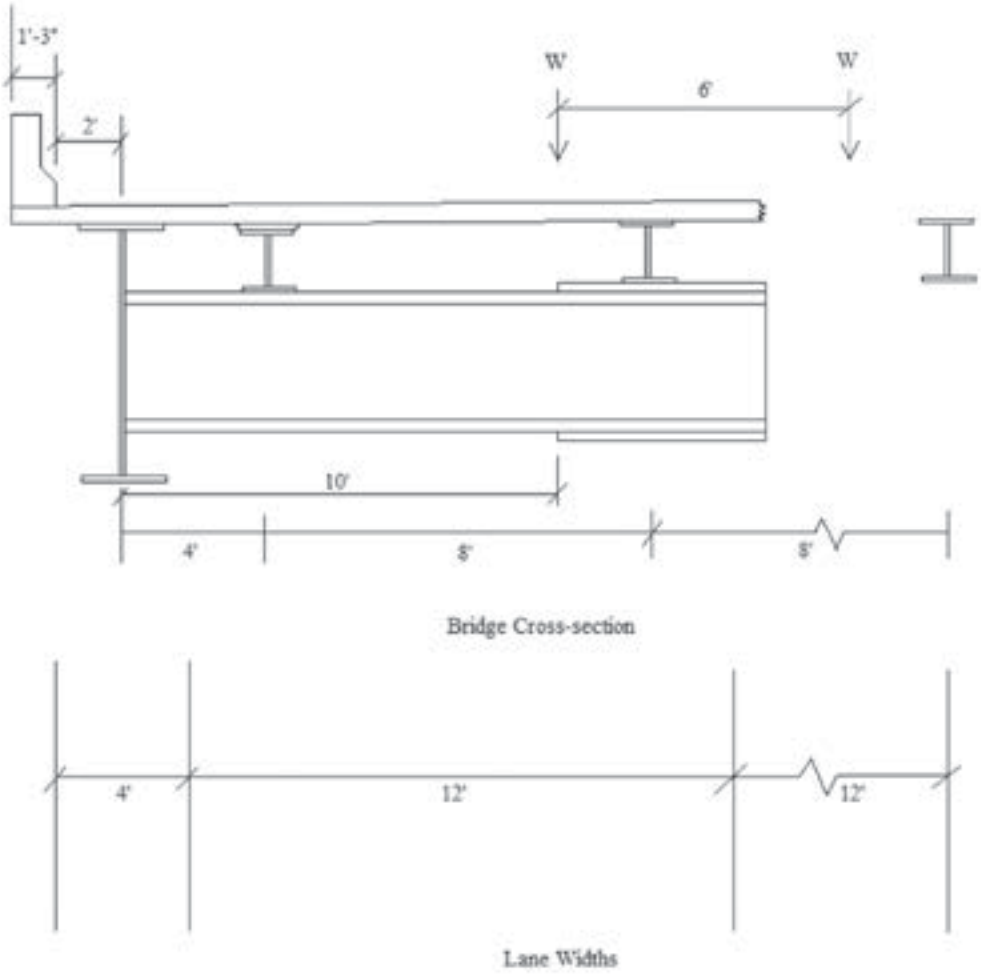

Figure 1: Bridge cross-section and lane widths.

The AASHTO LRFD design truck as specified in LRFD Article 3.6.1.4 and shown in the figure below shall be used to determine the critical stress range.

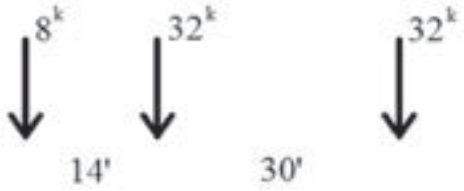

Assume that the floorbeam spacing is 25 . Also assume that the truck axle loads are transferred to the floor beams as simple beams.

Hence, maximum Truck Load to the floorbeams can be calculated by considering various positions of the truck axles:

$= 32^k + 8^k\left(\frac{25'-14'}{25'}\right) = 35.52^k \leftarrow$ Controls (One 32^k axle over floorbeam)

or $32^k\left(\frac{25'-5'}{25'}\right) + 8^k\left(\frac{25'-(14'+5')}{25'}\right) = 27.52^k$ (One 32^k axle 5ft on one side of floorbeam, and 8^k axle on opposite side)

or $\frac{32^k}{25'}\{(25'-(30'-x))+(25'-x)\} = 25.6^k$ (Floorbeam between two 32^k axles)

Fatigue Truck Wheel Load = 0.5 (35.52) = 17.76^k

The fatigue truck has been positioned such that the wheel load of the axle lies just above the location where the cover plate detail begins. This is done in order to maximize the stress range for the worst position of the fatigue truck load.

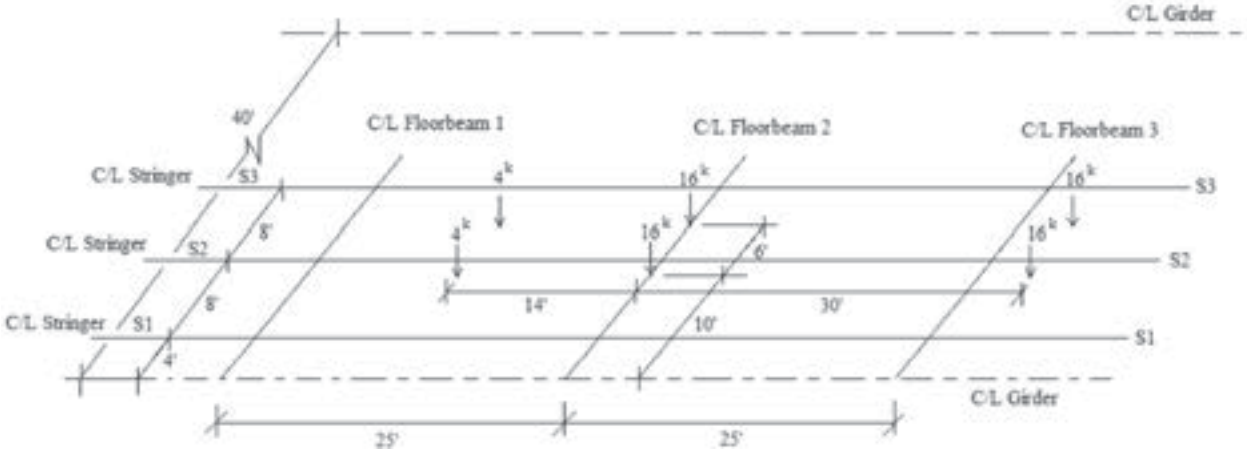

Figure 2: Distribution of wheel loads to stringers.

For distribution of 8^k axle and 32^k axle to stringers,

$$\text{Stringer S1 Reaction} = 4^k\left(\frac{1}{8}\right)(12-10)\left(\frac{11}{25}\right)+16^k\left(\frac{1}{8}\right)(12-10) = 4.44^k$$

$$\text{Stringer S2 Reaction} = 4^k\left(\frac{1}{8}\right)((10-4)+(20-16))\left(\frac{11}{25}\right)+16^k\left(\frac{1}{8}\right)((10-4)+(20-16)) = 22.2^k$$

$$\text{Stringer S3 Reaction} = 4^k\left(\frac{1}{8}\right)(16-12)\left(\frac{11}{25}\right)+16^k\left(\frac{1}{8}\right)(16-12) = 8.88^k$$

$$\text{Floorbeam Reaction@Girder} = \frac{1}{40}\left\{36(4.44^k)+28(22.2^k)+20(8.88^k)\right\}$$

$$= 23.98^k$$

$$\text{Floorbeam Live-Load Moment at x=10'} = 23.98^k(10') - 4.44^k(6') = 213.12^{k'}$$

Assume that the elastic section modulus of the floorbeam just beyond the cover plate is 1470 in^3.

Stress Range = M_r/S_x = 12 "/' x $213.12^{k'}$ / 1470 in^3 = 1.74 ksi

Impact factor IM = 15% *LRFD Table 3.6.2.1-1*

Critical Fatigue Section: Check fatigue at termination of bottom flange welded cover plate

Fatigue Case E

Use: A = $3.9x10^8$ *LRFD Table 6.6.1.2.5-1*

n = 1.0 *LRFD Table 6.6.1.2.5-2*

Threshold = 2.6 ksi *LRFD Table 6.6.1.2.5-3*

Hence, $(\Delta F)_{TH}$ = 2.6 ksi

Stress Ranges –

$\Delta f = \Delta f_{LL+IM}$ = LL + I = (1.00 + 0.15) x 1.74 *LRFD Table 3.6.2.1-1*

= 2.0 ksi

Nominal fatigue resistance for infinite life

$(\Delta F)_{TH}$ = 2.6 ksi for Detail Category E *LRFD Table 6.6.1.2.5-3*

Infinite-Life Fatigue Check *MBE 7.2.4*

R_p = 1.0 for transverse members *MBE 7.2.2.1*

R_{sa} = 1.0 *MBE Table 7.2.2.1-1*

R_{st} = 1.0

$R_s = R_{sa}$ x R_{st} = 1.0

$(\Delta f)_{eff} = (R_p)(R_s)(\Delta f_{FATIGUE\ II})$=(1.0)(1.0) (0.75)(2.0) = 1.5 ksi *MBE 7.2.2*

$(\Delta f)_{max} = (R_p)(\Delta f_{FATIGUE\ I})$ = (1.0)(1.50)(2.0)

= 3.0 ksi > 2.6 ksi *MBE 7.2.4*

Thus, $(\Delta f)_{max} > (\Delta F)_{TH}$.

The detail does not possess infinite fatigue life.

Evaluate fatigue life using procedures given in Section 7 of AASHTO's The Manual for Bridge Evaluation.

CALCULATION OF FATIGUE LIFE

Fatigue life determination will be based upon the finite fatigue life.

$$Y = \frac{\log\left[\frac{R_R A}{365n\left[(ADTT)_{SL}\right]_{PRESENT}[(\Delta f)_{eff}]^3} g(1+g)^{a-1}+1\right]}{\log(1+g)}$$ *MBE 7.2.5.1*

Assume $[ADTT]_{PRESENT}$ (One Direction, all lanes) = 1500

Use p = 0.80 *LRFD Table 3.6.1.4.2 -1*

Hence, $[(ADTT)_{SL}]_{PRESENT}$ = 0.80 x 1500 = 1200

Traffic Growth Rate g: 2%

Bridge Age a = 2011-1962 = 49 years

Assume that the owner decides to use Minimum Life for the bridge assessment.

Hence, R_R = 1.0 *MBE Table 7.2.5.1-1*

$(\Delta f)_{eff}$ = 1.5 ksi

A = 3.8 x 10^8 ksi^3 *LRFD Table 6.6.1.2.5-1*

n = 1.0 simple span girders with L > 40 ft. *LRFD Table 6.6.1.2.5-2*

$$Y = \frac{\log\left[\frac{(1.0)(3.9x10^8)}{365(1)(1200)(1.5)^3}(0.02)(1+0.02)^{49-1}+1\right]}{\log(1+0.02)} = 136 \text{ years}$$

CALCULATION OF FATIGUE SERVICEABILITY INDEX

Fatigue Serviceability Index $Q = \left(\frac{Y-a}{N}\right)GRI$ *MBE 7.2.6.1*

No. of Loadpaths (In this case, the minimum number of floorbeams loaded) = 3

G = 0.9 *MBE Table 7.2.6.1-1*

No. of Spans = 1 (Simple Span between floor beam ends)

R = 0.90 *MBE Table 7.2.6.1-2*

N = (larger of 100 or Y) = 136

Assuming that the bridge is on an Interstate Highway, I = 0.9 *MBE Table 7.2.6.1-3*

$$Q = \left(\frac{136-49}{136}\right)(0.9)(0.9)(0.9) = 0.47$$

The serviceability rating and assessment outcome are provided in MBE Table 7.2.6.2-1 for various ranges of the Fatigue Serviceability Index. In this example, a Q value of 0.47 means that the bridge will be rated as ‘Good’ from a fatigue standpoint and the assessment outcome would be ‘Continue Regular Inspection’.

Example 4: (Strategy to Increase Fatigue Serviceability Index – Accept Greater Risk)

If the bridge owner is willing to accept a greater likelihood of fatigue cracking for statistically more risk, the detail given in Example 3 can be evaluated for Evaluation 2 Life with a higher resistance factor R_R of 1.6. The example continues with a recalculation of the fatigue life and the Fatigue Serviceability Index.

CALCULATION OF FATIGUE LIFE

Fatigue life determination will be based upon the finite fatigue life.

$$Y = \frac{\log\left[\frac{R_R A}{365n\left[(ADTT)_{SL}\right]_{PRESENT}[(\Delta f)_{eff}]^3} g(1+g)^{a-1}+1\right]}{\log(1+g)} \qquad \textit{MBE 7.2.5.1}$$

$(ADTT)_{PRESENT}$ (One Direction) = 1500

$[(ADTT)_{SL}]_{PRESENT}$ = 0.80(1500) = 1200 *LRFD Table 3.6.1.4.2-1*

Traffic Growth Rate g: 2%

Bridge Age a = 2011-1962 = 49 years

$(\Delta f)_{eff}$ = 1.5 ksi

Assume Evaluation 2 Life to be used for bridge assessment.

Hence, R_R = 1.6 *MBE Table 7.2.5.1-1*

A = 3.9 x 10^8 ksi^3 *LRFD Table 6.6.1.2.5-1*

n = 1.0 simple span girders with L > 40 ft. *LRFD Table 6.6.1.2.5-2*

$$Y = \frac{\log\left[\frac{1.6(3.9x10^8)}{365(1)(1200)(1.5)^3}(0.02)(1+0.02)^{49-1}+1\right]}{\log(1+0.02)} = 158 \text{ years}$$

CALCULATION OF FATIGUE SERVICEABILITY INDEX

Fatigue Serviceability Index $Q = \left(\frac{Y-a}{N}\right)GRI$ *MBE 7.2.6.1*

No. of load paths (in this case, the minimum number of floorbeams loaded) = 3

G = 0.9 *MBE Table 7.2.6.1-1*

No. of Spans = 1 (Simple Span between floor beam ends)

R = 0.9 *MBE Table 7.2.6.1-2*

N = (larger of 100 or Y) = 158

Assuming that the bridge is on an Interstate Highway, I = 0.9 *MBE Table 7.2.6.1-3*

$$Q = \left(\frac{158-49}{158}\right)(0.9)(0.9)(0.9) = 0.50$$

The serviceability rating and assessment outcome are provided in MBE Table 7.2.6.2-1 for various ranges of the Fatigue Serviceability Index. In this example, a Q value of 0.50 means that the bridge will be rated as 'Excellent' from a fatigue standpoint and the assessment outcome would be 'Continue Regular Inspection'.

Example 5: (Strategy to Increase Fatigue Serviceability Index – More Accurate Data)

Field measurement is one of the methods that can be used to improve the accuracy of data. A more reliable value of the stress at the detail obtained through strain measurement at the critical detail will improve the life estimate. Suppose, for the detail given in Example 3, field measurements are performed which indicate a measured effective stress range of 0.9 ksi and a maximum measured stress range of 1.6 ksi.

Nominal fatigue resistance for infinite life

$(\Delta F)_{TH}$ = 2.6 ksi for Detail Category E *LRFD Table 6.6.1.2.5-3*

Infinite-Life Fatigue Check *MBE 7.2.4*

$(\Delta f)_{eff}$ = 0.9 ksi

$(\Delta f)_{max}$ = Larger of maximum (Δf_i) and $(2.0)[(\Delta f)_{eff}]$ *MBE 7.2.4*

= Larger of (1.6) and (2.0)(0.9)

= Larger of 1.6 and 1.8 = 1.8 ksi $<$ 2.6 ksi

Thus, $(\Delta f)_{max} < (\Delta F)_{TH}$.

Hence, the detail possesses infinite fatigue life.

Example 6: (Strategy to Increase Fatigue Serviceability Index – Use Inspection Information)

Consider a welded plate girder bridge with a welded partial length cover plate detail. The bridge, which was built in 1966, spans 70 ft and carries two lanes of traffic. The owner is using 'Evaluation 1 Life' to assess the bridge condition. Assume a cover plate weld detail of Category E.

Bridge age = a = 45 years

$[(ADTT)_{SL}]_{PRESENT}$ = 2,350

$(\Delta f)_{eff}$ = 3.75 ksi

n = 1 for 70 ft simple span

g = 2%

R_R = 1.2

A = 11.0 x 10^8 ksi^3 for Category E

$$Y = \frac{\log\left[\frac{R_R A}{365n\left[(ADTT)_{SL}\right]_{PRESENT}[(\Delta f)_{eff}]^3} g(1+g)^{a-1}+1\right]}{\log(1+g)} \qquad \textit{MBE 7.2.5.1}$$

$$Y = \frac{\log\left[\frac{1.2(11.0x10^8)}{365(1)(2350)(3.75)^3} 0.02(1+0.02)^{45-1}+1\right]}{\log(1+0.02)}$$

Y = 44 years

CALCULATION OF FATIGUE SERVICEABILITY INDEX

Fatigue Serviceability Index $Q = \left(\frac{Y-a}{N}\right) GRI$ *MBE 7.2.6.1*

No. of Load paths (In this case, girders) = 4

G = 1.0 *MBE Table 7.2.6.1-1*

No. of Spans = 1 (Simple Span)

R = 0.90 *MBE Table 7.2.6.1-2*

N = (larger of 100 or Y) = 100

Assuming that the bridge is on an Interstate Highway, I = 0.9 *MBE Table 7.2.6.1-3*

$$Q = \left(\frac{44-45}{100}\right)(1.0)(0.9)(0.9) = -0.01$$

The serviceability rating and assessment outcome are provided in MBE Table 7.2.6.2-1 for various ranges of the Fatigue Serviceability Index. A fatigue serviceability index less than zero gives a fatigue rating of 'Critical' with an assessment outcome of 'Consider Retrofit, Replacement, or Reassessment'. In this case the bridge owner decides to consider reassessment.

Since the bridge had been thoroughly inspected and no fatigue cracking or distress was found, it was decided to recompute the fatigue life using the truncation approach described in Article 7.2.7.2.3 of AASHTO's The Manual for Bridge Evaluation.

The calculation requires computation of the mean fatigue life, Y_{mean}. In making this calculation, the R_R value for the mean life should be taken from Table 7.2.5.1-1, and the stress range previously determined should be used.

R_R = 1.6 for mean life *Table 7.2.5.1-1*

$$Y_{mean} = \frac{\log\left[\frac{R_R A}{365n\left[(ADTT)_{SL}\right]_{PRESENT}[(\Delta f)_{eff}]^3} g(1+g)^{a-1}+1\right]}{\log(1+g)}$$

MBE 7.2.7.2.3

$$Y_{mean} = \frac{\log\left[\frac{1.6(11.0x10^8)}{365(1)(2350)(3.75)^3} 0.02(1+0.02)^{45-1}+1\right]}{\log(1+0.02)}$$

Y_{mean} = 53.1 years

Update the estimation for the lognormal distribution

$$P = \Phi\left[\frac{Ln\left(\frac{a}{2.19Y_{mean}}\right)+0.27}{0.73}\right] = \Phi\left[\frac{Ln\left(\frac{45}{2.19(53.1)}\right)+0.27}{0.73}\right]$$

$$= \Phi[-0.93] = 1-\Phi[0.93] = 1-(0.8238)$$

MBE Table 7.2.7.2-1

$$= 0.1762$$

$$Y'_{Eval1} = 2.19 Y_{mean} e^{0.73\Phi^{-1}[0.074(1-P)+P]-0.27}$$

$$= 2.19(53.1) e^{0.73\Phi^{-1}[0.074(1-0.1762)+0.1762]-0.27}$$

$$= 116.2 e^{0.73\Phi^{-1}[0.237]-0.27}$$

$$= 116.2 e^{0.73\{-\Phi^{-1}[1-0.237]\}-0.27}$$

$$= 116.2 e^{0.73\{-\Phi^{-1}[0.763]\}-0.27}$$

$$= 116.2 e^{0.73(-0.715)-0.27}$$ *MBE Table* 7.2.7.2-1

$$= 116.2 e^{-0.792} = 53 \text{ years}$$

Now compute the revised Fatigue Serviceability Index:

$$Q = \left(\frac{Y-a}{N}\right) GRI$$ *MBE 7.2.6.1*

$$Q = \left(\frac{53-45}{100}\right)(1)(0.9)(0.9)$$

Q = 0.06

The serviceability rating and assessment outcome are provided in MBE Table 7.2.6.2-1 for various ranges of the Fatigue Serviceability Index. Based upon the fatigue serviceability index of 0.06 of the reassessed life estimate, the cover plate detail now has a ‘Poor’ fatigue rating with an assessment outcome of ‘Assess Frequently’. The owner must decide how often to examine the detail prior to the next regular inspection.

Abbreviations and acronyms used without definitions in TRB publications:

AAAE	American Association of Airport Executives
AASHO	American Association of State Highway Officials
AASHTO	American Association of State Highway and Transportation Officials
ACI–NA	Airports Council International–North America
ACRP	Airport Cooperative Research Program
ADA	Americans with Disabilities Act
APTA	American Public Transportation Association
ASCE	American Society of Civil Engineers
ASME	American Society of Mechanical Engineers
ASTM	American Society for Testing and Materials
ATA	American Trucking Associations
CTAA	Community Transportation Association of America
CTBSSP	Commercial Truck and Bus Safety Synthesis Program
DHS	Department of Homeland Security
DOE	Department of Energy
EPA	Environmental Protection Agency
FAA	Federal Aviation Administration
FHWA	Federal Highway Administration
FMCSA	Federal Motor Carrier Safety Administration
FRA	Federal Railroad Administration
FTA	Federal Transit Administration
HMCRP	Hazardous Materials Cooperative Research Program
IEEE	Institute of Electrical and Electronics Engineers
ISTEA	Intermodal Surface Transportation Efficiency Act of 1991
ITE	Institute of Transportation Engineers
NASA	National Aeronautics and Space Administration
NASAO	National Association of State Aviation Officials
NCFRP	National Cooperative Freight Research Program
NCHRP	National Cooperative Highway Research Program
NHTSA	National Highway Traffic Safety Administration
NTSB	National Transportation Safety Board
PHMSA	Pipeline and Hazardous Materials Safety Administration
RITA	Research and Innovative Technology Administration
SAE	Society of Automotive Engineers
SAFETEA-LU	Safe, Accountable, Flexible, Efficient Transportation Equity Act: A Legacy for Users (2005)
TCRP	Transit Cooperative Research Program
TEA-21	Transportation Equity Act for the 21st Century (1998)
TRB	Transportation Research Board
TSA	Transportation Security Administration
U.S.DOT	United States Department of Transportation